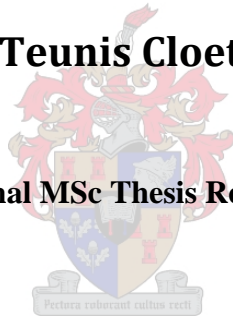# Benchmarking full-body inertial motion capture for clinical gait analysis

Teunis Cloete

Final MSc Thesis Report

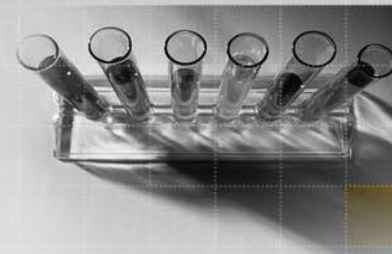**Department of Mechanical and Mechatronic Engineering**
University of Stellenbosch

29 January 2009
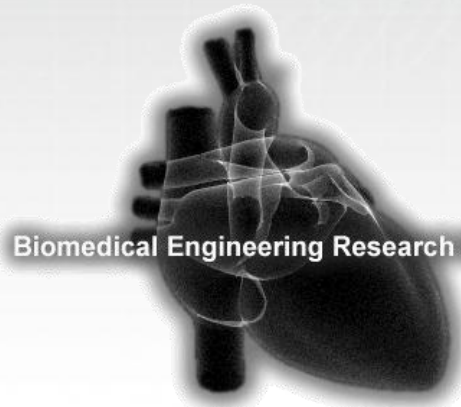
Benchmarking full-body inertial motion capture for clinical gait analysis

Final MSc Thesis Report

Teunis Cloete

Department of Mechanical and Mechatronic Engineering
Stellenbosch University

2nd Edition

29 January 2009

Benchmarking full-body inertial motion capture for clinical gait analysis

Final MSc Thesis Report

Author: **Mr. T. Cloete**
Supervisor: **Prof. C. Scheffer**

Department of Mechanical and Mechatronic Engineering
University of Stellenbosch

2nd Edition

29 January 2009

SUMMARY

Clinical gait analysis has been proven to greatly improve treatment planning and monitoring of patients suffering from neuromuscular disorders. Despite this fact, it was found that gait analysis is still largely underutilised in general patient-care due to limitations of gait measurement equipment. Inertial motion capture (IMC) is able to overcome many of these limitations, but this technology is relatively untested and is therefore viewed as adolescent.

This study addresses this problem by evaluating the validity and repeatability of gait parameters measured with a commercially available, full-body IMC system by comparing the results to those obtained with alternative methods of motion capture. The IMC system's results were compared to a trusted optical motion capture (OMC) system's results to evaluate validity. The results show that the measurements for the hip and knee obtained with IMC compares well with those obtained using OMC – with coefficient-of-correlation (R) values as high as 0.99. Some discrepancies were identified in the ankle-joint validity results. These were attributed to differences between the two systems with regard to the definition of ankle joint and to non-ideal IMC system foot-sensor design.

The repeatability, using the IMC system, was quantified using the coefficient of variance (CV), the coefficient of multiple determination (CMD) and the coefficient of multiple correlation (CMC). Results show that IMC-recorded gait patterns have high repeatability for within-day tests (CMD: 0.786-0.984; CMC: 0.881-0.992) and between-day tests (CMD: 0.771-0.991; CMC: 0.872-0.995). These results compare well with those from similar studies done using OMC and electromagnetic motion capture (EMC), especially when comparing between-day results.

Finally, to evaluate the measurements from the IMC system in a clinically useful application, a neural network was employed to distinguish between gait strides of stroke patients and those of able-bodied controls. The network proved to be very successful with a repeatable accuracy of 99.4% (1/166 misclassified). The study concluded that the full-body IMC system produces sufficiently valid and repeatable gait data to be used in clinical gait analysis, but that further refinement of the ankle-joint definition and improvements to the foot sensor are required.

OPSOMMING

Dit is bewys dat kliniese gang-analise tot groot verbeterings lei in die versorgingsbeplanning en monitering van pasiënte wat aan neuromuskulêre siektes ly. Ten spyte hiervan word daar gevind dat gang-analise steeds onderbenut word in algemene pasiëntesorg vanweë tekortkominge in gang-opnametoerusting. Inersie-bewegingsopname (IBO) bied oplossings vir vele van hierdie tekortkominge, maar die tegnologie is steeds relatief ongetoets en word dus as onvolwasse beskou.

In hierdie studie word dié probleem aangespreek deur die geldigheid en herhaalbaarheid van gang-parameters, wat met behulp van 'n kommersieel beskikbare IBO-stelsel gemeet is, te ondersoek deur die resultate met alternatiewe bewegingsopnamemetodes te vergelyk. Die IBO-stelsel is vergelyk met 'n betroubare optiese bewegingsopname (OBO)-stelsel om die geldigheid te bepaal. Resultate toon dat IBO-opnames goed vergelyk met dié van OBO wat geneem is van die heup en knie met waardes van koëffisiënt van korrelasie (R) wat strek tot 0.99. Geldigheidsresultate van die enkelgewrig toon swakker waardes. Die probleme word toegeskryf aan verskille in die definisie van die enkelgewrig en die nie-ideale ontwerp van die IBO-stelsel se voetsensor.

Die herhaalbaarheid van die IBO-resultate is gekwantifiseer met behulp van die koëffisiënt van variasie (KV), koëffisiënt van veelvoudige determinasie (KVD) en die koëffisiënt van veelvoudige korrelasie (KVK). Resultate het getoon dat gang-opnames met behulp van die IBO-stelsel goeie herhaalbaarheid toon vir sowel dieselfde-dag-toetse (KVD: 0.786-0.984; KVK: 0.881-0.992) en verskillende-dag-toetse (KVD: 0.771-0.991 ; KVK: 0.872-0.995). Resultate vergelyk goed met dié van soortgelyke studies wat gedoen is met behulp van OBO en elektromagnetiese bewegingsopname (EBO), veral vir verskillende-dag resultate.

Om gang-opnames van die IBO-stelsel in 'n nuttige kliniese toepassing te ondersoek, is 'n neurale netwerk ingespan om te onderskei tussen gang-opnames van pasiënte met beroerte en gang-opnames van 'n kontrolegroep. Die netwerk het goeie resultate getoon met 'n herhaalbare akkuraatheid van 99.4% (1/166 vals geklassifiseer). Die gevolgtrekking van hierdie studie is dus dat die IBO-stelsel voldoende geldigheid en herhaalbaarheid toon om van nut te wees vir kliniese gang-analise. Verdere verfyning van die enkelgewrig-definisie en verbetering van die voetsensors is egter nodig.

ACKNOWLEDGEMENTS

DECLARATION

I, the undersigned, hereby declare that the work contained in this thesis is my own original work and that I have not previously in its entirety or in part submitted it at any university for a degree.

Signature: …………………………………………………
                            Teunis Cloete

Date: …………………………………………………..

TABLE OF CONTENTS

NOMENCLATURE

Normal gait	Stride of an able-bodied human
Pathological gait	Stride patterns showing locomotive irregularities
Orthopaedics	A branch of surgery related to musculoskeletal injuries
Ambulation	Movement related to walking (while walking)
Hemiparesis	Loss of control of feeling in one half of the body

LIST OF ABREVIATIONS

IMC	Inertial motion capture
OMC	Optical motion capture
EMC	Electromagnetic motion capture
MEM	Microelectromechanical
GCS	Global coordinate system
BCS	Body coordinate system
JCS	Joint coordinate system
AL	Anatomical landform
ROM	Range of motion
PD	Parkinson's disease
HS	Heel-strike
TO	Toe-off
DOF	Degrees of freedom
R	Correlation coefficient
CMD	Coefficient of multiple determination
CMC	Coefficient of multiple correlation
SD	Standard deviation

LIST OF SYMBOLS

φ	Roll
θ	Elevation
ψ	Azimuth
φ_h	Hip abduction-adduction
θ_h	Hip flexion-extension
ψ_h	Hip internal-external rotation
φ_k	Knee varus-valgus
θ_k	Knee flexion-extension
ψ_k	Knee internal-external rotation
φ_a	Ankle eversion-inversion
θ_a	Ankle plantar-dorsiflexion
ψ_a	Ankle supination-pronation
M	Total number of days (Section 4.4.2)
N	Total number of runs (Section 4.4.2)
T	Total stride-time (Section 4.4.2)

LIST OF UNITS

Hz	Hertz
ms	Milliseconds
g	Gravitational acceleration
m/s	Meters per second
kg	Kilogram

LIST OF FIGURES

LIST OF TABLES

1. INTRODUCTION

1.1. Introduction

The analysis of human motion has progressed leaps and bounds from its origin in the times of Aristotle and Borelli (Baker, 2007). Gait analysis is used to quantify the mobility state of a person (Simon, 2004). This biomechanical information is useful in several fields and applications, including: the ongoing pursuit for improved performance and reduced injuries in athletes, the quest to make more believable humanoid characters in computer graphics and virtual reality, the planning of treatment protocols such as effective surgical intervention or orthopaedic prescription (Roetenberg, 2006, Steinwender *et al.*, 2000). Gait analysis also offers insight into the development of motor learning skills in children, training development, rehabilitation monitoring and the effect of neuromuscular injuries on a patient's daily living (Bronner, undated). The clinical applications mentioned are of greatest importance to this study.

Current diagnostic observations of posture and movement made by physicians are subjective and dependent on their judgment and experience (Lee *et al.*, 2000, Mackey *et al.*, 2005). With the backing of several examples, Simon (2004) found that gait analysis supplies a confidence not provided by regular clinical examination, that the correct number and selection of surgical procedures can be chosen in patients with cerebral palsy. This is also the case for patients with other neuromuscular disorders. In spite of obvious advantages, gait analysis has nevertheless seen hampered popularity and is still rarely used as a means of clinical diagnosis (Simon, 2004). The limited utilization has been attributed to factors such as ineffective application of current technologies and poor lab organization, test procedure, result interpretation and report generation as well as the high cost associated with most gait studies. There is often a need for gait analysis to be conducted outside of a laboratory environment as in-lab walking differs from everyday walking (Simon, 2004). This attribute is also a requirement in the field of telemedicine where doctors are unable to meet the demand of patients in rural areas. Most gait labs are however unequipped to satisfy this requirement.

In recent decades improvements in the field of photography have allowed researchers to conduct frame-by-frame analyses of the mechanics of human motion. Ever-increasing revelation of the clinical potential of gait analysis has united the medical and engineering communities in efforts to fashion more efficient, accurate and versatile ways of capturing and analysing human motion. Although originating from clinical studies, the industry of motion capture (Mocap) has seen noticeable growth with the more recent popularity of life-like computer animations in television and computer gaming. This has birthed a variety of methods of Mocap, each with their own advantages and limitations (as discussed in Section 2.1.3.2). The most common

limitation in Mocap systems is their high cost and spatial restrictions. In almost all cases Mocap is conducted indoors and within limited spatial boundaries (Vlasic *et al.*, 2007). Only recently has technology allowed for the development of untethered Mocap such as magnetic and inertial motion capture (IMC). This is largely because of recent advances in Micro Electro Mechanical System (MEMS) technologies encouraging the development of small and inexpensive sensors such as accelerometers, gyroscopes and magnetometers which form the key components of inertial motion sensor units. These sensors allow researchers to determine orientation based on passive measurements of physical quantities directly related to the motion and orientation of rigid bodies to which the sensors are attached (Bachmann, 2000). These, along with powerful microcontrollers, small batteries and high storage capacities directly facilitate long term, portable recordings of ambulatory measurements (Dejnabadi *et al.*, 2005).

With evident versatility and cost advantages over alternative, laboratory-based optical, acoustic and mechanical systems, it would seem that IMC offers solutions to several of the before-mentioned hampering factors. It is thus applicable to ask why IMC is still largely underutilized for clinical gait analysis. A possible answer lies in the adolescence of the technology in practice, and therefore the lack of confidence in its measurement accuracy. This study aims to address this hindrance by investigating the validity and repeatability of results obtained from a commercially available, full-body IMC system, by comparing them to results obtained from a proven and commonly used optical motion capture (OMC) system. Various studies have been conducted to compare these technologies (Dejnabadi *et al.*, 2005, Dejnabadi *et al.*, 2006, Favre *et al.*, 2006, Roetenberg, 2006, Simon, 2004), however the author has found no evidence of such a comparison done during a routine ambulatory gait analysis.

1.2. Problem statement

Mocap methods currently used for clinical gait analysis are sufficiently accurate and well accepted among professionals in the field. However, these Mocap systems often lack spatial versatility and are relatively costly. Cheaper, more flexible methods of recording motion have emerged in recent years, but these are relatively untested in relevant applications and therefore invoke uncertainties among physicians.

1.3. Motivation

As mentioned above, there are several factors which limit the widespread utilization of gait analysis as an everyday clinical tool. These are summarized below:

   i.   Gait analysis is primarily considered by most physicians to be a research tool rather than an aid to clinical decision-making. This view is often

supported by the fact that medical insurance companies do not cover gait analysis in their policies (Simon, 2004).

ii.   Gait laboratories are viewed as inefficient, unproductive and uneconomical because:

- o The laboratory setup and calibration procedures vary from test-to-test and patient-to-patient, making the procedure time consuming and therefore limiting the daily patient throughput.
- o In most cases trained professionals are employed to acquire process and interpret gait data. Associated labour costs are considered as the major contributor to the relatively high cost of gait tests.
- o Gait test reports, generated for physicians, are often tardy and contain vast amounts of unnecessary data (Simon, 2004).

iii.   Gait parameters are calculated using assumptions of skin movement and anatomical parameters to estimate joint angle centres rather than actual measured data (Simon, 2004). According to White *et al.* (1989) there are inherent errors associated with anatomical variability in bony contours and muscle attachment (White *et al.*, 1989). This forces physicians to question the validity of measured gait parameters.

iv.   Most gait analyses are conducted within laboratories which limits both the range of motion and duration of tests. In several applications, including rehabilitation and sports performance analysis, it may be necessary that gait recordings be done in larger and more versatile locations. Long term gait assessments are often required for patients with neuromuscular disorders and ideally in the patient's everyday home environments (refer to Section 2.1.1).

v.   Economic as well as logistical reasons cause trained physicians to be predominantly based in urban areas. This relates to hampered health care (such as gait analysis) for patients restricted to rural areas.

vi.   Current methods of recording the 3D kinematics suffer from several problems which cause uncertainty about their validity. According to Bachmann (2000) these include: Marginal accuracy, user encumbrance, range restrictions, susceptibility to interference, noise, poor registration, occlusion difficulties and high latency. These limitations in Mocap technologies are further discussed in Section 2.1.3.2

1.4. Objectives

In order to address the listed factors which have curbed gait analysis from becoming a commonly used diagnostic tool, the following objectives can be suggested:

i. To identify the most significant limitations to current means of conducting 3D kinematic gait analysis.

ii. To identify and define the requirements of a full-body motion capture system necessary for accurate and reliable gait analysis.

iii. To both qualitatively and quantitatively test whether IMC offers a solution to the above-mentioned limitations.

iv. To test the use of IMC in a clinical application through implementing a neural network, using IMC collected gait data, to distinguish between able-bodied subjects and stroke patients.

v. To discuss the aptness of IMC as a telemedicine tool.

vi. To suggest possible improvements to current methods of Mocap and subsequent gait data acquisition and analysis.

1.5. Scope of work

This study consists of four major sections, namely: 1) A literature review in which the current state of the art in motion capture methods are compared to the current requirements of clinical gait analysis. 2) A validity study in which inertial motion capture is compared to a generally accepted "gold standard" Mocap system on the grounds of statistical accuracy and precision. 3) A repeatability study in which the within-day and between test day repeatability is evaluated for both able-bodied and gait impaired ambulators. 4) The application of a neural network to test IMC collected gait data in a clinical application. This thesis represents the study findings and is organized as follows:

Chapter 2 defines and describes gait analysis and its historical background and continues with a look at its application in the diagnosis, assessment and treatment of patients with pathological (abnormal) gait. In Section 2.1.3.2, a qualitative comparison is drawn between the advantages and shortcomings of the most popular methods of Mocap. This includes an investigation into the ways in which gait parameters are acquired, calculated and represented. Finally, Section 2.2 contains a discussion of the procedures and findings of other studies related to this one.

Chapter 3 and 4 include the objectives, procedure, statistical approach and post-processing of the validity and repeatability studies respectively, as well as discussions on their findings with reference to related literature.

Chapter 5 discusses the planning, implementation, analysis and results of the neural network.

- 4 -

Chapter 6 examines IMC in everyday activities and considers its usefulness in telemedicine. The chapter then concludes the thesis by holistically discussing the results with reference to the objectives listed in Section 1.4 and, with these in mind, provides recommendations for future studies.

- 5 -

2. LITERATURE REVIEW

2.1. What is gait analysis?

Ambulation in humans can be defined as upright, bipedal locomotion, or gait (Whiting and Rugg, 2006). According to Whiting and Rugg (2006), gait analysis is the study of a particular form of human or animal[1] locomotion. Gait is typically used to describe a walking or running movement. Han, *et al.* (2006) describes gait as a cyclic movement of the feet in which one or the other alternate in contact with the ground. Gait analysis forms part of the field of biomechanics which includes statics and dynamics, the latter comprising of kinetic and kinematic parameter (Bronner, undated). Kinematic parameters may be further sub-divided into temporal-spatial and 3D joint angles. A human stride can be quantified by what is commonly referred to as the gait cycle. Phases of the gait cycle are shown in Figure 1:
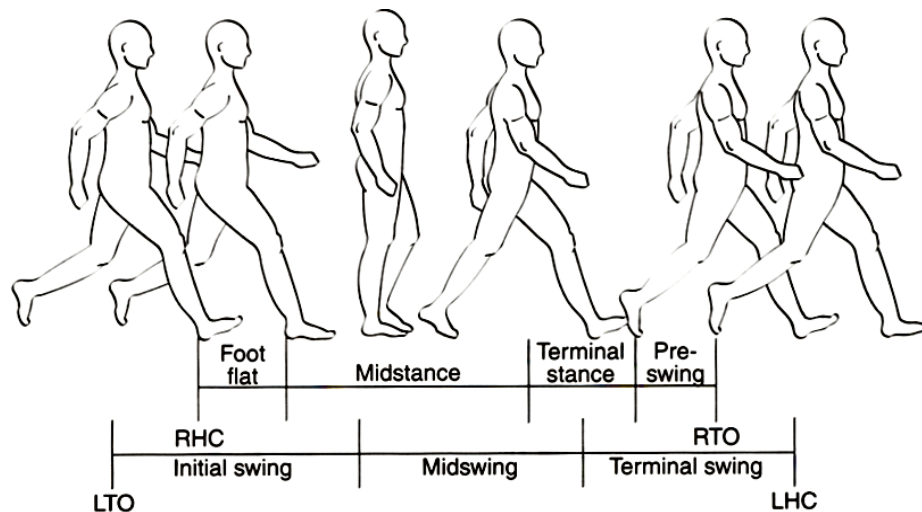
Figure 1: Gait cycle
Source: Whiting (2006)

Here LTO and RTO refers to left and right toe-off phases (terminal contact) and LHC and RHC refer to left and right heel-contact or heel-strike phases (initial contact).

In Figure 2 the gait cycle is represented by gait periods, tasks and phases. The temporal and spatial characteristics are obtained by measuring the distances and velocities between the feet at different phases of the gait cycle. These are then studied to provide clinical and scientific insight into both normal and pathological gait (Whiting and Rugg, 2006). Temporal (time dependant) measures include step time,

---

[1] From this point onwards, the word "gait" will refer to human gait only.

- 6 -

stride time, cadence and swing and stance phase durations. Spatial (distance dependant) measures include step length, stride length and step width. In addition clinicians also study the 2D or 3D joint angles in the sagittal, frontal or transverse planes when assessing subject gait (Favre *et al.*, 2006, Bronner, undated). These are sometimes referred to as gait patterns. The complexity of human walking is reflected by an abundance of gait studies related to sports, rehabilitation and orthopaedic surgery which has lead to a variety of parameters characterizing gait (Vardaxis *et al.*, 1998). A complete list of gait characteristics is given in Appendix A.
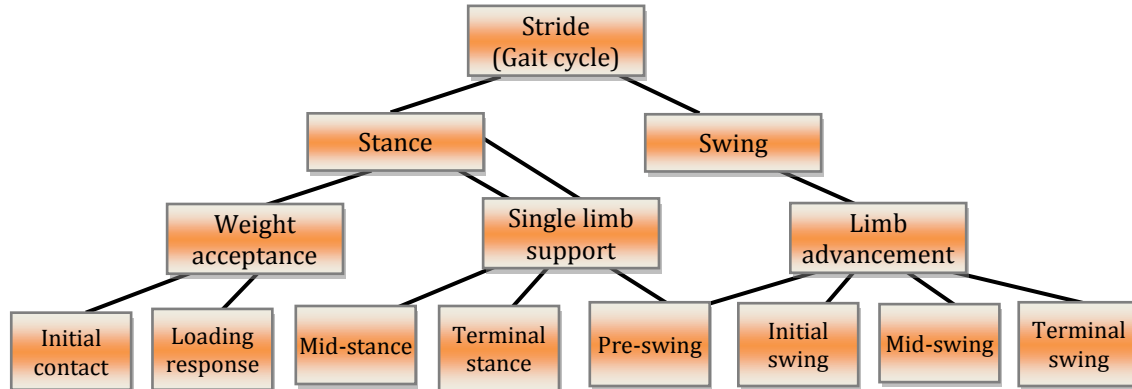
Figure 2: Division of gait cycle
Source: Whiting, 2006

The main reason for studying human gait is to identify irregularities or changes in the gait patterns of patients or athletes. Gait is often evaluated over time to monitor rehabilitative treatments or the extent of gait deterioration. Neural control of gait (organization and control of the activation of skeletal muscle and maintains balance by the nervous system) is very complex and is presently not completely understood (Molson Medical Informatics, 1999). Complex sensory, motor and central nervous systems are involved using muscles, tendons, ligaments, and skeletal structure as effectors. According to Molson Medical Informatics (1999) basic gait rhythm does not require input from the periphery.

An important element of studying gait abnormalities is the definition of able-bodied or normal gait (Vardaxis *et al.*, 1998). However, this is not a trivial exercise since vast amounts of gait data collected over several years from different labs and by different researchers show great variability, even when great efforts were made to maintain consistency (Vardaxis *et al.*, 1998).

2.1.1. Pathological gait

Two essential characteristics in human gait are equilibrium and locomotion, both of which are impaired during abnormal (pathological) gait (Han *et al.*, 2006). According to Ephanov and Hurmuzlu (2001) humans adapt their gait when affected by

pathological conditions to preserve their locomotive functionality. This is usually on a subconscious level. Adaptive mechanisms such as reduced stride length and gait cycle period are used by patients to reduce pain caused by joint moments (Gök *et al.*, 2002). This is exhibited by patients with Parkinson's disease (PD) who tend to walk slowly with short shuffling steps, reduced arm swing, stooped posture (Salarian *et al.*, 2004).

Stroke is a localized loss of brain function caused by a sudden lack of blood supply to an area in the brain. Stroke may occur as a result of an embolism or haemorrhage. Hemiparetic-stroke ambulation is characterised by asymmetry of temporal-spatial parameters and joint angles between the paretic and non-paretic sides. One example may be a lower hip extension measured on the paretic side compared to the unaffected side. Other factors such as muscle or tendon infection, disease, paralysis, injury and anatomical defects may also lead to abnormal gait. Gait disorders with varying severity and blatancy have been extensively studied, but despite this, gait analysis is rarely used to diagnose gait disorders (Simon, 2004). A list of structural and neurological gait disturbances is given in Appendix B.

In recent years healthcare systems have promoted the idea of patient monitoring in their own home environments (Roetenberg, 2006). This is particularly advantageous when monitoring patients with Parkinson's disease whose gait measurements are significantly affected by the amount of medication in their bodies at the time (Han *et al.*, 2006). Several studies have emerged focusing on portable, comfortable and user-friendly monitoring systems for stroke patients and patients suffering from Parkinson's disease and cerebral palsy (von Acht *et al.*, 2007, Zhou and Hu, 2004, Aminian *et al.*, 2001, Han *et al.*, 2006, Salarian *et al.*, 2004). These, along with statistical diagnostic algorithms could see future patient monitoring become both simple and affordable. Simon (2004) suggested the use of advanced semi-automated-diagnosis tools such as neural networks to assist in making gait analysis a part of a physician's referral process. With this in mind the focus must turn to optimizing current methods of gait measurement and analysis.

2.1.2. History of kinematic gait measurement

The earliest recorded comments of human walking characteristics can be dated back to Aristotle, who lived 384-322 BC. He stated that:

"If a man were to walk on the ground alongside a wall with a reed dipped in ink attached to his head the line traced by the reed would not be straight but zig-zag, because it goes lower when he bends and higher when he stands upright and raises himself" (Baker, 2007).

Further progress only continued with experiments by Giovanni Borelli (1608–1679). Several scientists wrote about walking through the enlightenment period, but it was

the brothers Willhelm (1804–1891) and Eduard (1806–1871) Weber who made the next significant contribution based on very simple measurements. Advancements in gait measuring technologies were made in the early 1900s by Eadweard Muybridge in California and Étienne-Jules Marey in Paris using still cameras. Refer to Figure 3 below.

Otto Fischer (1861–1917), in collaboration with Wilhelm Braune (1831–1892) further developed these methods using a calibrated mesh frame, shown in Figure 4. Their work on the effect of age and height variance on gait is still seen as definitive work on the subject (Baker, 2007). Before the recent advances in modern computers gait calculations were very tedious, containing up to 14000 numerical calculations, 72 curves plotted and 24 curves subject to graphical differentiation, all for a single stride. This required up to about 500 man hours. With some experience this could be reduced to about 250 man hours (Baker, 2007). Only in the late 1970s early 1980s a quicker and easier gait analysis system was designed using television cameras feeding data directly into a computer (Whittle, 1996).
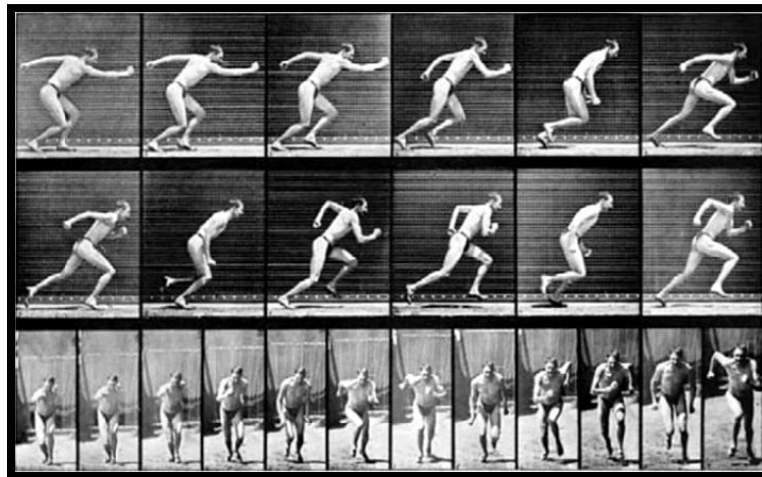
Figure 3: "The Human Figure in Motion" by Muybridge (1878)
Source: Roetenberg (2006)
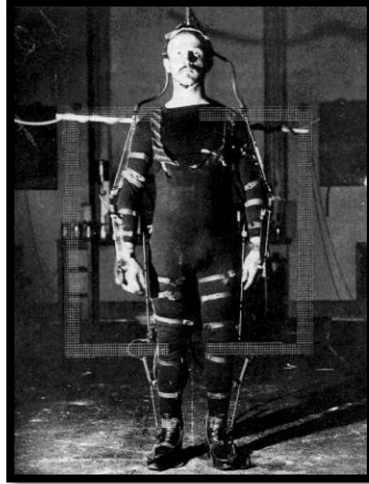
Figure 4: Braune and Fischer's subject wearing the experimental suit
Source: Baker (2007)

The last decade has seen substantial advancements in gait measuring (motion capture) technologies because of increased computational capabilities and sensor component size reduction. Current technologies include optical, acoustic and inertial motion capture and advanced software packages which reduces the level of expertise required to collect movement data. The most popular motion capture technologies are described in Section 2.1.3.2.

2.1.3. Methods of quantifying human gait

2.1.3.1. Requirements

Motion capture has seen significant advancement in the last two decades primarily because of the introduction of MEMS sensors and progress in computer technology (Roetenberg, 2006). Applications span the fields of medicine, television, computer gaming, engineering and more. Several surveys have been done on the subject (Meyer *et al.*, 1992, Frey, 1996, Hightower and Borriello, 2001, Welch and Foxlin, 2002) which emphasize the arsenal of systems currently available or being brought into production (Vlasic *et al.*, 2007). All these systems have unique advantages and limitations. It is therefore important to define the requirements of a Mocap system with reference to clinical gait measurement. Miller *et al.* (2004) listed cost, equipment size, communication and reliability as primary factors for choosing a system. Bachmann (2000) added resolution, registration, responsiveness, robustness and sociability as requirements. He quantified these characteristic in the context of human motion analysis as follows:

- 10 -

- o The hand is viewed as the part of the body that experiences the greatest motion and therefore governs the speed, force, frequency and precision requirements.

- o Fast hand motions occur at an average frequency of approximately 5 Hz. Based on the Nyquist sampling theorem a 10 Hz sampling frequency should be sufficient. However with the addition of noise from low cost sensors, and thus applying a low pass filter and a rule of thumb of 20 times over-sampling, the required sampling frequency is 100 Hz.

- o Under normal circumstances the hand reaches a velocity of 3 m/s, but under extreme conditions (such as throwing a baseball) it can reach up to 37 m/s.

- o Normal hand movements generate accelerations of between 5 and 6 g, but this may reach up to 25 g.

- o The minimum changes in rotation angles perceivable to humans are approximately 2.5°, 2° and 0.8° for the fingers, wrist and shoulders respectively. An angular precision of 0.5° should therefore suffice.

- o In applications where real-time movements are required (such as for patient feedback) it was found that a lag of greater than 100 ms will degrade response performance.

Sociability refers to the ability of the Mocap system to be used with other applicable equipment. This could include physiological measurement devices such as EMG force plates, or it may refer to equipment, such as a treadmill, sometimes necessary to fully analyse a person's gait. Frey *et al.* (1996) stated that a minimum of 15 body segments have to be tracked to achieve full-body tracking. Untracked segments may be added, but the kinematics of these would have to be calculated using reverse kinematics which is computationally demanding (Frey *et al.*, 1996).

2.1.3.2. Motion capture technologies

Some of the most popular Mocap technologies along with their relevant advantages and limitations are described below:

a. Mechanical (Electro-mechanical)

In the context of full-body Mocap, mechanical Mocap systems are rigidly mounted, body-based exoskeletons which make use of goniometers and potentiometers to sense relative joint angles. Figure 5b shows the Gypsy^{TM} system by Meta Motion. Because these tracking devices are rigidly mounted to the body, they are relatively cumbersome, but well-suited for measuring forces applied by segments when force-feedback devices are used (Frey *et al.*, 1996, Vlasic *et al.*, 2007).

- 11 -
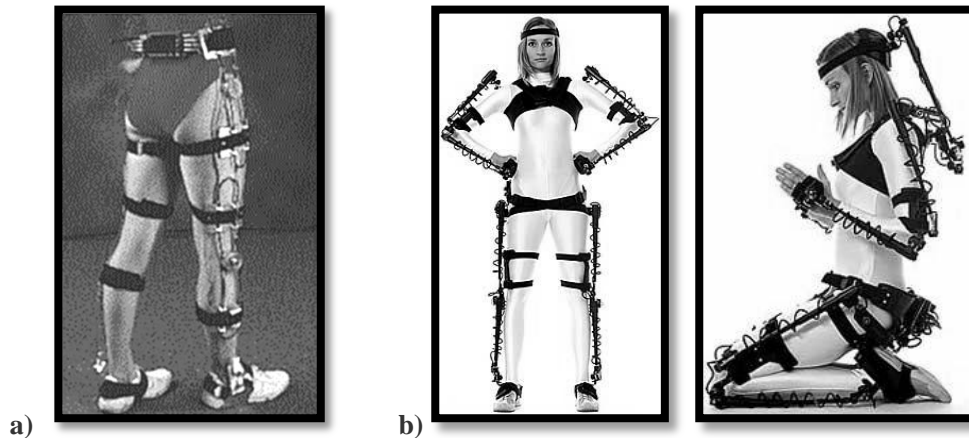
Figure 5: Mechanical motion capture devices
Source: (a) MIE Medical Research Ltd.; (b) www.metamotion.com

These systems are low in cost, and because no trigonometric calculations are required, they are able to track the body segment orientation in real time (Bronner, undated). These systems do not suffer from shadowing or interference problems associated with other methods. On the downside, mechanical Mocap systems are sensitive to soft-tissue artefacts and need a supplementary system to determine segment position in a global coordinate system (GCS) (Roetenberg *et al.*, 2007, Bronner, undated).

b. Electromagnetic

Electromagnetic systems are popular and relatively inexpensive. In a survey by Frey *et al.* (1996) he labelled this Mocap technique as "*the most widely used tracking method*". These systems are fairly compact and wireless models are readily available. A magnetic field transmitter produces three orthogonal magnetic fields. Body-worn trackers (receivers) then produce voltages proportional to the segment orientation using three orthogonal coils.

Two types of electromagnetic tracking systems are commercially available. These are direct current (DC) and alternating current (AC) systems. DC systems, in which DC excited magnetic fields are pulsed, boast a higher immunity to external electro-magnetic interferences associated with ferromagnetic materials. Nevertheless, this factor is still one of the most prominent limitations of electromagnetic Mocap (Bachmann, 2000). The strength of the tracking signal degrades with the distance between the transmitter and receivers which significantly limits the range of these systems (Roetenberg, 2006, Bachmann, 2000). Selling points include small user-worn receivers (Figure 6), the absence of line-of-sight requirements, multiple-segment tracking using a single transmitter and overall technology maturity (Welch and Foxlin, 2002).

- 12 -

Figure 6: Electromagnetic motion capture system
Source: Ascension Technology Corporation (2007)

c. Acoustic

Two methods of acoustic tracking are commonly in practice. The first employs the time-of-flight (TOF) of sound waves where the body or segment is tracked by measuring the distance between an acoustic pulse transmitter and a receiver at different intervals in time. The speed of sonic or ultrasonic sound waves is used to compute relative distances. Triangulation is used to track a relative position of a segment. Where the position of more than one segment needs to be tracked simultaneously, either a separate transmitter and receiver are required for every segment or multiple frequency acoustics are used. To track the orientation of a segment, two tracked points are required for each segment.

The second acoustic tracking technique uses the phase difference between incident and returning sound waves to determine the position and orientation of the segment. This technique is more accurate than TOF tracking, but is limited to calculating only relative positions between points in contrast to full 3D position in the GCS which TOF tracking is able to do (Frey *et al.*, 1996), (Welch and Foxlin, 2002).

Acoustic tracking demonstrate superior range to electromagnetic tracking, but requires a line-of-sight between emitters and receivers. Interference from echoing and environmental noise deteriorates measurement quality.

d. Optical

A multitude of Mocap techniques exist which utilize some method of sensing light. These include image based methods which use a combination of videography and image processing as well as opto-electric methods which sense TOF light intensity (Bronner, undated).

- 13 -
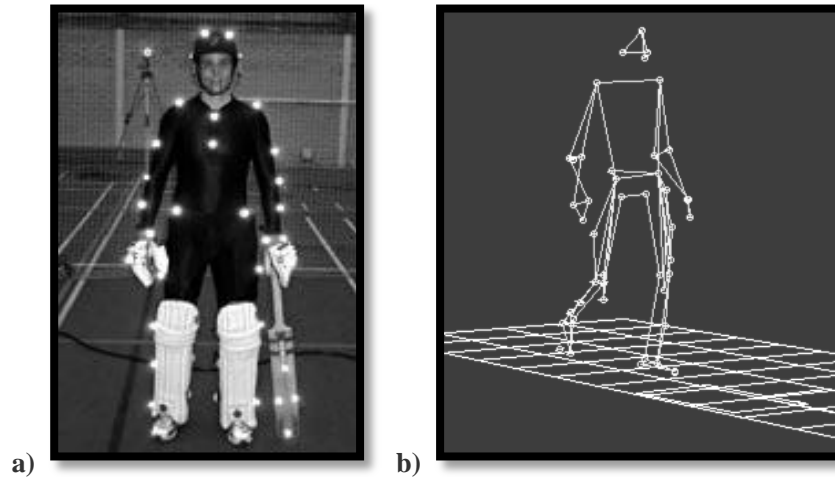
Figure 7: Optical motion capture - Vicon Oxford Metrics Ltd.
Source: (a) www.bbc.co.uk; (b) www.rehabtrials.org

Image-based methods may be markerless or employ active or passive markers. Active markers (usually infrared light-emitting diodes) are excited at unique frequencies to ensure differentiation from each other when sensed in multiple camera views. Passive markers (usually reflective balls) rely on variable sizing or software and accurate calibration procedures to distinguish one from another. Sensing may be outside-in or inside-out. With outside-in systems the sensors (light sensors or cameras) are placed on the ground and track markers on the body. Inside-out systems on the other hand employ sensors on the tracked body itself. The latter is hardly ever used for clinical applications due to the associated user encumbrance. Optical Mocap has achieved great popularity and commercial systems such as the Vicon (Oxford Metrics Ltd.) and Optotrak® are often viewed as the "golden standard" in the field human motion analysis (Roetenberg, 2006). These systems boast high accuracies and are able to sense full 6-DOF orientation and position. Optical Mocap systems are unfortunately relatively expensive, limited to laboratory use and suffer from shadowing. They also require substantial computing power.

As with most of the other Mocap techniques, surface markers move relative to the underlying bone because of soft-tissue artefacts. This leads to error propagation in position and orientation calculations (Lucchetti *et al.*, 1998). Many researchers feel that the final solution in human Mocap is markerless tracking (Bachmann, 2000). Boulgouris *et al.* (2000) foresaw the use of markerless optical gait measurements as a means of personal identification in the security sector. Markerless tracking is motivated by unreliable anatomical landmark identification, noisy data caused by soft-tissue artefacts, and marker inertia and marker loss, all common attributes of marker-based systems (Zhou and Hu, 2004). In recent work at Stanford University, accuracies of between 1° and 2° were found in sagittal and frontal joint knee angles using their eight camera markerless system shown in Figure 8 (Corazza *et al.*, 2006).

- 14 -

However, this type of system inherently relies on highly controlled laboratory conditions.
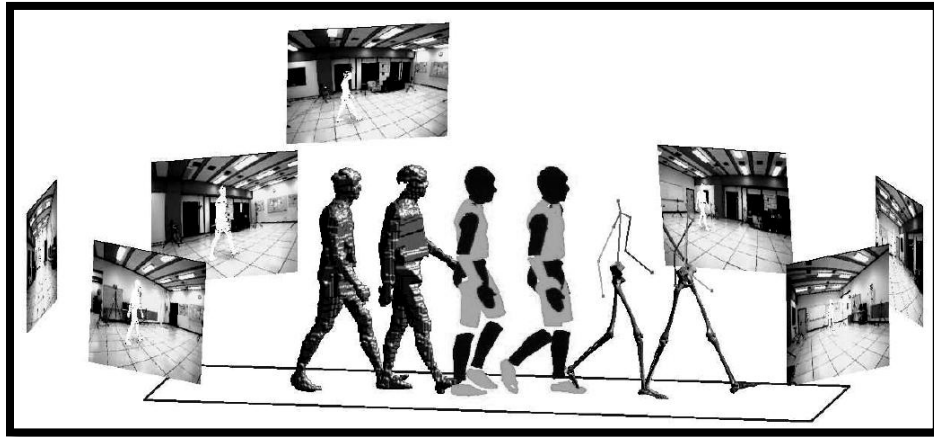
Figure 8: Markerless optical Mocap
Source: Corazza *et al.* (2006)

Opto-electric systems are less popular for full-body 3D motion tracing because of the difficulties experienced in distinguishing between markers.

e. Inertial

As stated earlier, the last few decades have spawned affordable micro-machined sensors which have lead to the feasibility of portable inertial sensors. According to Frey *et al*. (1996), this technique of tracking, "*has the potential to become the primary means of body tracking within the next few years*". Inertial motion capture sensor units generally use the integral of angular velocity, measured by tri-axial gyroscopes, to give the angular orientation of a tracked segment (Roetenberg, 2006). However, gyroscopes suffer from drift and therefore require continuous correction compensation. Tri-axial accelerometers can accurately sense inclination with respect to the Earth's gravitational force when accelerations are negligibly low, but this ability diminishes as accelerations become higher.

Accelerometers are also unable to sense rotations around the vertical axis and can therefore not be used alone to sense segment orientation (Luinge and Veltink, 2005). The solution is to fuse the useful attributes of these components using sensor fusion techniques such as a Kalman filter. In most cases accelerometer data is used to correct gyroscope drift. This is illustrated in Figure 9 (Luinge, 2002).

- 15 -
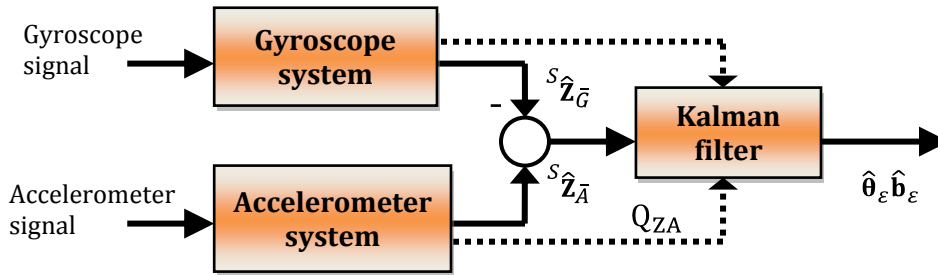
Figure 9: Structure of Kalman filter estimation.
Both the accelerometer and the gyroscope system are used to make an estimate of the global vertical unit vector (Z). The difference between the two estimates is written as a function of orientation error (θ_ε) and offset error (b_ε). A Kalman filter estimates θ_ε and b_ε using this function, together with the error covariances of the orientation (Q_θ), offset (Q_b) and inclination estimation (Q_{ZG} and Q_{ZA}). These estimated errors are used to correct the estimated orientation

Source: Luinge (2002)

Anatomical constraints can also be used to link different segments and enhance orientation estimates (Roetenberg *et al.*, 2007a). Position in the GCS (relative to an initial reference position) can also be calculated through double integration of acceleration values. Drift compensation can then be done by fusing accelerometer and magnetometer values to correct position and heading calculations with reference to the measured magnetic field of the Earth (Roetenberg, 2006). Figure 10a shows an Xsens inertial sensor which contains tri-axial accelerometers, tri-axial gyroscopes and tri-axial magnetometers. The Philips IMC sensor in Figure 10b, using the same technology as the one in Figure 10a, is fully untethered making these even less obtrusive.
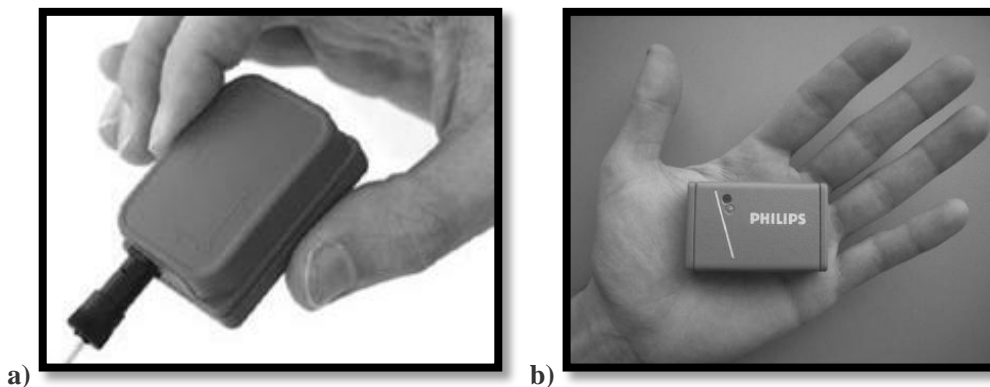
Figure 10: Inertial motion sensors
Source: (a) Xsens Technologies (2007); (b) von Acht *et al.* (2007)

Unlike electromagnetic systems, inertial systems use the Earth's magnetic field for orientation reference. This phenomenon affords IMC systems a definite

- 16 -

measurement-area advantage over other systems. Magnetometers are inherently sensitive to the presence of local magnetic disturbances caused by ferromagnetic metals. Roetenberg *et al.* (2007a) proposed fusion algorithms to compensate for this effect by sensing the local magnetic field and lowering the weighting of magnetometer heading correction whenever significant disturbances are measured.

Inertial sensors are larger than those used in magnetic, acoustic and optical Mocap, however only one sensor is required per tracked segment. Inertial sensors are relatively expensive, but less expensive than optical systems. Inertial tracking has a virtually unbound range and do not suffer from any occlusion or interference problems experienced by other techniques (Bachmann, 2000). IMC is very useful for sensing joint range of motion, but there is currently no method which is able to exactly define the neutral posture which corresponds to the zero-value of joint angles as defined by the ISB (International Society of Biomechanics, Favre *et al.*, 2006). Another major limitation is the fact that inertial tracking is still largely under-researched in certain applications and thus viewed as an adolescent technology. In this context this study proposes to investigate whether results from IMC are both valid and repeatable enough to be used in clinical gait analysis.

f. Hybrid systems

Welch and Foxlin (2002) stated that there is no "s*ilver bullet*" Mocap system capable of satisfying the needs of every application. Hybrid systems employ complementary features of two or more Mocap techniques to overcome their individual limitations (Vlasic *et al.*, 2007). A recent example of such a system combines inertial motion sensors with the TOF feature of acoustic tracking to avoid unbound sensor drift. This system eliminates the need for magnetometers which thus permits unbound motion capture even near ferromagnetic metals such as in treadmills or gymnasium equipment (often used in gait studies) (Vlasic *et al.*, 2007). Bachmann (2000) and Roetenberg (2006) both proposed hybrids of inertial and magnetic Mocap. Roetenberg also found improved tracking results by combining optical and inertial motion tracking.

- 17 -

g. Summary

To summarize, a comparison is drawn in Table 1 between the above-listed Mocap techniques:

Table 1: Summary of motion capture technologies

	Mechanical	Electromagnetic	Acoustic	Optical	Inertial
Accuracy / registration	Very accurate	Good	Good	Very good	Good
Resolution	Very good	Good	Good	Very good	Good
Shadowing	None	None	Sensitive	Very sensitive	None
Interference	Immune	Ferromagnetic materials	Ambient noise	Light sources	Ferromagnetic materials
Range	Unbound	Small	Small (In-lab only)	Small (In-lab only)	Unbound
Drift	None	Low	Low	None	Moderate
Encumbrance	Obtrusive	Comfortable	Comfortable	Comfortable	Comfortable
Sociability	Good	Medium	Medium	Medium	Good
Cost	Low	High	Moderate	Very high	High
Equipment size	Small	Very small	Require lab	Require lab	Very small
Kinematic Model	Limited	Good	Good	Very good	Good
Other	Accurate force measurement	Widely used and proven	Several transmitters required	Requires high computing power	Technology not adequately proven

2.1.3.3. Force plate and electromyography

Additional equipment commonly used for gait analysis includes pressure sensing force plates and electromyography (EMG) measuring systems. Ground reaction forces are used to calculate the moment and forces acting on joints. Force plates are usually imbedded into laboratory floors to avoid test subjects from trying to purposely step on them and thereby alter their gait patterns. Most commercial force plates require specific setup conditions and thus are not very mobile. EMG systems measure the muscle activity during locomotion. This is then used to calculate the amount of energy required to accomplish the analysed movement. The near future may dawn the development of a single self-contained suit which measures motion, ground reaction forces and EMG signals. This is possible because of a wide range of complimentary sensors and software packages currently available. These include in-shoe pressure sensor units, miniature EMG sensors and effective signal amplification and noise reduction software (Simon, 2004).

- 18 -

2.2. Related research

2.2.1. Using motion capture for clinical gait analysis

The utilization of gait analysis in patient care was questioned by Simon (2004) who cited findings by DeLuca, *et al.* (1997) showing that in a test of 91 children with cerebral palsy, experienced clinicians changed their initial opinions in 52% of cases after viewing quantitative gait analysis results. He still found gait analysis to lack popularity.

According to measurements by Salarian *et al.* (2004) gait phases in PD patients deviate significantly from able-bodied gait. They found that patients exhibit 52% slower step velocity, 60% shorter step length, 40% longer gait cycle and 59% longer double-stance than those with able-bodies. Han *et al.* (2006) found difficulty in detecting gait in patients with PD. They also used only able-bodied subjects during data acquisition. Lackovic *et al.* (2000) went further by using simplified gait cycle analyses in distinguishing between able-bodied subjects and those with gait disorders. In other studies such as those by Ebersbach *et al.* (1999) and Stolze *et al.* (2001), attempts were made to use gait patterns to diagnose and/or distinguish between certain movement disorders. Salarian *et al.* (2004) viewed the effect of deterioration of gait patterns with increased progression of Parkinson's disease. Finally, Lee *et al.* (2000) went as far as to use a neural network combined with video analysis to diagnose the presence of movement disorders. They employed only simple spatial parameters and attained accurate diagnoses of between 82.5% and 85% for the patient group. This study is still limited to only distinguishing between able-bodied persons and those with movement abnormalities. Studies such as those by Han *et al.* (2006) and Aminian *et al.* (2001) investigated autonomous gait cycle detection methods but these studies do not give sufficient gait information for detecting more complex gait abnormalities.

2.2.2. Verification of inertial motion capture

From studies conducted in the last decade it is apparent that IMC is continuously evolving. Some researchers made use of gyroscopes alone to determine temporal and spatial parameters (Aminian *et al.*, 2001, Salarian *et al.*, 2004). Salarian *et al.* (2004) used their own peak detection algorithm to identify toe-off and heel-strike gait cycle stages and a double pendulum anatomical model to determine the stride and step lengths. Aminian *et al.* (2001) were only interested in temporal parameters and used footswitches to correlate their results. They tested ten able-bodies subjects and ten subjects with PD. Spatial parameters were normalized to height to test inter subject variation. Han *et al.* (2006) found temporal parameters in PD patients using tri-axial accelerometers. They achieved automated gait disorder detection accuracies in excess of 90%.

- 19 -

Accelerometers and gyroscopes were combined by Dejnabadi *et al.* (2005), Favre (2006) and Luinge and Veltink (2005). Dejnabadi *et al.* (2005) proposed a new method of estimating flexion angles. They created algorithms which eliminated the need for integration in finding absolute joint angles in real time. Their results required no filtering, were free from drift and made no cyclic assumptions. Compared to an ultrasonic reference system (Zebris), their results showed excellent accuracy. However, they only considered 2D sagittal plane knee angles which are the most repeatable and easily measured of the nine lower-body joint angles. They furthered their research by developing an algorithm in which accelerometer inclination measurements were used to compensate for drift (Dejnabadi *et al.*, 2006). As stated in Section 2.1.3.2, accelerometers only sense inclination accurately when accelerations are infinitesimal. For this reason they created a means of compensation correction during the stance phase when accelerations are lowest and interpolation of the compensation function during other gait cycle phases. They also found excellent correlation with the ultrasonic reference system, but again only assessed knee flexion-extension angles. Favre *et al*. (2006) went further by looking at 3D joint angles of the knee. They used an electromagnetic Mocap system as reference (Polhemus Liberty®) and found differences ranging from 1.2° to 12°. Again sagittal plane knee angles showed the least difference. Luinge and Veltink (2005) used a Kalman filter to fuse sensor types and compared their results with those obtained from using gyroscopes alone. As expected, the Kalman filter significantly reduced the drift error found in gyroscope readings. They used an optical Mocap system (Vicon) as baseline and concluded that achieved accuracies were inadequate for applications where heading is important.

Thies *et al.* (2007) investigated linear acceleration measurements from inertial sensors during "reach and grasp" movements of two different manufacturers compared to a Vicon (Oxford Metrics Ltd.) optical Mocap system. They found exceptional correlations between all three systems which prove the repeatability and validity of acceleration measurements. They also confirmed the existence of bias errors due to misalignment of sensors and differences in calibration procedures. In 2000 Bachmann proposed a filter which used magnetometers and accelerometers to determine orientation when movement frequency is low and gyroscopes for higher frequency motion. It was tested for 2D motion and proved robust and accurate with reference to results obtained using a Vicon system (Bachmann, 2000). Inertial sensors have thus evolved to a point where drift-free tracking is possible using accelerometers gyroscopes and magnetometers. As gait analysis is often conducted near ferromagnetic materials such as in a gymnasium, it was necessary to come up with solutions for subsequent drift errors. Roetenberg *et al.* (2007a) proposed a filter which lowered such errors from 50° to 3.6°. They achieved this by lowering the compensation weighting from magnetometers whenever the measured local magnetic disturbances became significant. However this approach only remains valid for short periods. Long term magnetic disturbances, such as those present when driving in a

car, requires another solution. Vlasic *et al.* (2007) eliminated the need for magnetometers by using ultrasonic sensors. These sensors use the measured absolute distance between sensors to reduce orientation drift. This method showed great promise but is still relatively untested.

2.2.3. Repeatability in gait patterns

Repeatability is one of the most important attributes of gait analysis equipment. In the case of rehabilitation monitoring or intervention evaluation, a physician often looks at relative gait parameter ranges as opposed to absolute angles, times or distances. Here it is of paramount importance that an identical parameter, measured using an identical test procedure, reflects the actual changes in that parameter without a significant equipment measurement variability error. Several studies have looked at the repeatability of gait patterns measure using an OMC system: (Yavuzer *et al.*, 2006, Besier *et al.*, 2003, Mackey *et al.*, 2005, Kadaba *et al.*, 1989).

Mills *et al*. (2007) tested the within- and between-day repeatability and the inter- and intra-tester repeatability of ten able-bodied adults using an electromagnetic Mocap (EMC) system. Most of the above-mentioned studies used the approach presented by Kadaba *et al*. (1989) to quantify temporal-spatial and joint angle repeatability. Mackey *et al.* (2005) investigated the difference in gait repeatability between ten able-bodied children and ten children with cerebral palsy. He used an optical Mocap system and found acceptable and comparable and repeatability. In Section 4, repeatability values obtained using the IMC system are compared to results obtained by Kadaba *et al*. (1989) and Mills *et al*. (2005).

3. VALIDITY STUDY

According to Favre, *et al.* (2006), no existing Mocap system produces sensor or marker orientation measurements which exactly reflect the underlying bone orientation. It is however important that the results from the chosen system adequately exceeds the measuring error (Yavuzer *et al.*, 2006). This concept is evaluated in this section by comparing of results obtained by the IMC system gait recording with those measured using a trusted OMC system.

3.1. Test participation

3.1.1. Inclusion criteria

Routine gait assessments were conducted on 14 able-bodied male subjects. Test subjects were chosen under the condition that they do not suffer from any neurological pathology and/or have not experienced any injury which may affect gait function. Subjects were male and aged between 20 and 27 years. All the subjects were fairly fit. This reduced the prevalence of sensor movement which was the main concern when concurrently comparing the two systems.

3.1.2. Ethical approval / Protocol

Test subjects were used as controls in a separate study by Dr. Regan Arendse of the faculty of Health Sciences at the University of Stellenbosch. Ethical approval was obtained for this study. All subjects gave informed consent before being tested.

3.2. Apparatus

3.2.1. Vicon – Optical motion capture system

The Vicon OMC system (Oxford Metrics Ltd.) has been used for clinical gait analysis for many years. It uses high-resolution, high-speed CMOS VICON cameras specially designed for motion tracking. These cameras boast a resolution of up to 1280×1024 pixels and sampling rates of between 200 and 1000 Hz. Reflective markers are placed on the objects (segments) to be tracked. Vicon Tracker software automatically calculates the centres of each marker and reconstructs their position in the GCS. Markers are combined to model the 3D spatial orientation and position of body segments. This is usually accomplished in less than 7 ms. (Zhou and Hu, 2004)

In this study eight Vicon cameras were set up and calibrated within a 6×11 m laboratory space. Reflective markers, of diameter 10 mm were used.

3.2.2. Moven – Inertial motion capture system

3.2.2.1. Description

The Moven system (Xsens Technologies) is a full-body inertial motion capture suit that utilizes 16 tracking sensors, each comprising of tri-axial gyroscopes, tri-axial accelerometers, tri-axial magnetometers as well as a temperature sensor. Sensors, wireless data transmitters and cables are enclosed within a Lycra suit that weighs 1.9 kg in total. Sensors are located as is shown in Figure 11. Movement data is sampled at up to 120 Hz and is sent via wireless communication to a computer. Data include sensor orientation and position in the GCS as well as absolute sensor velocity, acceleration, angular velocity and angular acceleration. The Moven Studio software uses this data to construct a 23 segment body model in quasi-real time. Model segment dimensions are calculated using either user defined measurements or uses entered subject height and foot size to estimate anthropometric dimensions. The software allows for the estimation of foot clearance during walking which is not possible with orientation only driven Mocap systems. Sections 3.2.2.2 and 3.2.2.3. give a more detailed account of the operation principles of the Moven system (Roetenberg *et al.*, 2007c)
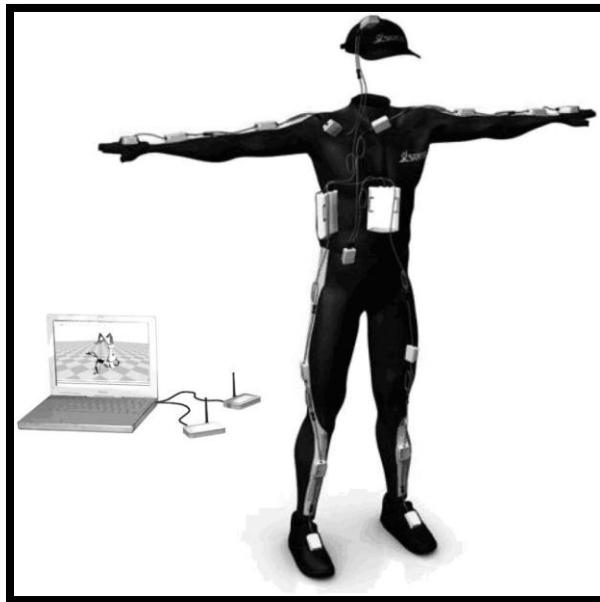
Figure 11: Moven motion capture system
Source: (Xsens Technologies, 2007)

After an initial pilot study, it was postulated that greater repeatability could be achieved if the sensors are removed from the Lycra suit and adhered directly onto the skin of the subject. For this purpose double-sided adhesive tape was used along with covering elastic straps which secured the sensors in place (refer to Figure 13b).

- 23 -

3.2.2.2. Position and orientation calculation

The following two sections offer a short description of the working principals of the Moven (Xsens Technologies) full-body IMC system. For a more in-depth explanation refer to Roetenberg *et al.* (2007a), Roetenberg (2006) and Roetenberg *et al.* (2007c).

a. Sensor orientation

Angular velocity $\boldsymbol{\omega}$ of the IMC sensor, measured using tri-axial gyroscopes, is integrated over time to give the change in angle from an initially known angle. This is done using Equation (1):

$$
{}^{GS}\dot{\boldsymbol{q}}_t = \frac{1}{2}{}^{GS}\boldsymbol{q}_t \otimes \Omega_t \tag{1}
$$

where ${}^{GS}\boldsymbol{q}_t$ is the quaternion describing the rotation of the sensor in the GCS at time t and $\Omega_t = (0, \omega_x, \omega_y, \omega_z)^T$ is the quaternion which represents $\boldsymbol{\omega}_t$. (Roetenberg *et al.*, 2007c)

b. Definition of Moven Studio v2.1 body model segment axes
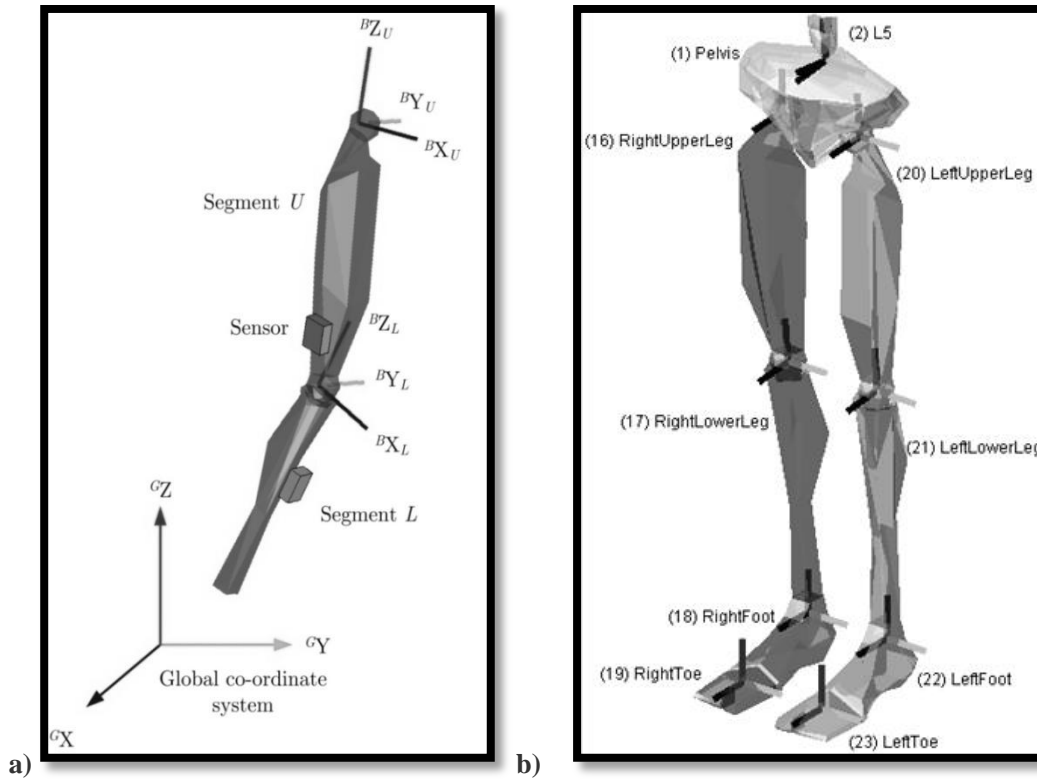
Figure 12: Body segment coordinate system in global coordinate system
Source: (Roetenberg *et al.*, 2007c)

- 24 -

As shown in Figure 12, Moven Studio software defines the x-axis in the anterior-posterior direction (anterior as positive), the y-axis in the medial-lateral direction (left as positive) and the z-axis as vertically (up as positive). This is similar to the joint coordinate system (described in Section 3.4.1) except that the x- and y-axes are switched.

c. Sensor position

The position of the IMC sensor in the GCS (with reference to a calibrated starting point) is calculated with the help of recordings from both linear accelerometers and the gyroscopes used in orientation calculation. After removing the gravitational component from acceleration signals using Equation (2) the sensor position in the GCS is calculated by Equation (3).

$$ {}^{G}\mathbf{a}_t - {}^{\mathbf{G}}\mathbf{g} = {}^{GS}\boldsymbol{q}_t \otimes ({}^{S}\boldsymbol{a}_t - {}^{S}\mathbf{g}) \otimes {}^{GS}\boldsymbol{q}_t^* \tag{2} $$

$$ {}^{G}\ddot{\mathbf{p}}_t = {}^{G}\boldsymbol{a}_t \tag{3} $$

where ${}^{G}\mathbf{a}_t$ and ${}^{G}\mathbf{g}$ are the linear acceleration and gravity vectors in the GCS respectively and $\mathbf{p}_t$ is the position vector. (Roetenberg *et al.*, 2007c)

d. Segment orientation and position

The body model, of which the lower body is depicted in Figure 12b, is comprised of 23 segments each considered as rigid bodies linked by joints. The sensors are assumed to be rigidly attached to these segments.

The orientation of each segment is therefore assumed to be that of the corresponding sensor with the exception of the spine, torso and toes which use a biomechanical model to determine their orientation. Moven Studio defines contact points between the body and the *xy*-plane of the GCS. These are used to determine the toe segment orientations

Finding the position of each segment requires a bit more work. Because of sensor drift it is necessary to limit the freedom of movement of each sensor relative to their original calibration position. To accomplish this, segments are assumed to be joined in a kinematic chain with the pelvis defined as the primary reference position. The joint centres between proximal and distal segments now form the new reference position for the distal segment. This joint centre position is calculated from the proximal segment reference position, the segment (sensor) orientation and the segment length (user-defined or anthropometrically calculated). This is achieved by using Equation (4) below.

- 25 -

$$^{G}\mathbf{p}_{U1} = \ ^{G}\mathbf{p}_{U0} + \ ^{GB}\mathbf{q}_U \otimes \ ^{B}\mathbf{s}_U \otimes \ ^{GB}\mathbf{q}_U^* \qquad (4)$$

where $^{G}\mathbf{p}_{U1}$ and $^{G}\mathbf{p}_{U0}$ are the reference positions of the distal and proximal segments at time $t = 0$. Here the orientation $^{GB}\mathbf{q}_U$ and length $\mathbf{s}_U$ of the proximal segment U are known.

Because the segments considered are not in fact rigid bodies as is assumed by the body model, statistical constraints are applied to avoid unlikely joint motions (e.g. large varus-valgus of the knee). Each joint is constrained using its own characteristic properties. (Roetenberg *et al.*, 2007c)

3.2.2.3. Drift and magnetic interference compensation

The Moven IMC system uses complimentary sensor components and a Kalman filter approach to correct propagating errors caused by sensor drift and/or magnetic field interference. Using a Kalman filter update, joint position uncertainties are reduced by correcting the drift. The sensor-noise, as well as statistical information about the joint constraints is used to determine the Kalman gain. (Roetenberg *et al.*, 2007c)

The segment orientation error is corrected by entering information about the heading and gravitational vector components from magnetometers and accelerometers into a Kalman filter. This is similar to the one illustrated in Figure 9 (refer to Section 2.1.3.2) which uses accelerometer measurements to correct orientation values.

According to Roetenberg *et al.* (2007c), local magnetic interferences from metallic objects easily disturb the Earth's magnetic field which in turn causes inaccurate magnetometer readings. A compensation algorithm is therefore employed to reduce these errors. This algorithm uses measurements of local magnetic disturbances to reduce the weighting of the magnetometer component of the drift compensation filter. This naturally increases the uncertainty of segment orientation calculations, but according to a study by Roetenberg *et al.* (2007a), this method practically eliminated the error caused by short term magnetic interferences.

3.3. Data acquisition and processing

3.3.1. Test protocol

Validity tests were conducted in a Mocap laboratory at the University of Cape Town, in their Department of Sport Science. The following section discusses the procedure followed during each gait assessment.

3.3.1.1. Sensor and marker application

Moven sensors were worn in a Lycra suit (Figure 13a) by 8 of the 14 test subjects. For the remaining six subjects, sensors were applied using double-sided adhesive tape

and secured using elastic straps (Figure 13b) as proposed by Dejnabadi *et al.* (2005). Markers were positioned according to manufacturer specifications (Xsens Technologies, 2008) as shown on Figure 13b. To ensure inter-tester repeatability, sensors placement was done by the same researcher for each test.

a)   b)
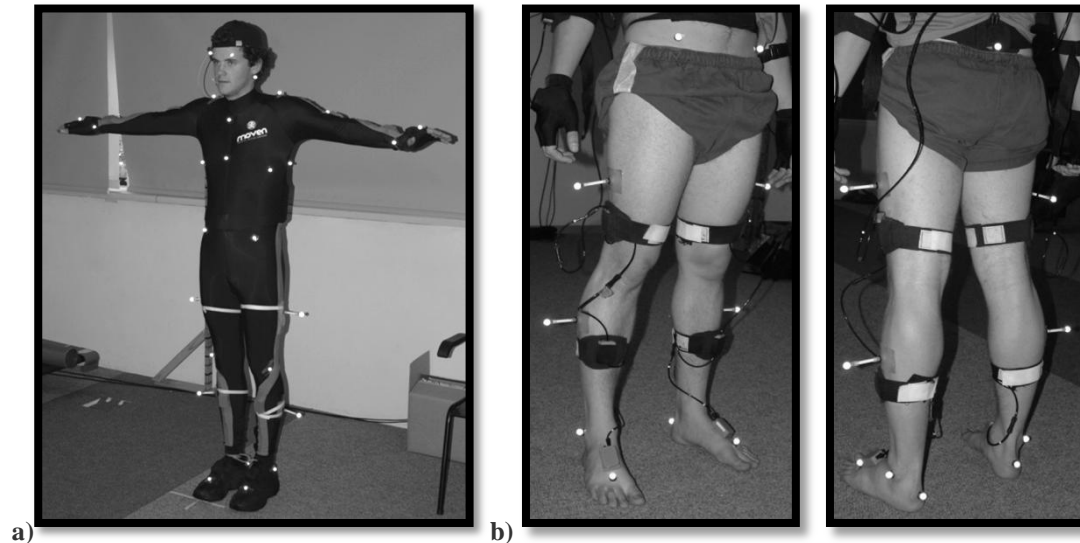
Figure 13: Marker and sensor placement
Using: a) Lycra suit, b) Elastic straps

When straps were used, the IMC wireless receivers were fastened in a harness over the shoulders. Special care was taken to avoid the receivers from interfering with the pelvic sensor located on the sacrum.

Vicon markers were positioned according to the Helen Hayes marker set (Richards, 2008). Appropriate placement of upper and lower leg wands minimized their interference with the Moven sensors or cables. In this study only lower limb markers were considered.

3.3.1.2. Calibration
Figure 14 illustrates the static and dynamic calibration of the OMC laboratory performed on each new test day (as described by Richards, 2008) as well as the subject specific calibration shown in Figure 14b.

- 27 -
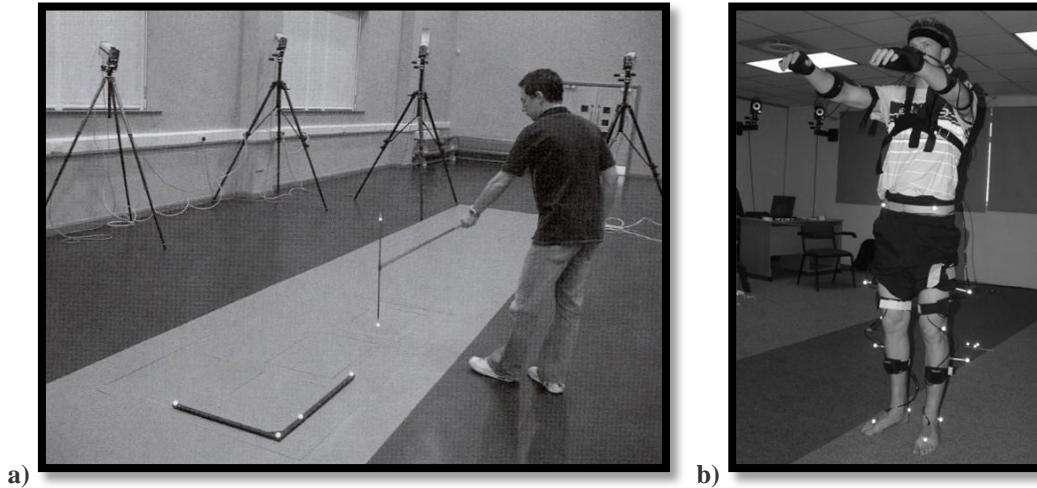
Figure 14: OMC calibration procedures
Source: a) Richards (2008)

Calibration of the IMC involved two five-second poses as represented in Figure 15. These calibration poses define the zero positions from which changes in segment orientation and position are calculated. Moven Studio software calibrates to an initial 10° anterior pelvic tilt. This detail is important when analysing the absolute hip and pelvic motion.
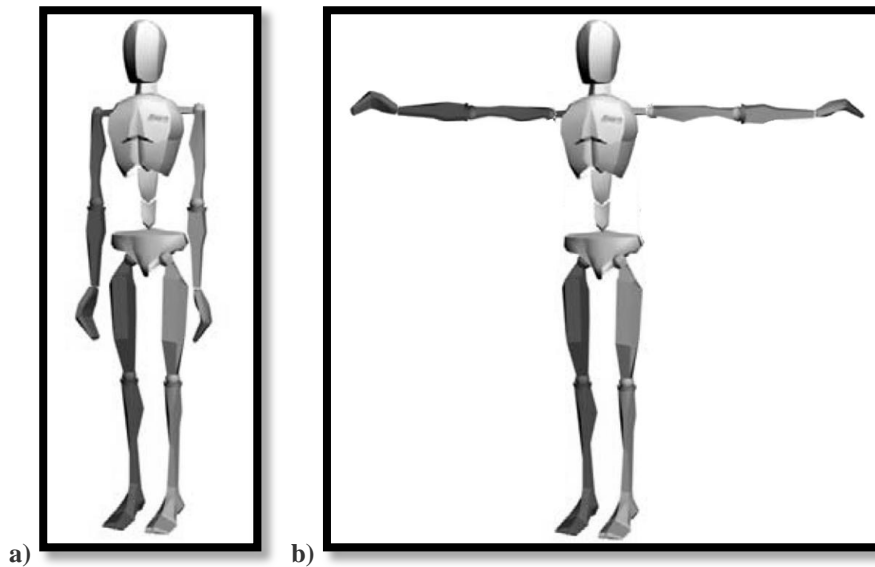
Figure 15: IMC calibration procedures
a) T pose, b) Neutral pose
Source: Xsens Technologies (2008)

3.3.1.3. Procedure

Each gait assessment included the following steps:
1. Static calibration of the OMC system (Vicon)
2. Dynamic calibration of the OMC system
3. IMC (Moven) sensors applied to the subject (refer to 3.3.1.1)
4. Wires secured to avoid interference with OMC markers
5. OMC markers applied
6. Subject calibration of the OMC system
7. Subject calibration of the IMC system
8. Two unrecorded runs at a self-selected speed
9. Two runs recorded at a fast walking speed
10. Two runs recorded at a slow walking speed
11. Two runs recorded at a normal walking speed
12. Sensors and markers removed

Steps 3 to 12 were repeated for all test subjects tested on a single test day.

3.3.2. File format

IMC data was recorded in a proprietary *.MVN file format and converted to *.MVNx file format which contains position and orientation data in ASCII format.

All kinematic data in the *.MVNx file is expressed in the global coordinates system with the positive Z-axis defined as vertically up. The file contains calibration, anthropometric scaling and recording setting information followed by a data matrix which contains the orientation and position data of each segment for each sample frame. This is illustrated on the abstract below taken from the Moven user manual:

Sample 1   <F v=" $^{GB}q_{seg1}$ $^{G}pos_{seg1}$ $^{GB}q_{seg2}$ $^{G}pos_{seg2}$ ... $^{GB}q_{seg23}$ $^{G}pos_{seg23}$ " />
Sample 2   <F v=" $^{GB}q_{seg1}$ $^{G}pos_{seg1}$ $^{GB}q_{seg2}$ $^{G}pos_{seg2}$ ... $^{GB}q_{seg23}$ $^{G}pos_{seg23}$ " />
...
Sample n   <F v=" $^{GB}q_{seg1}$ $^{G}pos_{seg1}$ $^{GB}q_{seg2}$ $^{G}pos_{seg2}$ ... $^{GB}q_{seg23}$ $^{G}pos_{seg23}$ " />

Here $^{GB}q_{seg}$ is the quaternion vector (q_0, q_1, q_2, q_3) describing the rotation of the segment in the global frame and $^{G}pos_{seg}$ is the position vector (x,y,z) of the segment from the origin in the global frame (Xsens Technologies, 2008).

OMC data was recorded in the more widely used *.C3D format. Gait data was calculated within the Vicon software and exported in *.TXT format.

- 29 -

3.4. Data analysis

3.4.1. Gait data representation

Kinematic data may be evaluated with the help of a variety of parameters. These include primary parameters such as segment orientation, position and linear and angular velocities and accelerations, which may be used to extract secondary parameters such as temporal and spatial gait parameters as well as kinematic joint angle.

For evaluating IMC performance in a gait analysis environment, the following temporal and spatial parameters were considered: Step length (SL), stride length (STL), velocity and cadence. Appendix A contains a description of these and other temporal-spatial gait parameters.

Joint angles are typically described by Euler orientation angles, namely the roll (φ), elevation (θ) and azimuth (ψ) about the x, y and z axes in the GCS respectively (Bachmann, 2000, Frey *et al.*, 1996). Angle calculations may be done using trigonometric manipulations of these angles, however, a singularity or "gimbal lock" may occur because of trigonometric discontinuities. For this reason, angle calculations are often made using quaternion mathematics. Quaternions are an extension of complex numbers which create a fourth dimension, effectively eliminating the singularity. Quaternions describe a four dimensional space by means of one real component r and three imaginary components x, y and z as presented by $\boldsymbol{q}$ $= r + x\boldsymbol{i} + y\boldsymbol{j} + z\boldsymbol{k}$ or as shown in Equation (5) below (Miller *et al.*, 2004).

$$\boldsymbol{q} = \begin{bmatrix} r \\ x \\ y \\ z \end{bmatrix} = \begin{bmatrix} q_0 \\ q_1 \\ q_2 \\ q_3 \end{bmatrix} \tag{5}$$

In this study lower body kinematic joint angles in the BCS $\left({}^{B}\boldsymbol{q}_{UL} \right)$ were found by calculating the joint orientation of the distal L segment with respect to the proximal segment U in the GCS (refer to Figure 12a). This is achieved by means of a quaternion multiplication $\otimes$ of the complex conjugate of the proximal segment quaternion, ${}^{GB}\boldsymbol{q}_{U}^{*}$, and the distal segment quaternion, ${}^{GB}\boldsymbol{q}_{L}$. (See Equation (6)) (Roetenberg *et al.*, 2007c)

$$ {}^{B}\boldsymbol{q}_{UL} = {}^{GB}\boldsymbol{q}_{U}^{*} \otimes {}^{GB}\boldsymbol{q}_{L} \tag{6}$$

When compared to Euler angles, quaternions are difficult to visualize. For this reason the joint angle quaternions were converted back to Euler angles. This was achieved with the help of Cardan sequences. Cardan sequences are series of three orthogonal rotations around the three major axes in a strictly specific order. The most popular of

- 30 -

these sequences is the Joint Coordinate System (JCS) proposed by Grood and Suntay (1983) and used in the majority of gait research publications. If the axes are chosen as: x – medial-lateral, y – anterior and z – up, then the JCS is defined as the sequence xyz. Richards (2008) reported significant errors occurring when these sequences are interchanged. It was therefore important to ensure that the same Cardan sequence was used in IMC calculations as was employed by the OMC software.

The joint angles of the IMC system were therefore calculated using the JCS (employed by the OMC software) with the aid of Equation (7) below as proposed by Diebel (2006). These angles, representing rotations in the sagittal, frontal and transverse planes, are used by most physicians or researchers to describe the gait of a subject.

$$
\begin{bmatrix} \varphi \\ \theta \\ \psi \end{bmatrix} = \begin{bmatrix} \text{atan2}(2q_2q_3 + 2q_0q_1, q_3^2 - q_2^2 - q_1^2 + q_0^2) \\ -\text{asin}\,(2q_1q_3 - 2q_0q_2) \\ \text{atan2}(2q_1q_2 + 2q_0q_3, q_1^2 + q_0^2 - q_2^2 - q_3^2) \end{bmatrix}
\tag{7}
$$

Here atan2 and asin are MATLAB (Mathworks, Natick, MA) commands for the four quadrant inverse tangent and the inverse sine respectively.

Because of the difference in x- and y-axis definition between the JCS and that of the IMC software, φ and ψ are then simply interchanged. The following joint angles (Table 2) were calculated and used for both the validity and repeatability studies as well as in training and testing a diagnostic neural network presented in Section 5. Note the symbols in the first column as these are used in the result tables in later sections:

Table 2: Joint angles evaluated

Symbol	Description	Proximal segment	Distal segment
φ_h θ_h ψ_h	Hip abduction-adduction Hip flexion-extension Hip internal-external rotation	Pelvis (Sacral sensor)	Femur (upper leg sensor)
φ_k θ_k ψ_k	Knee varus-valgus Knee flexion-extension Knee internal-external rotation	Femur (upper leg sensor)	Tibia (lower leg sensor)
φ_a θ_a ψ_a	Ankle eversion-inversion Ankle plantar-dorsiflexion Ankle supination-pronation	Tibia (lower leg sensor)	Calcaneus and Metatarsal (foot sensor)

φ, θ and ψ in Table 2 represent Euler angles in the frontal, sagittal and transverse planes, respectively.

Appendix A contains a more complete list of parameters commonly measured during a gait study along with anatomical illustrations of joint angles[2]. Figure 16 chronologically depicts how the temporal-spatial and joint angle gait parameters were calculated. Appendix C explains the function and structure of the MATLAB subfunctions (e.g. `gaitpar.m`) referred to in the figure.
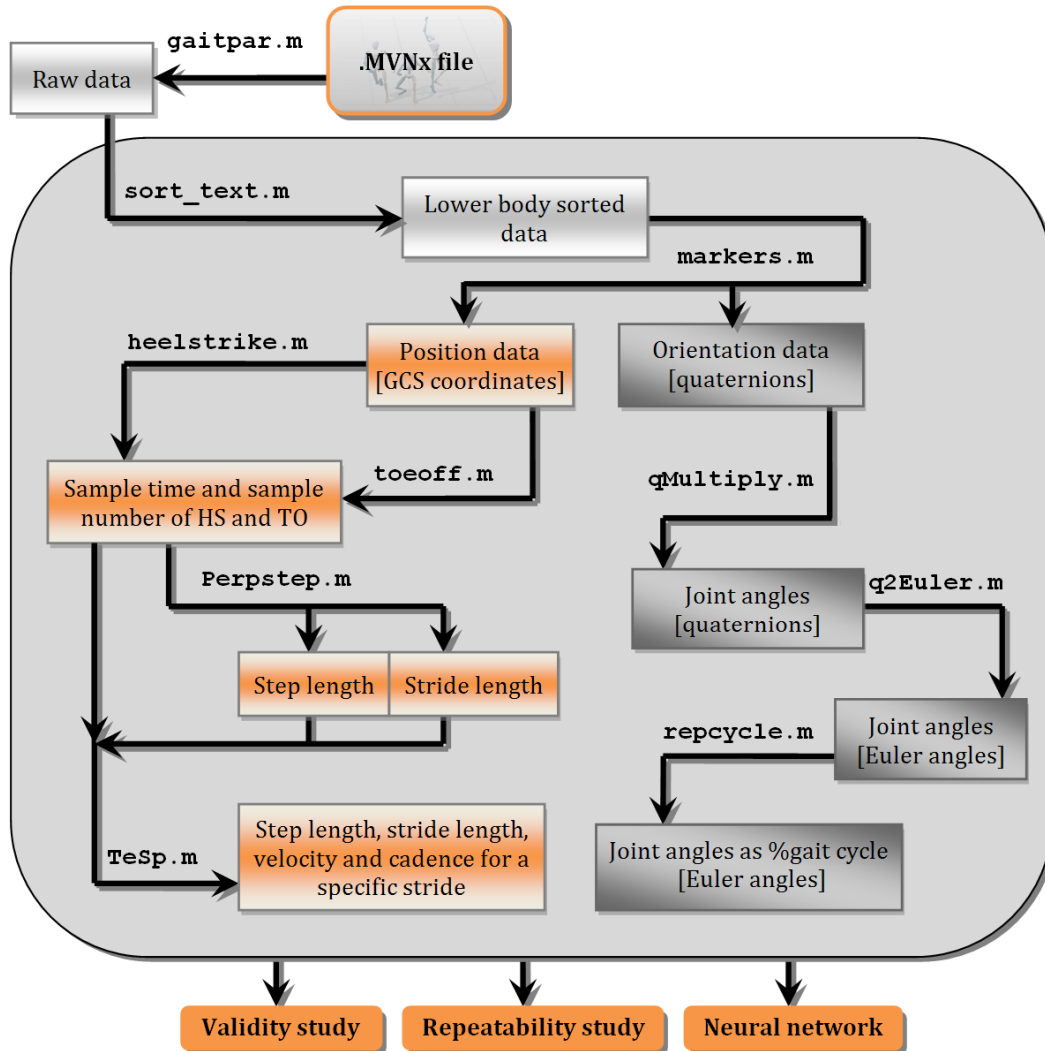
Figure 16: Schematic of gait parameter calculation script

3.4.2. Graphical user interface

To simplify IMC data processing a graphical user interface (GUI) was created within MATLAB. The GUI allowed researchers to view a variety of gait parameter of a recorded *.MVNx file. These include any of the joint angles of the hip, knee or ankle,

---

[2] Gait analysis may be applied to the entire body, but this study focussed on the lower body only.

medial-lateral and anterior-posterior pelvic tilt and average values of velocity, cadence step length and stride length. The layout and operation of the GUI are explained below.

Figure 17 shows the main graphical user interface created to simplify data handling and to visually verify calculated gait patterns.
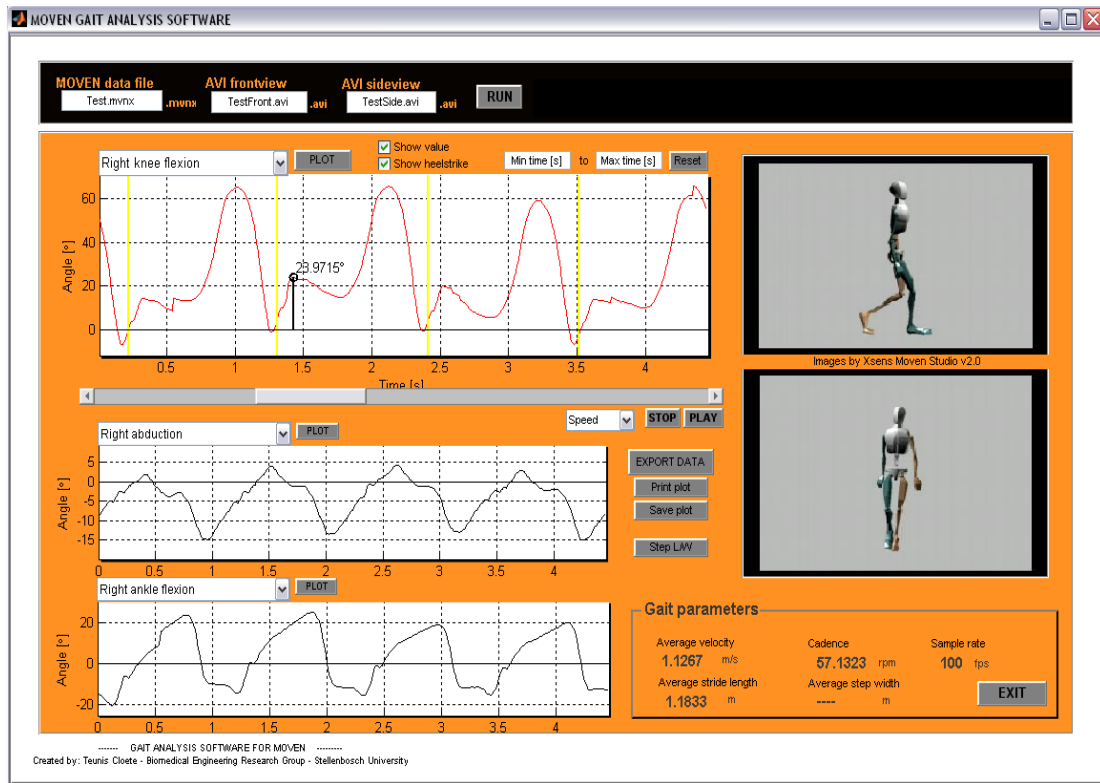
Figure 17: Graphical user interface

The user may start by entering the filename of a recorded *.MVNx file in an edit box at the top of the GUI window and clicking on the "RUN" button. Calculations, as described in Appendix C, are done from the raw data. When these calculations are complete, a "RUN COMPLETE!!" message will display in the status bar to the right of the "RUN" button. At the same time the sagittal plane angles of the right knee, hip and ankle will be plotted. Tick-boxes above the main plot window allow the user to plot the heel-strike incidence (yellow vertical lines above) and the value of the specific angle at a selected slider position.

The number of strides displayed may be selected by setting the time limits in the edit boxes at the top right of the main plot window. Drop-down bars above each of the three plot windows allow the user to view any of the nine major joint angles as well as the anterior-posterior or medial-lateral pelvic tilt. Front and/or side view video

- 33 -

files (in .AVI format) may be created using Moven Studio. After being uncompressed using alternative software, they may be copied to the active directory and their filenames entered with the corresponding *.MVNx file. This allows for a frame-by-frame analysis of gait patterns.

The window at the bottom right of the GUI displays the sampling frequency along with average values of step and stride length as well as the velocity and cadence for the run. It is important that the *.MVNx file only contains walking data (no jumping, squatting, etc) if these values are to be valid. The "EXPORT DATA" button may be used to export all the calculated kinematic and temporal-spatial gait data to a Microsoft EXCEL file with the same name as the evaluated *.MVNx file. The "PRINT" button creates a new figure which displays the parameter which is plotted on the main plot window along with the heel-strike instances (if the user ticks the "SHOW HEELSTRIKE" tick-box). A printer selection window is opened from which the figure may be printed. The "SAVE" button also creates a new figure and saves it in the form of a .JPG file in the current directory. The filename of the *.JPG file is a combination of the *.MVNx filename and the selected gait parameter.

3.4.3.   Synchronizing IMC and OMC data

In order to accurately compare IMC and OMC gait parameters, it was important to synchronise the data acquired from these systems. This was achieved during post processing by using a basic least squares fit of the OMC data onto the IMC data. A single OMC recorded stride was isolated by identifying consecutive heel-strike instances. Here heel-strike was defined as the local minima of the z-axis displacement of the foot. This is illustrated in Figure 18.

Because sagittal plane angle comparison of the knee showed the greatest inter-system correlation, this parameter was used to pinpoint matching stride start-times. The OMC stride data was superimposed onto the IMC data and the sum of the least squares was calculated over all the time samples. The OMC stride was incrementally shifted across the timeline of the IMC data until a minimum summed difference was found. A visual confirmation was done in each case to ensure that corresponding strides were compared. All the remaining joint angles were then compared for the determined starting timeframe.

- 34 -
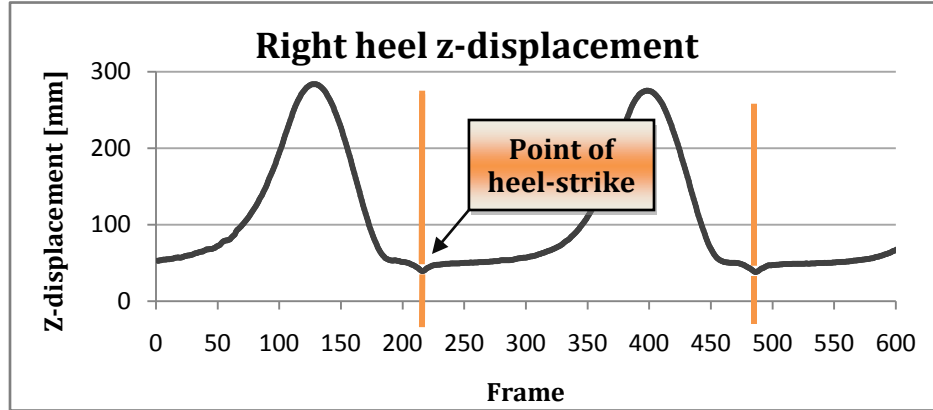
Figure 18: Heel-strike identification

Bias errors are common in gait analysis measurement because of differences in marker placement with reference to the BCS (Besier *et al.*, 2003), irrespective of the Mocap system used. This bias error was removed by applying another least squares fit along the y-axis (joint angle magnitude) of the parameter curves. The relative differences in angle waveforms could then be compared. Difference calculations were done with and without the y-axis bias error correction and both cases reported in Section 3.5.

3.4.4. Statistical approach

Two statistical quantifiers were used to describe the correlation between the IMC and OMC collected data. Namely, the Root Mean Square difference (E_{RMS}) and the Correlation Coefficient (R):

3.4.4.1. Root mean square (RMS) difference

The first method used to compare data is the *RMS* value which is calculated by taking the square root of the mean squared difference between the data sets at each timeframe (Equation 8).

$$E_{RMS} = \sqrt{\frac{1}{T} \sum_{t=1}^{T} (x_t - y_t)^2} = \sqrt{\frac{(x_1 - y_1)^2 + (x_2 - y_2)^2 + ... + (x_t - y_t)^2}{T}} \tag{8}$$

where x_t and y_t are the joint angle values (in degrees) of the IMC and OMC at time frame t, respectively.

3.4.4.2. Coefficient of correlation

Weisstein (2008), proposed the use of a correlation coefficient (also called the cross-correlation coefficient), R, in comparing the correlation between two datasets. This coefficient is a quantity which describes the quality of a least-squares fitting to the original data and is given by (9).

- 35 -

$$R = \frac{n\sum xy - (\sum x)(\sum y)}{\sqrt{n(\sum x^2) - (\sum x)^2}\sqrt{n(\sum y^2) - (\sum y)^2}} \qquad (9)$$

If R approaches 1, the correlation between the data sets is strong whereas for dissimilar data sets, R approaches 0. This coefficient is also unaffected by the bias error commonly found in joint angle measurements.

3.5. Results

3.5.1. Temporal-spatial comparison

Average temporal and spatial parameters measured during the validity study are given in Table 3 below.

Table 3: Temporal-spatial results - Normal walk

	Avg. results (straps)		Difference	Avg. results (suit)		Difference
	IMC	OMC		IMC	OMC	
	Mean ± SD	Mean ± SD	E_{RMS} #	Mean ± SD	Mean ± SD	E_{RMS} #
Stride length#	1.38 ± 0.12	1.41 ± 0.13	0.045	1.50 ± 0.14	1.49 ± 0.13	0.046
Step length	0.685 ± 0.06	0.713 ± 0.07	0.051	0.759 ± 0.08	0.751 ± 0.07	0.067
Velocity	1.281 ± 0.17	1.297 ± 0.18	0.037	1.329 ± 0.14	1.315 ± 0.12	0.060
Cadence	111.9 ± 7.5	109.1 ± 10.1	5.749	105.1 ± 5.15	105.0 ± 4.00	5.670

Units for gait parameters are as follows: Stride length [m], step length [m], velocity [m/s] and cadence [steps/min]

Values of step and stride length calculated using IMC data vary slightly from those calculated by the OMC software. The average differences between the compared step lengths are 67 mm (8.9%) and 51 mm (7.3%) when using the suit and straps, respectively. Values calculated for stride length are found to be more accurate with an average difference of 46 mm when using the suit. Cadence values vary in the order of 5.7 steps per minute (5.3%). The best results were obtained for velocity using the straps, with an average difference of 0.037 m/s (2.9%).

3.5.2. Joint angle comparison

Table 4 and Table 5 below show the RMS difference and correlation coefficient obtained when comparing joint angle waveforms at a self-selected (normal) walking speed.

- 36 -

Table 4: Joint angle validity results - Normal walk (Straps)

	E_{RMS} [°] (Mean ± SD)		E_{RMS} (bias corrected) [°] (Mean ± SD)		R (Mean ± SD)	
	Right	Left	Right	Left	Right	Left
φ_h	3.27 ± 1.71	3.12 ± 0.65	2.05 ± 0.47	2.29 ± 0.27	**0.91 ± 0.08[#]**	**0.86 ± 0.06**
θ_h	17.82 ± 7.23	17.26 ± 5.69	3.84 ± 1.73	3.46 ± 1.01	**0.97 ± 0.03**	**0.98 ± 0.02**
ψ_h	9.68 ± 4.70	10.65 ± 3.83	4.51 ± 2.51	5.55 ± 1.89	**0.50 ± 0.24**	0.44 ± 0.27
φ_k	8.86 ± 1.01	8.09 ± 0.89	5.56 ± 2.62	6.69 ± 0.75	0.49 ± 0.28	0.39 ± 0.29
θ_k	7.76 ± 4.51	7.90 ± 3.29	3.41 ± 0.86	3.04 ± 0.83	**0.99 ± 0.00**	**0.99 ± 0.01**
ψ_k	10.48 ± 5.16	15.61 ± 7.93	3.95 ± 0.96	4.40 ± 1.27	**0.78 ± 0.15**	**0.57 ± 0.29**
φ_a	6.12 ± 2.31	8.66 ± 3.17	5.35 ± 1.04	7.50 ± 1.94	0.28 ± 0.16	0.23 ± 0.18
θ_a	25.57 ± 5.07	22.57 ± 2.23	21.42 ± 2.78	20.65 ± 2.23	0.25 ± 0.11	0.28 ± 0.07
ψ_a	6.64 ± 2.13	15.33 ± 7.09	4.86 ± 2.42	6.80 ± 1.32	0.41 ± 0.30	0.13 ± 0.13

Values in bold and colour are those with correlation coefficient > 0.5

Table 5: Joint angle validity results - Normal walk (Suit)

	E_{RMS} [°] (Mean ± SD)		E_{RMS} (bias corrected) [°] (Mean ± SD)		R (Mean ± SD)	
	Right	Left	Right	Left	Right	Left
φ_h	5.83 ± 2.48	5.28 ± 4.30	4.86 ± 1.96	2.11 ± 0.39	**0.83 ± 0.12[#]**	**0.84 ± 0.04**
θ_h	13.62 ± 6.71	11.78 ± 4.74	2.80 ± 0.98	3.40 ± 1.07	**0.99 ± 0.00**	**0.99 ± 0.01**
ψ_h	10.42 ± 4.54	14.43 ± 11.58	5.61 ± 0.72	6.26 ± 2.74	**0.56 ± 0.21**	0.42 ± 0.27
φ_k	7.48 ± 5.82	8.94 ± 3.49	5.02 ± 3.23	7.25 ± 2.80	**0.59 ± 0.34**	0.49 ± 0.31
θ_k	6.92 ± 3.64	8.99 ± 9.12	3.02 ± 1.07	4.83 ± 2.42	**0.99 ± 0.01**	**0.99 ± 0.01**
ψ_k	10.45 ± 4.43	11.94 ± 7.82	5.39 ± 2.84	5.02 ± 1.03	0.36 ± 0.23	**0.58 ± 0.23**
φ_a	6.81 ± 3.23	7.36 ± 4.53	5.84 ± 2.21	6.78 ± 4.41	**0.52 ± 0.22**	0.37 ± 0.26
θ_a	26.55 ± 4.70	27.89 ± 2.32	22.61 ± 2.68	24.89 ± 2.79	0.14 ± 0.11	0.31 ± 0.27
ψ_a	11.21 ± 7.42	14.34 ± 10.89	3.53 ± 0.94	6.79 ± 5.31	0.49 ± 0.33	0.43 ± 0.27

Values in bold and colour are those with correlation coefficient > 0.5

As expected, the sagittal plain angles of the hip and knee, θ_h and θ_k, display high correlation coefficients with average hip flexion-extension correlation slightly higher when using the suit (R = ±0.99). Hip abduction-adduction figures also display acceptable results. Abduction-adduction results in the knee show moderate validity with *R* values between 0.39 and 0.59. During normal walking, ψ_h has *R* values of between 0.42 and 0.56. These however go up to 0.71 for slow walking. The results of slow and fast walking trials are given in Appendix D.

Differences found by comparing results of the ankle joint are far more significant with an *R* value as low as 0.13 during internal-external rotation. An irregularity was found however when using the Lycra suit. Here *R* for ψ_a during slow walking is 0.63 on the right ankle while the left ankle only obtained a value of 0.49. The same

phenomenon was observed during fast walking with right and left values 0.56 and 0.27, respectively.

Table 6 gives a comparison between average results obtained using the Lycra suit or the elastic straps at a normal walking speed. The table shows that there is on average little advantage when using straps instead of the Lycra suit. This difference increases slightly at a fast walking speed (Table 7) which confirms the significance of an error caused by sensor movement relative to the skin.

Table 6: Difference between joint angle validity results of suit and straps - Normal walk

	ΔE_{RMS} [°]		ΔE_{RMS} *(bias corrected)* [°]		ΔE_R	
	Right	Left	Right	Left	Right	Left
φ_h	**2.567#**	**2.155**	**2.800**	0.179	**0.080**	**0.024**
θ_h	4.198	5.479	1.040	0.057	0.024	0.006
ψ_h	**0.740**	**3.783**	**1.098**	**0.706**	0.059	**0.016**
φ_k	1.381	**0.844**	0.535	**0.558**	0.096	0.096
θ_k	0.835	**1.092**	0.392	**1.787**	0.003	**0.003**
ψ_k	0.027	3.673	**1.448**	**0.619**	**0.414**	0.009
φ_a	**0.694**	1.307	**0.489**	0.722	0.243	0.142
θ_a	**0.981**	**5.327**	**1.189**	**4.233**	**0.112**	0.032
ψ_a	**4.566**	0.994	1.330	0.012	0.076	0.298

#Values in bold and colour is where straps showed higher correlation than the suit

Table 7: Difference between joint angle validity results of suit and straps - Fast walk

	ΔE_{RMS} [°]		ΔE_{RMS} *(bias corrected)* [°]		ΔE_R	
	Right	Left	Right	Left	Right	Left
φ_h	**4.014#**	**4.821**	**4.310**	**0.244**	**0.221**	**0.092**
θ_h	3.889	3.389	**0.799**	**0.488**	**0.009**	**0.004**
ψ_h	**2.984**	**1.923**	**4.730**	**2.372**	**0.174**	**0.137**
φ_k	3.582	**2.721**	1.412	**2.991**	0.201	0.099
θ_k	1.009	0.241	**1.290**	**0.950**	**0.017**	**0.016**
ψ_k	4.116	**0.150**	**0.765**	**2.359**	**0.382**	0.059
φ_a	**0.385**	1.703	**0.325**	2.302	0.001	0.113
θ_a	**0.903**	**8.663**	**1.456**	**9.649**	**0.161**	0.233
ψ_a	**4.077**	**0.347**	0.701	**0.961**	0.070	**0.128**

#Values in bold and colour is where straps showed higher correlation than the suit

Figure 19 and Figure 20 show the joint angle comparison of a representative test subject. The figures also better illustrate the effect of removing the bias error. A good correlation is again observed between IMC and OMC recorded joint angles of the hips and knees. Bias errors are significant in the rotation angles of these joints with constant offsets in the order of 10°. This was also the case for hip flexion-extension

- 38 -

values. Ranges and maxima of ankle plantar-dorsiflexion calculated from IMC data are noticeably higher than those produced by OMC software. Also at toe-off (±66% of gait cycle) a phenomenon was observed where localized peaks in results from the two systems deviate in opposite directions (e.g. in the left foot of the representative subject, IMC calculations suggest pronation in contrast to supination as reported by the OMC system).

- 39 -
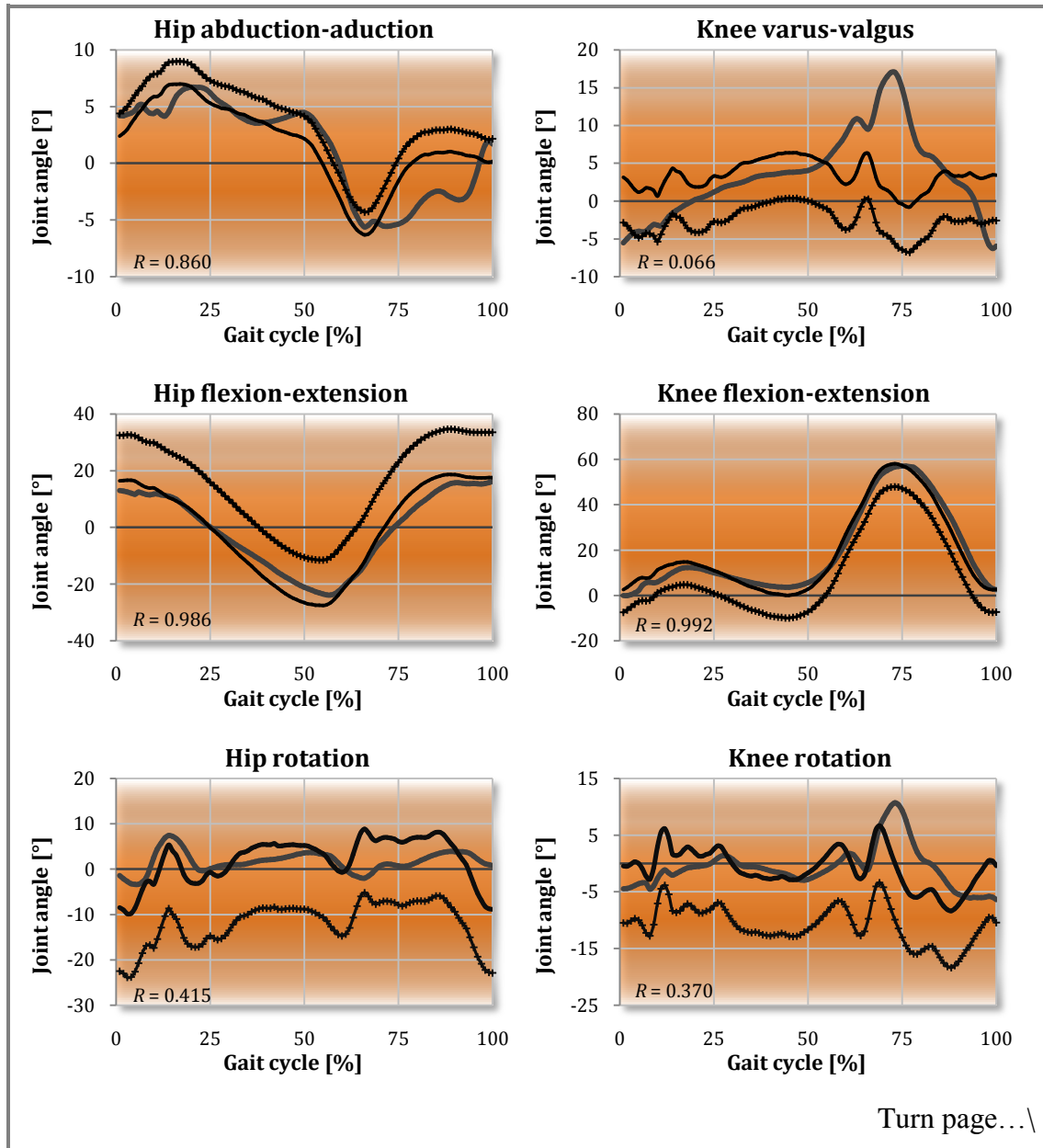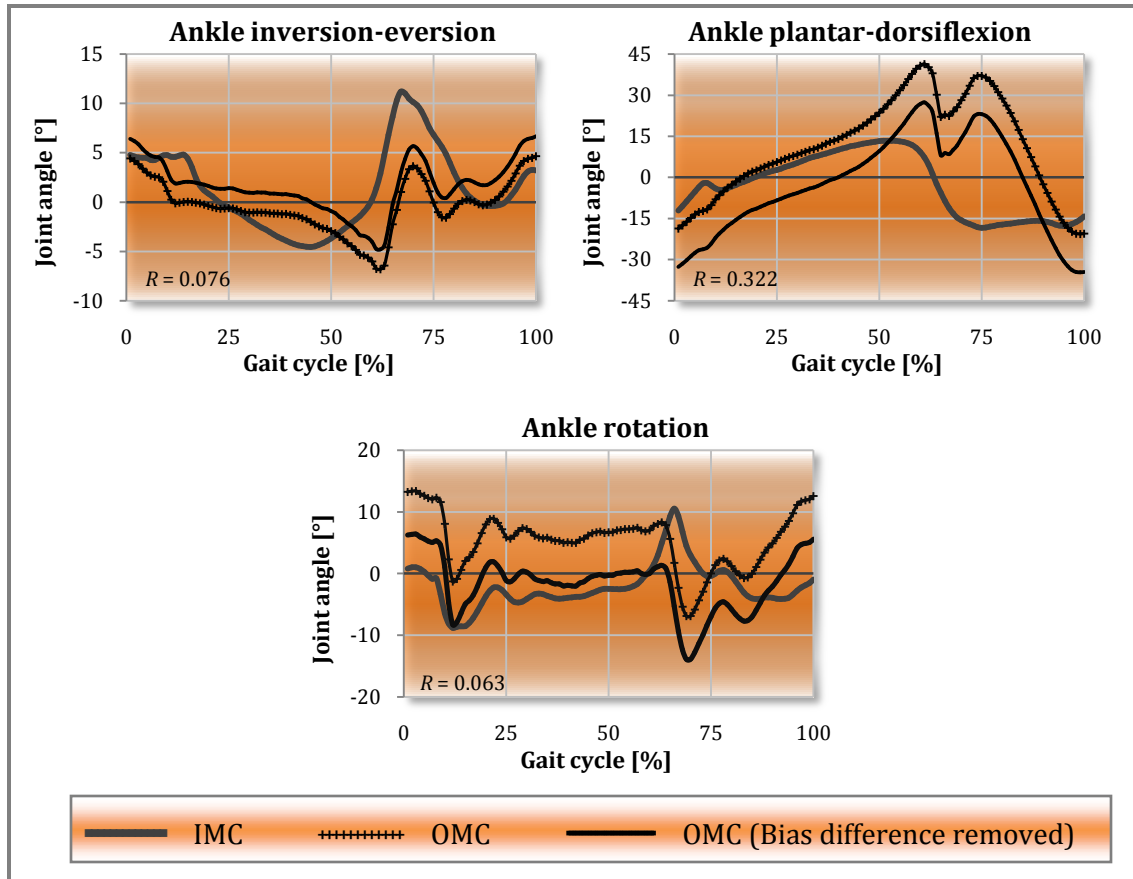
Figure 19: Comparative data validity for the *left side* of a representative subject
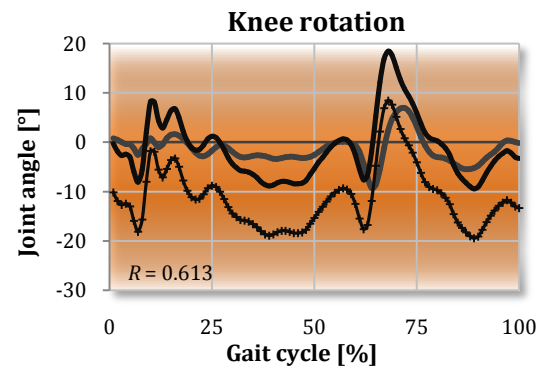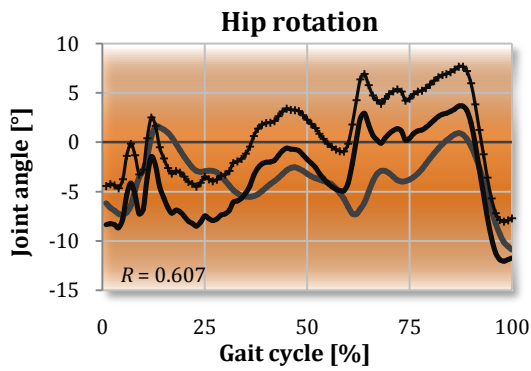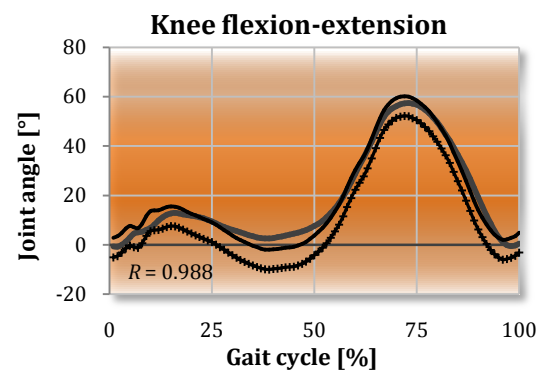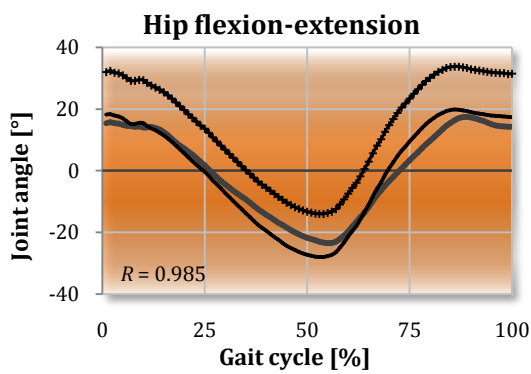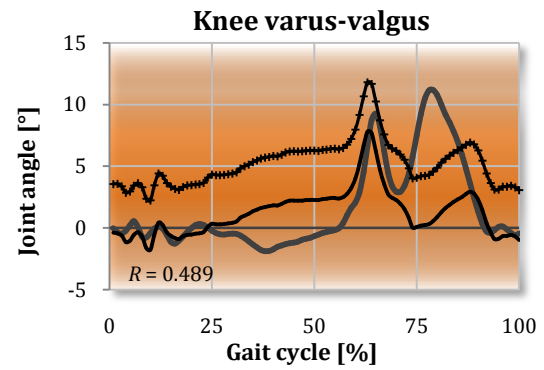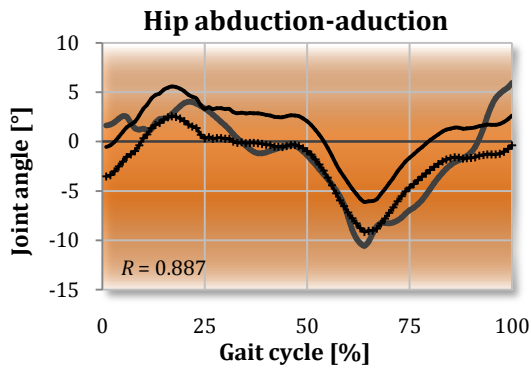
Turn page…\
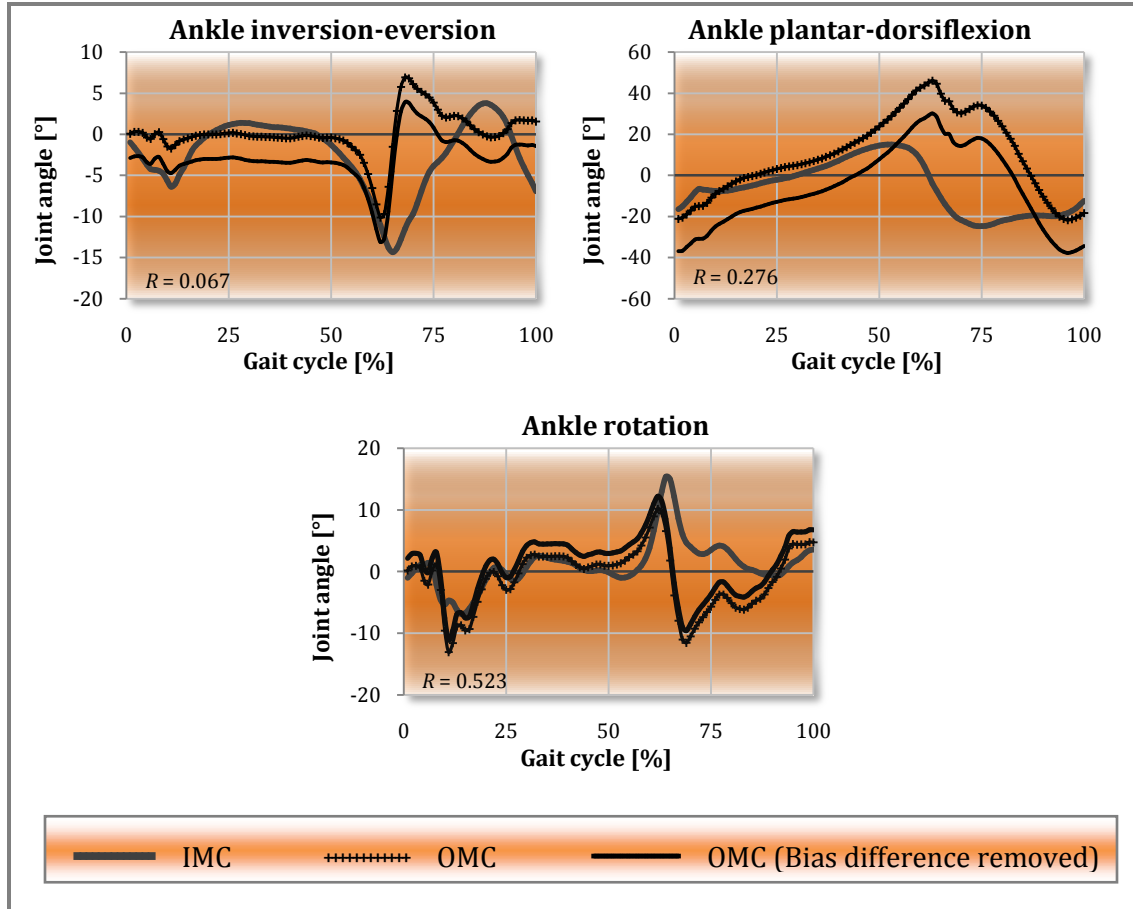
Figure 20: Comparative data validity for the right side of a representative subject

3.6. Discussion

One attribute of the full-body IMC that sets it apart from other acceleration or strictly orientation based systems, is its ability to determine 3D segment position in the GCS. As stated earlier, this is achieved through double integration of acceleration values and drift compensation from complementary component outputs. The validity of temporal-spatial parameters is therefore dependent on two factors: the accuracy of foot position calculations by Moven Studio software, and the correct identification of heel-strike instances, as calculated by the author of this study.

The position measurements of the OMC are very accurate due to the use of several pre-calibrated, high resolution cameras and the subsequent absence of measurement drift. The differences between OMC and IMC results are therefore assumed to be fully attributed to operational errors of IMC such as drift, magnetic interference, calibration and joint centre calculation.

- 42 -

Velocity was calculated using the total distance displaced by the pelvic sensor divided by the time between consecutive heel-strike instances of one side (over one stride). This value therefore indicates the average velocity between two positional points in time and is therefore considered good indication of the position validity of Moven Studio results.

As discussed in Appendix C, step and stride length calculations relied upon the definition of a direction vector. Step lengths were calculated as the vector components parallel to the direction vector, whereas stride length utilized the absolute distance between foot coordinates at consecutive heel-strike instances. Lower average differences of stride length (Straps: 3.2%, Suit: 4.5%) to step length (Straps: 8.9%, Suit: 7.3%) indicate that position calculations are acceptable and that the directional vector approach of calculating step length requires refinement. Even with the current software, however, the temporal-spatial parameters show acceptable validity.

Besier *et al*. (2003) cited Della Croce *et al*. (1999) in saying that the errors associated with the imprecise location of anatomical landforms (ALs) are noted to be the greatest source of error in motion analysis compared to instrument error and skin artefacts. Whether it is the inaccurate positioning of markers or the miscalculation of joint centres, this is the case for all motion analysis systems. Besier *et al*. (2003) went on to state that the greatest error in AL location occurs in the foot. This was confirmed by the validity results in Section 3.5.2. Unlike with temporal-spatial parameters, the OMC values also suffer from errors such as marker vibration and inertia (especially in the wands). Keeping this in mind, the OMC was still considered as the "golden standard" because of its widespread use and acceptance.

High correlation values in sagittal joint angles were found in the hips and knees. This suggests that the validity of joint angles, calculated from IMC data, may be affected by the rotational freedom of the joint around non-primary rotation axes and/or the range of motion around the primary axis, as both these characteristics are more prevalent in sagittal plane angles. Acceptable correlation values were recorded for hip and knee abduction-adduction. Differences may stem from a misalignment of IMC sensors or inaccurate positioning of OMC markers leading to mismatched rotation centres or axes. A higher *R* value for knee rotation during slow walking suggests that sensor or marker movement relative to the BCS adds to errors in this plane.

Low correlation values in the ankle joints could be as a result of the following factors:
- o Incorrect allocation or calculation of angle axes (e.g. the OMC software uses a marker on the lateral malleoli and an estimation based on a measured ankle width to calculate the sagittal plane angle of the ankle, while the IMC software uses an axis defined during static calibration).
- o Movement of the IMC sensor on the soft tissue on top of the foot.

- 43 -

- A small area of contact between the sensor and the foot due to the flat base of the sensor.
- Interference of the IMC sensor cable with the lower tip of the tibia. This is illustrated in Figure 21 below in which the arrow points to the position of possible interference at maximum dorsiflexion.
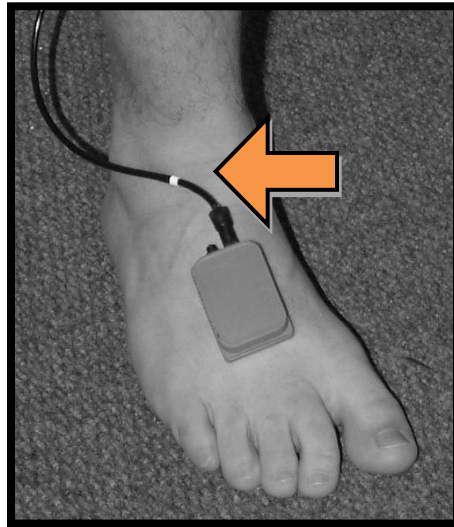
Figure 21: Foot sensor position

The last two factors are most likely responsible for the discrepancies observed between left and right ψ_a values as well as the pronation-supination phenomenon at toe-off described in Section 3.5. These differences may be reduced through better sensor design or placement. Unfortunately there is no means of determining the weighting that each of the above-mentioned factors had on the total difference. Upon studying Table 6 and Table 7, the initial hypothesis of using double-sided tape and straps in instead of the Lycra suit was confirmed by the slight improvements in validity during fast walking trials. The highest achievable accuracy and repeatability is obligatory in clinical gait applications. It was for this reason that the Lycra suit was not used in the repeatability study described in Section 4.

A relatively constant bias difference of approximately 10° in the hip joint may be a result of the initial anterior pelvic tilt defined by Moven Studio software. The removal of this bias difference is a valid step as this difference is purely due to varying sensor or marker positioning which is a common problem in all Mocap systems.

In conclusion the IMC produced temporal-spatial and joint angle parameters (except for ankle joint angles) are sufficiently valid for clinical gait analysis. However, improvements are required in spatial parameter calculation and in foot sensor design.

4. REPEATABILITY STUDY

Several studies have been conducted to investigate the repeatability of recorded gait parameters using the Vicon OMC system. These include measurements on able-bodied controls as well as subjects with gait pathologies (Kadaba *et al.*, 1989, Mackey *et al.*, 2005, Steinwender *et al.*, 2000, Yavuzer *et al.*, 2006). Mills *et al.* (2007) evaluated the repeatability of ten able-bodied subjects using an electromagnetic Mocap system. However, no studies were found which investigate the repeatability of gait parameters measured using full-body IMC.

4.1. Test participation

30 young, healthy men were used in the study. Their physical characteristics were as follows:

Table 8: Test subject characteristics (repeatability study)

	Mean ± SD	Max	Min
Age [years]	22.6 ± 1.9	25	19
Height [cm]	180.6 ± 5.7	196	168
Weight [kg]	81.4 ± 10.1	110	64

Subjects were selected under the condition that they had no prior history of musculoskeletal problems. Subjects were also questioned before every trial to ensure that they were not experiencing any muscle stiffness or fatigue possibly caused by sporting activities. Kadaba *et al*. (2007) did not use any female subjects in their study. It was therefore also decided to omit female subjects from this study to provide a more accurate comparison of results.

4.2. Apparatus

For this study the Moven IMC system was used with double-sided adhesive tape and elastic straps. Refer to Section 3.2.2.

4.3. Data acquisition and processing

This study evaluated the within-day and between-day repeatability of 30 able-bodied subjects. Each subject was tested three times on each of three test days. The test days were at least one week apart to simulate an entirely new experience on each test day.

Sensor placement and calibration procedures were identical to those performed for the IMC in Sections 3.3.1.1 and 3.3.1.2. Subjects were asked to walk at a self-

- 45 -

selected speed along a 12 m walkway. The first two runs were not recorded. This allowed the subject to become comfortable with the surroundings and procedure. Seven runs were recorded in the same direction for each subject on each test day. A tape line was made on the walkway, 5 m from the start position. Using the Moven Studio software a time marker was inserted when the subject passed over this line. At this point the subject would have achieved a uniform walking pattern and velocity. Three strides were isolated after the time marker and from these; the middle stride on each side was used in calculating gait repeatability.

4.4. Data analysis

4.4.1. Gait data representation

As in Section 3.4.1, SL, STL, velocity, cadence and the same nine joint angles were analysed for repeatability.

4.4.2. Statistical approach

All of the abovementioned studies done on gait parameters repeatability (Besier *et al.*, 2003, Mackey *et al.*, 2005, Yavuzer *et al.*, 2006, Mills *et al.*, 2007, Steinwender *et al.*, 2000, Kadaba *et al.*, 1989), use repeatability quantifiers as proposed by Kadaba, *et al.* (1989). They employed the coefficient of variance (CV) for temporal-spatial parameters and either the coefficient of multiple determination (CMD) or the coefficient of multiple correlation (CMC) for evaluating joint angle kinematics. The coefficient of variance is defined as the ratio of standard deviation (SD) to the mean, expressed as a percentage. CV will approach zero as values of SD decrease, thus implying repeatability between values. The CMC, or also sometimes written as *r*, is the positive square root of the adjusted *R*-squared (R_a^2) statistic also called the CMD (Besier *et al.*, 2003). Equation (10) shows the calculation of the adjusted *R*-squared for within-day repeatability while Equation (13) is used for between-day repeatability (Kadaba *et al.*, 1989). Here *M* is the total number of days, *N* is the total number of runs (strides) and *T* is the total stride-time of a specific stride.

$$R_a^2 = 1 - \frac{\sum_{i=1}^{M}\sum_{j=1}^{N}\sum_{t=1}^{T}(Y_{ijt} - \overline{Y}_{it})^2 / MT(N-1)}{\sum_{i=1}^{M}\sum_{j=1}^{N}\sum_{t=1}^{T}(Y_{ijt} - \overline{Y}_{i})^2 / M(NT-1)} \tag{10}$$

Here Y_{ijt} is the tth time point of the jth run on the ith test day, $\overline{Y}_{it}$ is the average at time point t on the ith test day given by Equation (11)

$$\overline{Y}_{it} = \frac{1}{N} \sum_{j=1}^{N} Y_{ijt} \qquad (11)$$

and $\overline{Y}_i$ is the grand mean on the ith day and given by Equation (12)

$$\overline{Y}_i = \frac{1}{NT} \sum_{j=1}^{N} \sum_{t=1}^{T} Y_{ijt} \qquad (12)$$

For between-day repeatability, mean values of gait parameters were calculated for each subject for each of the three test days.

$$R_a^2 = 1 - \frac{\sum_{i=1}^{M} \sum_{j=1}^{N} \sum_{t=1}^{T} (Y_{ijt} - \overline{Y}_t)^2 / T(MN-1)}{\sum_{i=1}^{M} \sum_{j=1}^{N} \sum_{t=1}^{T} (Y_{ijt} - \overline{Y})^2 / (MNT-1)} \qquad (13)$$

Here $\overline{Y}_t$, given by (14), is the average at time point t over NM gait cycles and $\overline{Y}$, given by (15), is the grand mean over time.

$$\overline{Y}_t = \frac{1}{MN} \sum_{i=1}^{M} \sum_{j=1}^{N} Y_{ijt} \qquad (14)$$

$$\overline{Y} = \frac{1}{MNT} \sum_{i=1}^{M} \sum_{j=1}^{N} \sum_{t=1}^{T} Y_{ijt} \qquad (15)$$

The CMCs of these values were then calculated by taking the positive square root of Equations (10) and (13). Another quantifier often used to analyse repeatability is the interclass correlation coefficient which presents increasing repeatability on a scale from of 0 to 1. The CMC value was preferred in this study because (unlike the ICC) it allowed the author to compare more than two data sets or joint angle curves.

4.5. Results

4.5.1. **Temporal-spatial repeatability**

Table 9 contains the temporal and special gait parameter repeatability results for the IMC system along with results obtained by Kadaba *et al*. (1989) using the Vicon OMC system. Results show that the OMC system produces more repeatable results in all but one of the calculated parameters. The within-day coefficient of variance for the IMC recorded velocity is almost double what was presented by Kadaba *et al*. (1989) Between-day repeatability of cadence is slightly better than that of the OMC system.

Table 9: Comparison of intra-subject repeatability of temporal-spatial parameters

	Average results (Mean ± SD)		CV% (within-day) (Mean ± SD)		CV% (between-day) (Mean ± SD)	
	IMC	OMC	IMC	OMC	IMC	OMC
Stride length#	1.33 ± 0.11	1.36 ± 0.12	2.0 ± 0.42	1.7 ± 0.6	3.6 ± 1.2	3.0 ± 1.3
Step length	0.66 ± 0.53	- -	5.5 ± 1.8	- -	6.6 ± 1.9	- -
Velocity	1.183 ± 0.12	1.306 ± 0.05	5.4 ± 1.7	2.9 ± 3.3	7.5 ± 2.4	6.1 ± 7.1
Cadence	107.1 ± 6.21	111.6 ± 8.3	2.2 ± 0.6	1.9 ± 0.8	**3.2 ± 1.3**[*]	3.4 ± 1.8

\# Units for gait parameters are as follows: Stride length [m], step length [m], velocity [m/s] and cadence [steps/min]

* Values in bold and colour are those in which the IMC show a higher degree of repeatability than the OMC

Figure 22 present the within-day and between-day variation in SL, STL, velocity and cadence for a representative subject.
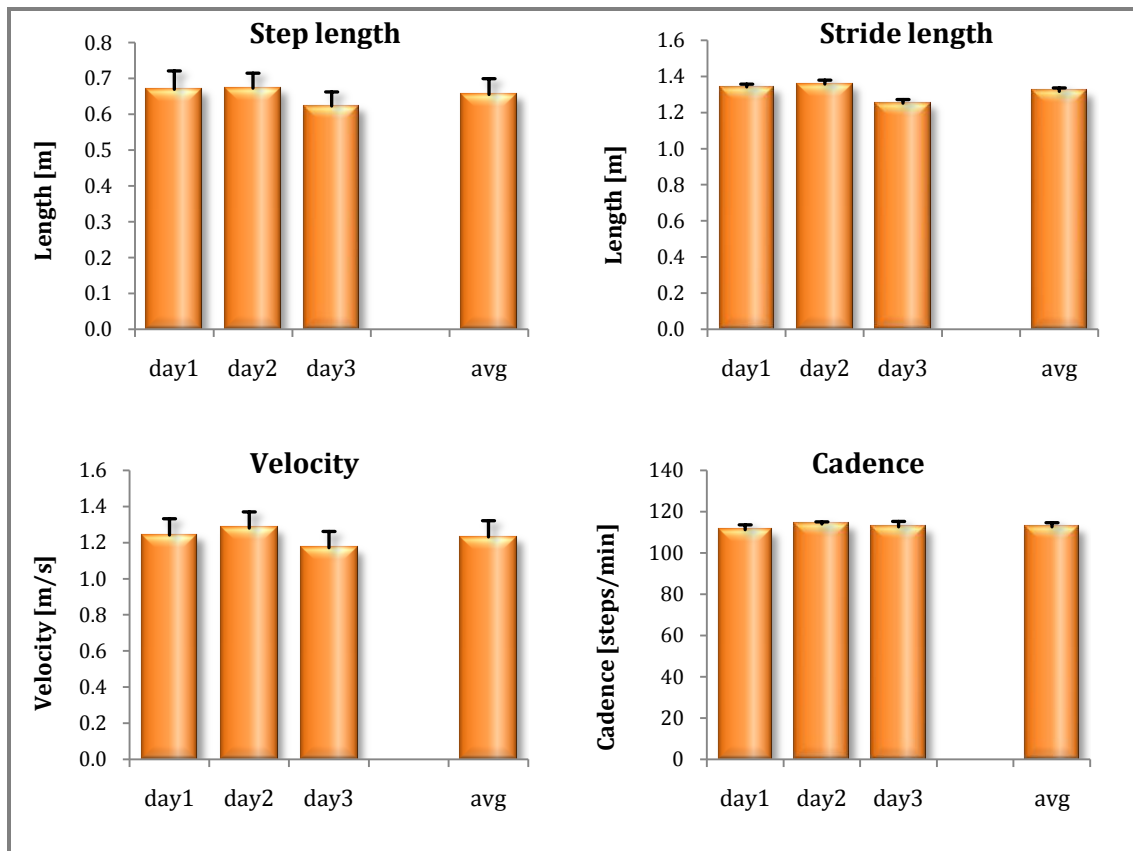
Figure 22: Mean and standard deviation of temporal-spatial parameter repeatability for a representative subject

- 48 -

4.5.2. Joint angle repeatability

4.5.2.1. Within-day repeatability

Table 10 and Table 11 contain the average joint angle repeatability results and corresponding standard deviations obtained between different trials within test days for the 30 able-bodied subjects.

Table 10: Within-day repeatability of joint angles – IMC vs. OMC

	CMC ($\sqrt{R_a^2}$ Mean ± SD) Inertial		CMC ($\sqrt{R_a^2}$ Mean ± SD) Optical (Kadaba *et al.* 1989)	
	Right	Left	Right	Left
φ_h	**0.981 ± 0.009***	**0.981 ± 0.008**	0.964 ± 0.030	0.957 ± 0.088
θ_h	0.992 ± 0.005	0.991 ± 0.004	0.996 ± 0.003	0.995 ± 0.005
ψ_h	0.881 ± 0.079	0.889 ± 0.068	0.893 ± 0.064	0.893 ± 0.072
φ_k	**0.958 ± 0.041**	**0.970 ± 0.016**	0.942 ± 0.044	0.962 ± 0.029
θ_k	0.992 ± 0.004	0.990 ± 0.004	0.994 ± 0.005	0.994 ± 0.003
ψ_k	**0.919 ± 0.045**	**0.935 ± 0.047**	0.911 ± 0.090	0.918 ± 0.053
φ_a	0.913 ± 0.046	0.967 ± 0.017	- -	- -
θ_a	**0.981 ± 0.012**	0.966 ± 0.032	0.975 ± 0.018	0.978 ± 0.010
ψ_a	**0.910 ± 0.042**	**0.952 ± 0.025**	0.853 ± 0.080	0.885 ± 0.053

* Values in bold and colour are those in which the IMC show higher values of repeatability than the OMC

Table 11: Within-day repeatability of joint angles – IMC vs. EMC

	CMD (R_a^2 Mean ± SD) Inertial		CMD (R_a^2 Mean ± SD) Electromagnetic (Mills *et al.* 2007)	
	Right	Left	Right	Left
φ_h	0.963 ± 0.017	0.962 ± 0.015	0.977 ± 0.013	0.980 ± 0.010
θ_h	0.984 ± 0.011	0.983 ± 0.008	0.994 ± 0.003	0.995 ± 0.002
ψ_h	0.786 ± 0.131	0.799 ± 0.111	0.932 ± 0.023	0.938 ± 0.024
φ_k	**0.921 ± 0.072***	**0.942 ± 0.030**	0.901 ± 0.074	0.903 ± 0.087
θ_k	0.983 ± 0.008	0.981 ± 0.008	0.989 ± 0.007	0.992 ± 0.005
ψ_k	0.848 ± 0.080	0.876 ± 0.081	0.956 ± 0.017	0.947 ± 0.027
φ_a	0.840 ± 0.078	**0.936 ± 0.032**	0.932 ± 0.032	0.819 ± 0.081
θ_a	0.962 ± 0.023	0.935 ± 0.055	0.967 ± 0.023	0.972 ± 0.014
ψ_a	0.832 ± 0.072	**0.908 ± 0.045**	0.888 ± 0.041	0.872 ± 0.081

* Values in bold and colour are those in which the IMC show higher values of repeatability than the EMC

Within-day repeatability of IMC calculated joint angles are high across the board. Sagittal plane angles of the hips and knees are especially high with CMD = ±0.983 and CMC = ±0.991. Ankle plantar-dorsiflexion display excellent repeatability despite the extrinsic factors named in Section 3.6. Here right-side CMD and CMC values of

0.962 and 0.981 were achieved, respectively. Interestingly, the IMC system outperforms the OMC system for ankle joint repeatability. Repeatability values reported by Mills *et al.* (2007) are in most cases higher than those produced by the IMC system. Reported values for transverse plane angles ψ_h and ψ_k of the hips and knees were significantly higher in the EMC results than in the IMC results. Except for these divergences, all the results show a high degree of repeatability and are in the same order of magnitude as reported EMC and OMC results.

4.5.2.2. Between-day repeatability

Table 12 shows the between-day repeatability results obtained without removing the mean of each day (bias difference).

Table 12: Between-day repeatability of joint angles – IMC vs. OMC

	CMC ($\sqrt{R_a^2}$ Mean ± SD)			CMC ($\sqrt{R_a^2}$ Mean ± SD)	
	Inertial			**Optical (Kadaba *et al.* 1989)**	
	Right		Left	Right	Left
φ_h	**0.934 ±**	**0.034***	**0.933 ± 0.039**	0.885 ± 0.067	0.882 ± 0.101
θ_h	0.980 ±	0.014	**0.983 ± 0.009**	0.983 ± 0.012	0.978 ± 0.019
ψ_h	**0.911 ±**	**0.115**	**0.866 ± 0.088**	0.410 ± 0.210	0.483 ± 0.236
φ_k	**0.839 ±**	**0.223**	**0.905 ± 0.066**	0.611 ± 0.172	0.783 ± 0.159
θ_k	**0.991 ±**	**0.007**	**0.991 ± 0.006**	0.981 ± 0.014	0.985 ± 0.009
ψ_k	**0.831 ±**	**0.140**	**0.854 ± 0.105**	0.490 ± 0.191	0.534 ± 0.221
φ_a	0.832 ±	0.121	0.942 ± 0.038	- -	- -
θ_a	**0.969 ±**	**0.019**	**0.954 ± 0.030**	0.937 ± 0.030	0.933 ± 0.034
ψ_a	**0.789 ±**	**0.080**	**0.913 ± 0.048**	0.582 ± 0.176	0.612 ± 0.200

* Values in bold and colour are those in which the IMC show higher values of repeatability than the OMC

All but one of the calculated CMC values calculated for the analysed joint angles are higher for IMC than OMC. The exception being θ_h for the right side, in which the difference is 0.003˚. IMC results for ψ_h, ψ_k and ψ_a significantly outperforms OMC results reported by Kadaba *et al.* (1989). Between-day, sagittal plane CMC values for the knees are in the same order as those calculated between trials, within test days. As expected, however, the CMCs of trials measured between test days are virtually all slightly lower than those measured within test days. Only ψ_h for the right side deviates from this trend.

The following two tables provide the between-day repeatability results for the case in which the bias difference for each day was removed. All the joint angle curves measured on a particular day were normalized by subtracting the mean curves of that day from each of the curves. These mean curves were calculated by summing the angle at a specific time frame and dividing the answer by the number of runs of that day. The CMC and CMD values therefore indicate the relative repeatability of nine

measured trial strides (three trials on each of three test days) each with the mean of the specific test day removed.

Table 13: Between-day repeatability of joint angles with mean of each day removed – IMC vs. OMC

	CMC ($\sqrt{R_a^2}$) Inertial			CMC ($\sqrt{R_a^2}$) Optical (Kadaba *et al.* 1989)		
	Right		Left	Right		Left
φ_h	**0.964 ± 0.028**[*]	**0.958 ±**	**0.023**	0.943 ± 0.035	0.948 ± 0.062	
θ_h	0.992 ± 0.003	0.991 ±	0.004	0.994± 0.003	0.994 ± 0.004	
ψ_h	**0.975 ± 0.020**	**0.950 ±**	**0.037**	0.820 ± 0.100	0.841 ± 0.084	
φ_k	**0.875 ± 0.200**	**0.934 ±**	**0.040**	0.737 ± 0.197	0.858 ± 0.106	
θ_k	**0.995 ± 0.002**	**0.995 ±**	**0.002**	0.990 ± 0.009	0.991 ± 0.004	
ψ_k	**0.906 ± 0.084**	**0.910 ±**	**0.056**	0.844 ± 0.086	0.849 ± 0.091	
φ_a	0.872 ± 0.103	0.960 ±	0.025	- -	- -	
θ_a	**0.976 ± 0.017**	0.964±	0.027	0.964 ± 0.018	0.967 ± 0.013	
ψ_a	**0.950 ± 0.021**	**0.965 ±**	**0.015**	0.834 ± 0.074	0.858 ± 0.055	

* Values in bold and colour are those in which the IMC show higher values of repeatability than the OMC

Table 14: Between-day repeatability of joint angles with mean of each day removed – IMC vs. EMC

	CMD (R_a^2 Mean ± SD) Inertial			CMD (R_a^2 Mean ± SD) Electromagnetic (Mills *et al.* 2007)		
	Right		Left	Right		Left
φ_h	**0.930 ± 0.053**[*]	**0.919 ±**	**0.043**	0.929 ± 0.052	0.871 ± 0.093	
θ_h	**0.984 ± 0.007**	**0.992 ±**	**0.007**	0.969 ± 0.021	0.970 ± 0.019	
ψ_h	**0.951 ± 0.038**	**0.903 ±**	**0.068**	0.839 ± 0.126	0.806 ± 0.112	
φ_k	**0.804 ± 0.265**	**0.874 ±**	**0.073**	0.598 ± 0.220	0.659 ± 0.260	
θ_k	**0.991 ± 0.004**	**0.990 ±**	**0.004**	0.988 ± 0.012	0.978 ± 0.036	
ψ_k	0.827 ± 0.135	0.832 ±	0.099	0.877± 0.108	0.849 ± 0.112	
φ_a	0.771 ± 0.164	**0.921 ±**	**0.048**	0.863 ± 0.102	0.722 ± 0.273	
θ_a	0.953 ± 0.033	0.930±	0.051	0.967 ± 0.027	0.946 ± 0.080	
ψ_a	**0.903 ± 0.039**	**0.932 ±**	**0.029**	0.731 ± 0.255	0.719 ± 0.273	

* Values in bold and colour are those in which the IMC show higher values of repeatability than the EMC

With the bias difference removed, CMC and CMD values recorded indicate excellent between-day repeatability. When compared to the studied OMC and EMC systems, results show that angle measurement from all three joints are highly repeatable with CMC values ranging from 0.872 ± 0.103 to 0.995 ± 0.002 and CMD values ranging from 0.771 ± 0.164 to 0.992 ± 0.007. Sagittal plane angles of the knees show particularly good repeatability (CMC: ±0.995, CMD: ±0.991). Unlike the phenomenon noted for within-day testing, the results for transverse plane angles ψ_h

and ψ_k of the hips and knees recorded using EMC are not found to be significantly higher than those of the IMC system. These values seem to exhibit a contrary trend, especially when comparing results with the findings of Kadaba *et al*. (1989).

Figure 23 and Figure 24 illustrate the means and corresponding variance of CMC results for the right and left side joint angles of a representative subject.
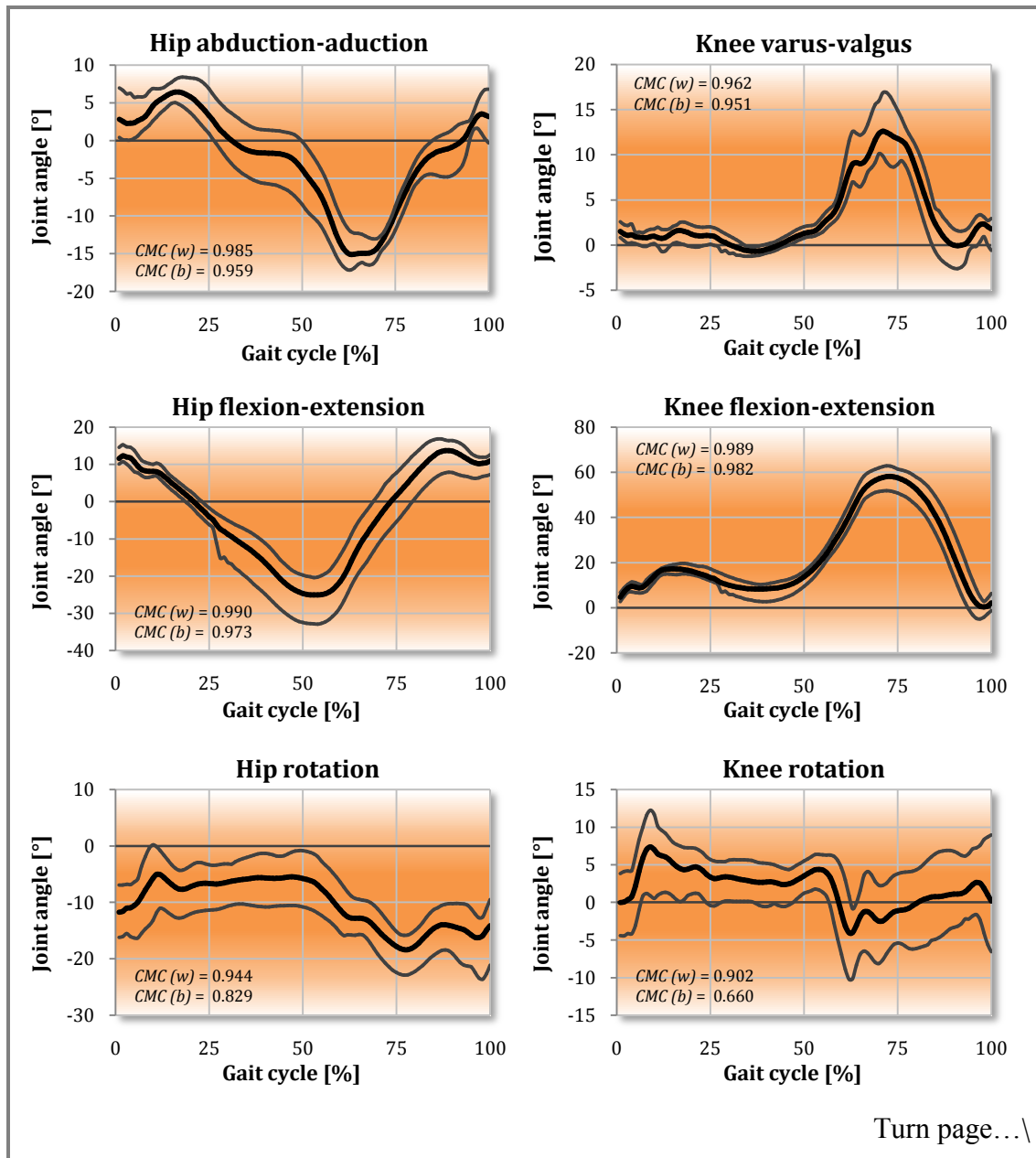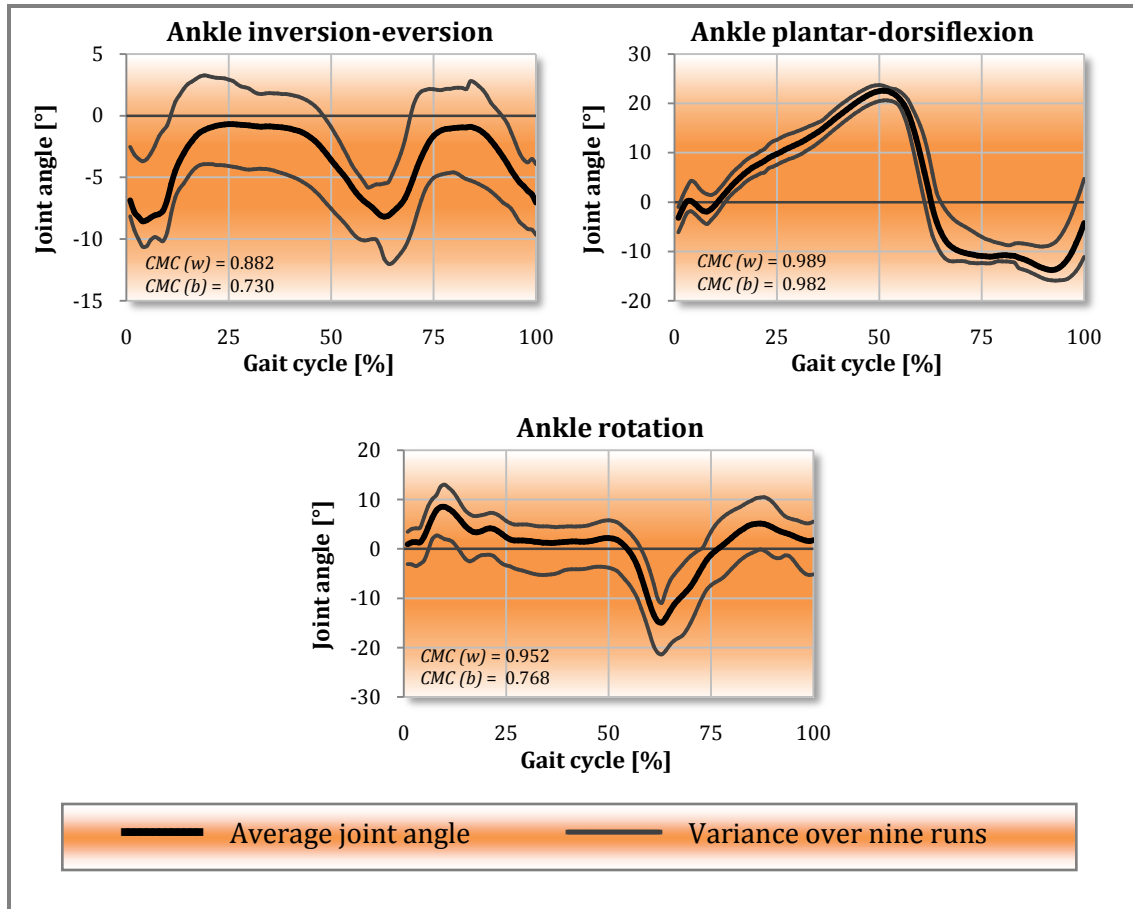
Figure 23: Mean and variance of joint angle motion of the *right side* for the representative subject over nine runs (three runs on each of the three days)

Hip abduction-aduction

CMC (w) = 0.976
CMC (b) = 0.910

Knee varus-valgus

CMC (w) = 0.969
CMC (b) = 0.912

Hip flexion-extension

CMC (w) = 0.990
CMC (b) = 0.938

Knee flexion-extension

CMC (w) = 0.989
CMC (b) = 0.988

Hip rotation

CMC (w) = 0.965
CMC (b) = 0.822

Knee rotation

CMC (w) = 0.911
CMC (b) = 0.801

Turn page…\
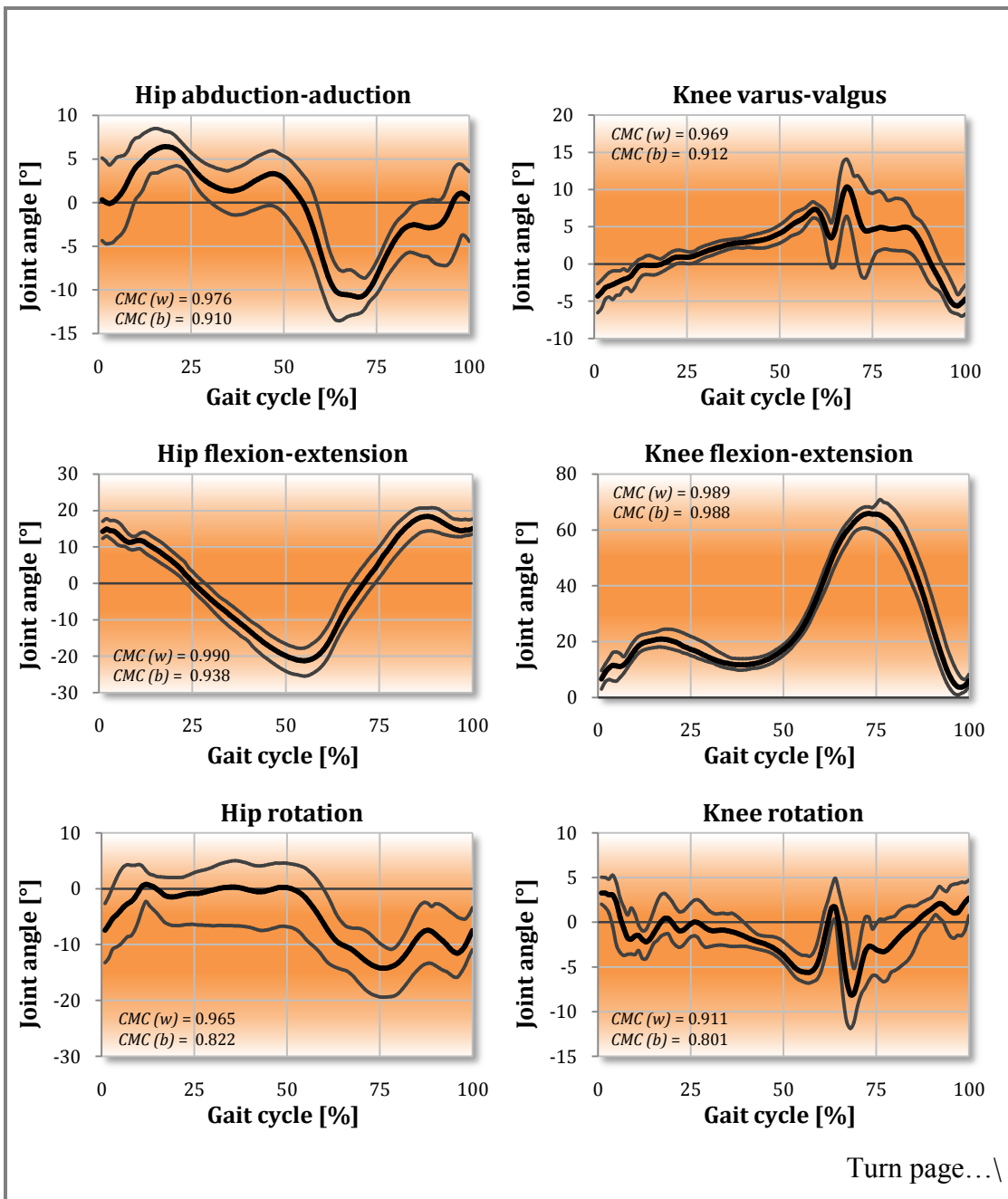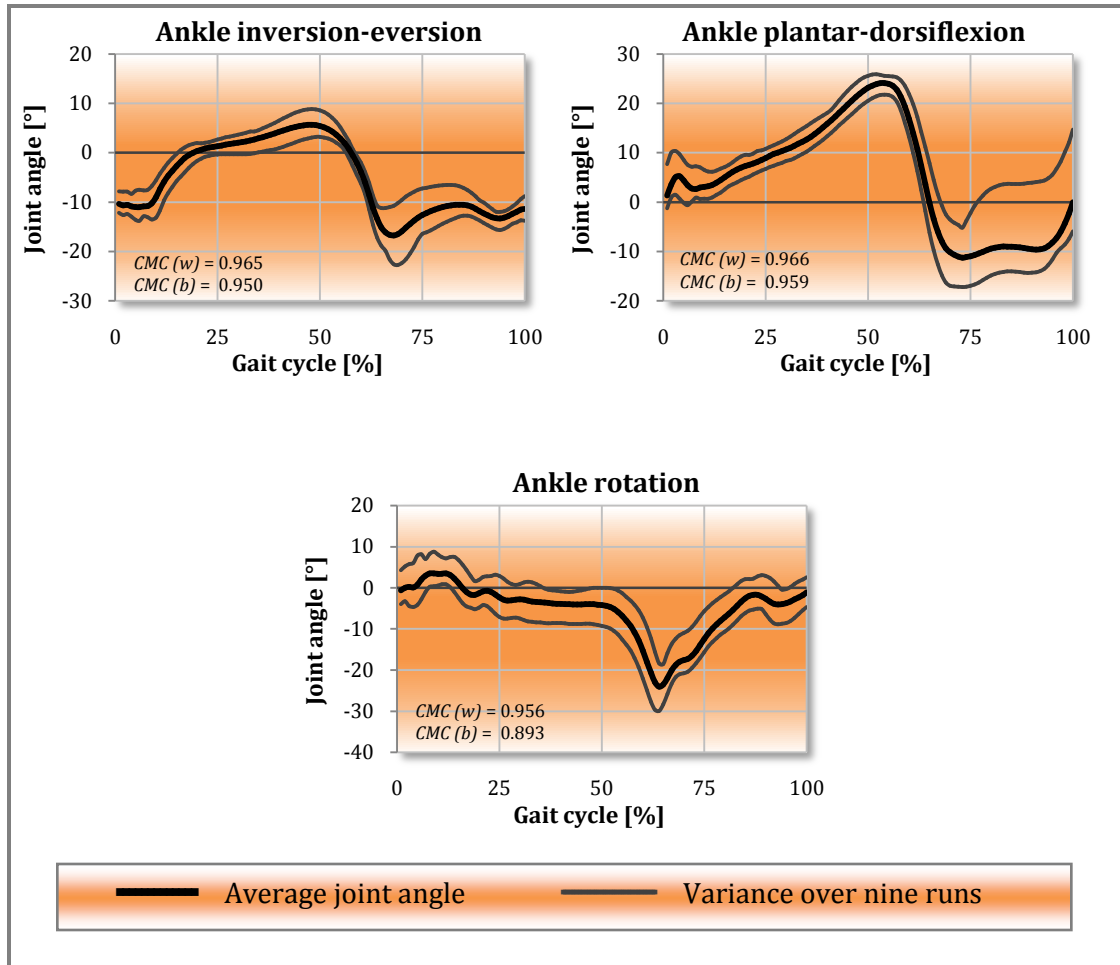
Figure 24: Mean and variance of joint angle motion of the *left side* for the representative subject over nine runs (three runs on each of the three days)

Again the general trend of higher repeatability in the knee and hip joints was observed, especially in the sagittal plane.

4.6. Discussion

According to Yavuzer *et al*. (2007), errors in repeatability may be as a result of two types of errors, namely, intrinsic and extrinsic errors. Intrinsic errors occur naturally and cannot be reduced through improvements of measuring techniques but should be measured as a baseline for analysis. On the other hand, extrinsic errors such as those caused by skin movement, calibration, anthropometric measurements and the definition of gait cycle phases (such as heel-strike and toe-off phases), may be minimized by careful and meticulous testing procedure and improvements in tracking equipment (Yavuzer *et al.*, 2006). When compared to OMC and EMC systems, the

- 55 -

IMC sensors are quite large (38 × 53 × 21 mm, 0.030 kg). This causes more sensor inertia and subsequent increased skin artefacts, especially during faster ambulation. On the other hand, a greater area of contact between the sensors and skin was possible which ensured negligible sensor-to-skin movement. Heel-strike and toe-off identification differences played a definite role, and further refinement of these calculations is still required. Finally, calibration and anthropometric measurement errors were minimized by using a single trained researcher to conduct segment measurement and calibration for all the tests. Tester-tester effects were studied by Besier *et al*. (2003) and Mills *et al*. (2007). Besier *et al*. concluded that the repeatability results were fairly independent of the examiner.

Variation in marker reapplication also leads to an extrinsic bias error (Kadaba *et al.*, 1989). According to Mackey *et al*. (2005), small changes in marker positioning of knee and ankle markers lead to noticeable differences in transverse plane kinematics. This is consistent with findings by other researchers and apparent in the comparatively lower between-day repeatability. In general however the between-day repeatability results were high for both bias-uncorrected (CMC: 0.789 – 0.991) and bias-corrected (CMC: 0.872 – 0.995) cases and comparable to those by Kadaba *et al*. (1989) (CMC: 0.410 – 0.985 and 0.737 – 0.994) and Mills *et al*. (2005) (CMD: 0.598 – 0.988). This implies that marker reapplication errors were acceptably low.

Kadaba *et al.* (1989) stated that lower repeatability in the pelvic tilt was as a result of both small range of motion (ROM) and the lack of a well defined pattern of movement. This statement is true for most joint angles which display these characteristics. Sagittal plane angles have higher ranges of motion and well defined motion patterns (refer to Figure 23 and Figure 24). As expected these angles show the highest CMCs. This is true for other studies (Kadaba *et al.*, 1989, Mills *et al.*, 2007). Since the study conducted by Kadaba *et al*. (1989) OMC systems may have improved, hence their reported values of repeatability may be slightly lower than those achievable by present OMC systems, but to the knowledge of the author, no such results have been reported.

Based on repeatability results obtained, this study has proven that researchers and/or physicians can base diagnosis about the gait of a test subject or patient on a single IMC-recorded gait analysis. Kadaba *et al*. (1989) however aptly stated that the repeatability of pathological gait patient may decrease from those recorded from able-bodied subjects, particularly because of greater skin looseness and a higher average body-fat index often found in stroke and Parkinson's disease sufferers.

5. NEURAL NETWORK

5.1. Introduction

The aim, in earlier sections, was to show that IMC (more specifically full-body IMC) exhibits sufficient accuracy and repeatability to be utilized for clinical gait analysis. The results obtained in Sections 3 and 4 indicate that this is indeed the case. This section aims to compliment these findings by employing and evaluating IMC in a clinical application namely to train and test a neural network using IMC collected data, to distinguish between stroke patients and able-bodied controls. Although a seemingly trivial problem, human gait is observed to be very complex and variable, even within an able-bodied group. Subjects from one group may display characteristics common to the other group.

The use of semi-automated-diagnosis tools such as neural networks has seen a continual growth in popularity because of their clinical potential and diagnostic success. As will be shown in later sections, it is often very difficult to provide accurate diagnoses by looking at only a few parameters at a time. However, a neural network is able to perform a weighted comparison of several input parameters simultaneously to distinguish between known output groups. This aids medical professionals with patient assessment by supplying a primary diagnosis, which may provide both an increase in the number of patients that a doctor is able to treat as well as improve the choice and quality of treatment.

5.2. Objectives

In this section the author aims to prove, through the use a neural network in a specific clinical application, the usefulness of employing a neural network for gait analysis over the use of conventional qualitative or quantitative statistical methods. This section also aims to highlight the present and future advantages of combining IMC and semi-automated-diagnosis tools (e.g. neural networks or fuzzy logic) in gait analysis. Such advantages may be especially useful in telemedicine.

5.3. Procedure

5.3.1. Data collection

5.3.1.1. Inclusion criteria

Sufficient pathologic and normal gait data was required to train and test a chosen neural network. Data from the 30 able-bodied subjects used in the repeatability study (Section 4) was re-used for the required normal input data. Stroke patient data was recorded in a collaborative study done in cooperation with Mr Wasim Labban from

- 57 -

the Department of Physiotherapy of the University of Stellenbosch. Ethical approval for this study was obtained from the Committee for Human Research of the University of Stellenbosch, Faculty of Life Sciences. Written informed consent was obtained from each patient prior to their participation in the study. Routine gait analysis was conducted on 28 hemiparetic stroke patients with varying degrees of locomotive dysfunction. The stoke-patient group were aged between 25 and 64 years with a mean (STD) of 51.2 (±10.1) compared to the control group who were aged between 19 and 25 with a mean of 22.6 (±1.9). Also, the stroke-patient group contained 40 % female subjects compared to the control group who were exclusively male.

5.3.1.2. Gait assessment

Tests were conducted with the aid of Mr Labban at the Western Cape Rehabilitation Centre. All test subjects were asked to walk at a self-selected speed along a 10 m walkway. Measurements were recorded in one direction only. Stroke patients were given sufficient opportunity to rest between trials. This minimized the effect of fatigue on gait recordings. At least five trials, each with at least four full strides, were recorded for each subject. 375 strides[3] from 25 of the able-bodied subjects and 327 strides[3] from 22 of the stroke patients were isolated as train data and 73 strides[3] from the remaining five able-bodied subjects and 66 strides[3] from the remaining five stroke patients were used as test data for the neural network. All strides were re-sampled to 100 data points which represent 100% of the gait cycle.

5.3.2. Network input parameters

This section deals with the selection of input parameters with which the neural network was trained. The first step was to calculate the Statistical Overlap Factor (SOF) as proposed by Mdlanzi *et al.* (2007). The SOF between two variable distributions is a calculation of the ratio of the distance between the averages of the two distributions, to the mean of the two standard deviations. This is represented by Equation (16) below:

$$SOF = \left| \frac{\bar{x}_1 - \bar{x}_2}{(\sigma_1 + \sigma_2)/2} \right| \tag{16}$$

where $\bar{x}_1$ and $\bar{x}_2$ are the averages of the distributions and σ_1 and σ_2 are their respective standard deviations (Mdlanzi *et al.*, 2007).

High SOF values indicate a greater degree of separation between the respective distributions. This is indicated in Figure 25 which shows the stroke-patient and able-bodied control group distributions for the input parameters having the ten highest calculated SOF values.

---

[3] In this context, the term "strides", refers to a combination of concurrent left and right-side strides. This was necessary to calculate parameters such as SL and double-stance and swing phases.
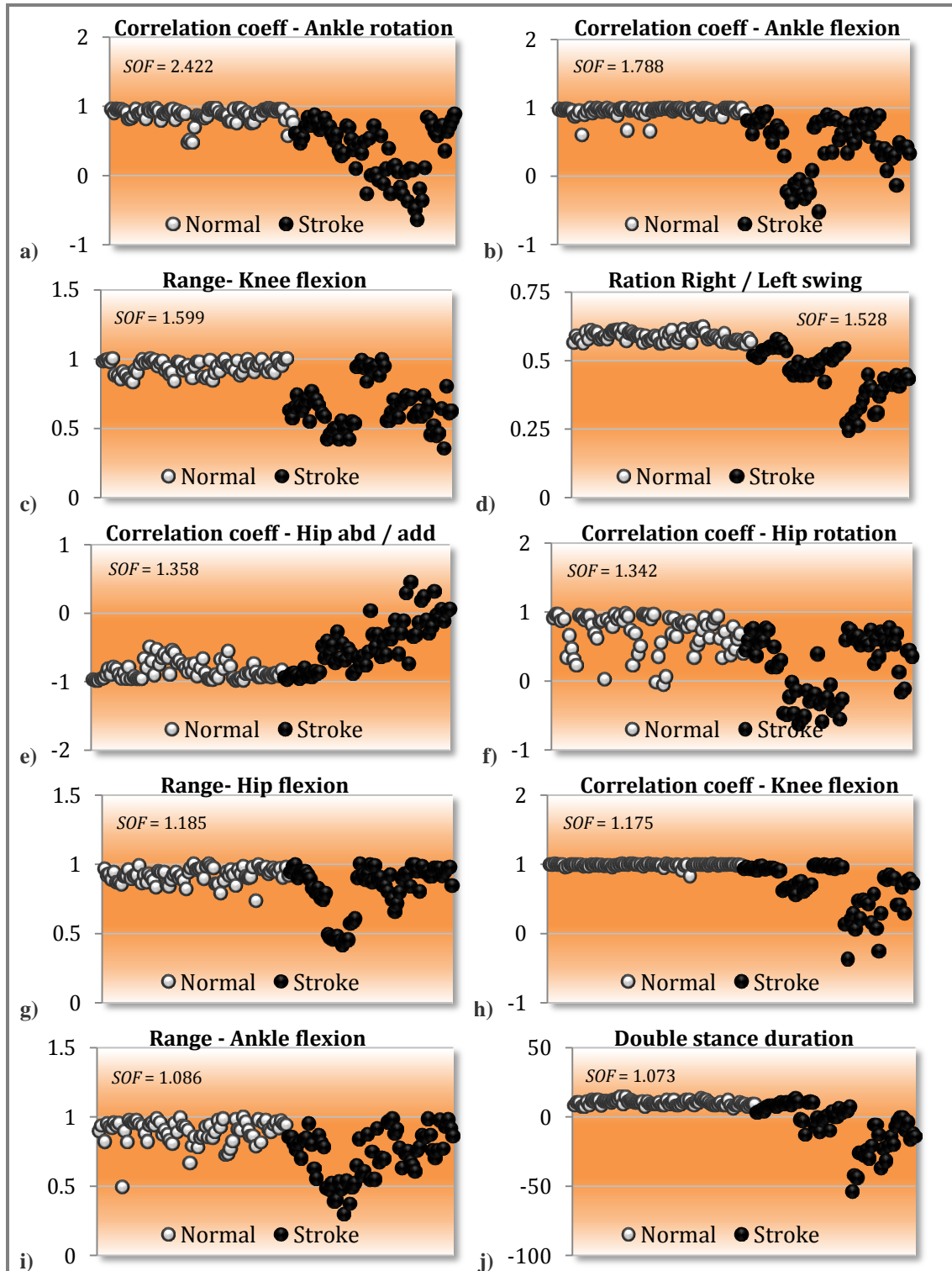
Figure 25: Scatter plots of neural network input variables
(Arranged from 1ˢᵗ (a) to 10ᵗʰ (j) highest SOF value)

These plots also allow for a visual confirmation that the two groups cannot simply be distinguished by comparing average values or standard deviations of subject parameters. Most of the input variables in Figure 25 display a greater variance for stroke patient values than in the normal group (e.g. Figure 25h). Even so, several of the stroke patient values lie in the same range as normal subject values and vice versa. Conventional statistical methods would thus cause a false classification of several of the studied test subjects.

In this study, 24 input parameters were identified with which to train and test the network. These are arranged, in Table 15, from highest to lowest value of SOF.

Table 15: Neural network input parameters

	Input parameters	SOF
1	Correlation coefficient - Ankle rotation	2.422
2	Correlation coefficient - Ankle flexion-extension	1.788
3	L/R Range of motion - Knee flexion-extension	1.599
4	L/R swing ratio	1.528
5	Correlation coefficient - Hip abduction-adduction	1.358
6	Correlation coefficient - Hip rotation	1.342
7	L/R Range of motion - Hip flexion-extension	1.185
8	Correlation coefficient - Knee flexion-extension	1.175
9	L/R Range of motion - Ankle flexion-extension	1.086
10	Double support duration	1.073
11	Correlation coefficient - Hip flexion-extension	0.872
12	L/R step length ratio	0.816
13	L/R Range of motion - Ankle rotation	0.698
14	Correlation coefficient - Knee rotation	0.576
15	Minimum step length (normalized to velocity)	0.572
16	L/R Range of motion - Hip abduction-adduction	0.483
17	L/R stride length ratio	0.387
18	L/R Range of motion - Ankle abduction-adduction	0.330
19	L/R Range of motion - Knee abduction-adduction	0.291
20	Minimum peak hip flexion	0.250
21	L/R Range of motion - Hip rotation	0.246
22	L/R Range of motion - Knee rotation	0.175
23	Correlation coefficient - Knee abduction-adduction	0.086
24	Correlation coefficient - Ankle abduction-adduction	0.050

L/R refers to the ratio between left and right side values.

The choice of parameters were made based on findings by Kim and Eng (2004), Chen *et al.* (2005), Olney and Richards (1996) and Den Otter *et al.* (2007) who studied a variety of differences in gait patterns between able-bodied individuals and those who had suffered a hemiparetic stroke. Chen *et al.* (2005) studied the gait differences between six subjects with post-stroke hemiparesis and six able-bodied controls at

matched speeds and found a noticeable distinction between swing-time and step-length asymmetry of the left and right sides. Asymmetry of swing-time in post-stroke subjects was found to be more than 40% higher than the average value calculated for the able-bodied group (Chen *et al.*, 2005). Otter *et al.* (2007) analysed temporal gait in 24 hemiparetic stroke patients and 14 able-bodied controls and found significant differences in double-stance and single-stance values. Olney and Richards (1996) stated that only 23 - 37% of persons having suffered hemiparetic stroke are able to walk independently within the first week. This value increases to between 50 - 80% after 3 weeks.

Notice that the asymmetry between the left and right side ankle joint angles in the transverse and sagittal planes produce the highest values of SOF. The asymmetry was calculated by taking the correlation coefficient of the left and right side joint-angle curves. Other input parameters include: the ratio between the left and right side maximum range of motion (ROM) for all nine joint angles, the ratio of left and right swing phase to gait cycle, the double-support duration, the minimum step length, the minimum peak hip flexion-extension and the ratio of left to right step and stride lengths. The ROM was calculated from the displacement between the minimum and maximum joint angles measured during a single gait cycle for a specific side. The ratio of left to right side ROMs were then taken as input parameters. The term *L/R* in Table 15 refers to the ratio between the left and right side values. However, since different stroke patients exhibit hemiparesis in different sides of the body, the ratio of *L/R* was corrected to represent the ratio of the lower of the two values to the higher. These values are therefore always equal to, or lower than one, where a value of one implies perfect symmetry between the left and right sides. Figure 25 clearly illustrates this feature. The swing phase for a specific side is the time period between the toe-off instance and the following heel-strike instance. This parameter was chosen because stroke patients tend to display a shorter swing phase in their unaffected side than on their affected side. Similarly stroke patients tend to exhibit a prolonged double-support to aid in their stability. The double-support phase is calculated as the period between the heel-strike instance of one side and the toe-off instance of the other side. During this phase both feet are in contact with the ground.

Stroke patients have a tendency to walk at a lower average velocity than able-bodied subjects. Although this attribute is significant and fairly consistent, a possibility is there that an able-bodied subject walks at a slow speed or that a stroke patient walks at a near normal speed. It was therefore decided to eliminate the effect of velocity by normalizing the step length and evaluating the minimum normalized step length. Stroke patients demonstrate a significantly reduced hip extension. To compensate for this they often exhibit a decrease in hip flexion on the affected side. This characteristic was employed by comparing the minimum peak hip flexion of the two sides. Finally the asymmetries of the step and stride lengths were assessed by taking the ratio between the left and right side lengths.

- 61 -

5.3.3. Training and testing the model

Neural network training and testing parameter matrices were prepared as instructed by the MATLAB2007b neural network toolbox. To achieve the best possible diagnostic performance, network variables such as the goal function (tolerance), the number of hidden-layer neurons and the number of input parameters were optimized. This was accomplished by varying these values within pilot-test-determined ranges and comparing the number of misclassified strides. The goal function was varied between 0.025 and 0.2 in increments of 0.025. The number of input parameters was incrementally decreased from 24 to 4. The parameter with the lowest SOF value was eliminated after each iteration. A rule-of-thumb is that the number of hidden-layer neurons be twice the number of input parameters. This was taken as a reference point around which the number of neurons was varied from seven less to seven more than this point. This is illustrated in the tables shown in Section 5.4.

It was found that the network was unstable at certain combinations of these parameters. It was therefore necessary to test the repeatability of the network at different input scenarios. This was achieved by running the same optimization procedure, mentioned above, 15 times. By doing so, the mean and standard deviation of each scenario could be evaluated over 15 identical runs in order to find the optimum combination of neural network input variables. Optimization results are shown in Section 5.4.

5.3.4. Network training function selection

The MATLAB 2007b neural network toolbox contains several network training functions to choose from. To select the most apt of these functions for the gait data used, three functions were tested using the optimization technique described above. Results were then tabulated as shown in Appendix E. This section will provide a short description of each of the tested training functions followed by a discussion of the selection process used to identify the most apt function for gait data:

5.3.4.1. TRAINLM

The network training function, `trainlm.m`, uses Levenberg-Marquardt optimization to update weight and bias values. This function can train any network provided its net input, weight, and transfer functions have derivative functions. According to the MATLAB Help-menu, this train function assumes that the network has the `mse` performance function which is a basic assumption of the Levenberg-Marquardt algorithm.

The Jacobian (`jX`) of performance (`perf`) is calculated using back-propagation with respect to the weight and bias variables (`X`) and each variable is adjusted according to the Levenberg-Marquardt optimization as shown below:

$$jj = (j_X)(j_X)$$
$$je = (j_X)(E)$$
$$dX = -\frac{[jj + I(mu)]}{je}$$

Here *E* is all errors and *I* is the identity matrix. (according to MATLAB2007b Help menu)

5.3.4.2. TRAINGDM

The postfix `gdm` in `traingdm.m` is an acronym for "gradient descent with momentum back-propagation" which is the method used by this function to update weight and bias values. Again `traingdm.m` can train any network under the condition that its weight, net input, and transfer functions have derivative functions. However, in this case each variable is adjusted according to gradient descent with momentum in appose to the Levenberg-Marquardt optimization used above.

$$dX = mc(dX_{prev}) + lr(1 - mc)(\frac{dperf}{dX})$$

where, according to MATLAB2007b Help menu, dX_{prev} is the previous change to the weight or bias and *dperf/dX* is the derivative of the performance.

5.3.4.3. TRAINGDX

As with `traingdm.m`, each weight and bias variable is adjusted according to gradient descent with momentum, however, this function builds on `traingdm.m` in that it employs an adaptive learning rate. The derivative function is shown below:

$$dX = mc(dX_{prev}) + lr(mc)(\frac{dperf}{dX})$$

5.3.4.4. Selection process

The functions described above were compared for stability and performance using the method explained in Section 5.3.3. A choice had to be made on how to select the optimal combination of these criteria since the input-variable combination producing the best network performance did not match the input combination producing network stability. This was the main argument behind using a visual based optimization procedure. The tables in Section 5.4 and Appendix E depict areas with lower misclassifications using darker shadings. This allowed for a visual investigation of network performance vs. input variable scenario. Conventional methods of optimization does not allow for such a comparison.

- 63 -

5.4. Results

Table 16: Average misclassifications in neural network results over 15 identical runs

	Number of hidden layer neurons (2j+i)														
	-7	**-6**	**-5**	**-4**	**-3**	**-2**	**-1**	**0**	**1**	**2**	**3**	**4**	**5**	**6**	**7**
23	0.6	0.6	0.3	1.1	0.9	1.2	1.1	0.9	0.5	1.1	0.5	1.2	0.6	0.8	0.5
22	0.6	0.7	0.7	0.7	0.5	0.7	0.7	0.8	0.8	0.5	0.6	0.7	0.6	1.2	1.0
21	0.2	0.3	0.2	0.9	0.5	0.7	0.3	0.7	0.8	0.9	0.9	0.5	0.5	0.6	0.6
20	0.5	0.5	0.9	0.8	1.1	0.9	0.7	0.9	0.9	0.9	1.2	1.3	0.6	0.7	1.1
19	2.0	1.5	1.7	1.1	2.0	1.4	1.9	1.7	1.7	1.8	1.9	2.1	1.7	2.0	1.5
18	1.3	1.4	1.2	1.2	1.1	1.4	1.1	1.1	1.2	1.1	1.3	1.5	1.5	1.6	1.5
17	1.6	1.8	1.5	1.5	1.7	1.1	1.1	1.3	1.4	1.0	1.5	1.1	0.7	0.9	1.5
16	1.3	1.3	1.4	1.7	1.1	1.7	1.3	1.5	1.5	1.4	1.3	1.3	1.1	1.2	1.5
15	1.4	1.6	1.0	1.7	1.7	1.3	1.3	1.5	1.5	0.8	1.4	1.1	1.3	1.5	1.3
14	1.8	1.5	1.9	1.9	1.3	1.7	1.7	1.6	1.6	1.7	1.5	1.5	1.3	1.1	1.7
13	1.1	1.1	1.0	1.1	1.0	1.1	1.1	0.9	1.0	1.0	1.1	1.1	1.1	0.9	1.1
12	0.9	1.0	0.9	1.0	1.0	1.0	0.9	1.0	1.0	1.0	1.0	1.0	1.0	1.0	1.0
11	0.9	1.0	0.9	0.9	1.0	1.0	1.0	0.9	0.8	1.0	0.9	1.0	1.0	1.0	1.0
10	0.9	1.0	1.0	1.0	1.0	0.9	1.0	1.0	1.0	0.9	1.0	0.9	0.9	0.9	1.0
9	1.0	1.0	1.0	1.0	1.0	1.0	0.9	0.9	1.0	1.0	1.0	1.0	1.0	1.0	1.0
8	1.0	1.0	0.9	1.0	1.0	1.0	0.9	0.9	1.0	1.0	1.0	0.9	1.0	0.9	0.9
7	1.4	1.1	1.2	1.3	0.9	1.2	1.1	0.9	1.3	1.0	1.1	1.1	1.0	1.1	1.0
6	1.1	1.1	1.0	0.9	1.0	1.0	1.0	1.1	1.0	1.0	0.9	0.9	1.0	0.9	1.0
5	0.9	0.9	1.0	0.9	0.9	1.0	0.8	0.9	0.9	0.9	1.1	0.9	1.1	0.8	0.9
4	1.0	1.0	0.9	0.7	0.8	0.7	0.7	0.7	0.9	0.9	0.8	0.8	0.7	0.5	0.7

Number of input parameters used (j)

Low misclassification ——— High misclassification

Table 17: Standard deviation in neural network results over 15 identical runs

	Number of hidden layer neurons (2j+i)														
	-7	**-6**	**-5**	**-4**	**-3**	**-2**	**-1**	**0**	**1**	**2**	**3**	**4**	**5**	**6**	**7**
23	1.1	0.8	0.5	1.0	1.0	1.5	1.4	0.6	0.7	0.8	0.8	1.4	1.3	0.9	0.6
22	0.9	1.0	0.8	0.7	0.6	0.8	0.9	0.9	0.8	0.7	0.7	1.2	0.6	1.1	0.9
21	0.4	0.8	0.4	1.2	0.7	1.0	0.5	0.9	0.9	0.7	1.2	0.7	0.6	0.7	0.7
20	1.1	0.6	0.8	0.9	1.0	0.7	0.7	0.9	0.7	0.7	1.2	0.8	0.7	0.7	1.1
19	0.5	0.6	0.8	1.0	0.8	0.6	0.8	0.9	0.7	0.7	1.0	1.0	0.5	1.3	1.4
18	0.6	0.9	0.8	0.9	0.6	0.6	0.6	0.8	0.9	0.8	0.7	0.5	0.6	0.7	1.0
17	0.6	0.9	0.7	0.6	1.0	0.8	0.5	0.7	0.6	0.8	0.8	0.7	0.6	0.5	0.8
16	0.6	0.9	0.5	0.9	0.5	0.6	0.6	0.6	0.8	0.5	0.5	0.9	1.1	0.8	0.5
15	0.7	0.7	1.1	1.1	0.8	0.5	0.6	0.6	0.6	0.6	0.5	0.7	0.8	0.5	0.8
14	0.7	0.8	0.8	0.9	0.7	0.8	0.6	0.6	0.8	0.7	0.6	0.6	0.6	0.7	0.5
13	0.3	0.3	0.0	0.3	0.0	0.4	0.5	0.4	0.0	0.0	0.4	0.4	0.5	0.5	0.3
12	0.3	0.0	0.3	0.0	0.0	0.0	0.3	0.0	0.0	0.0	0.0	0.0	0.0	0.0	0.0
11	0.4	0.0	0.4	0.3	0.0	0.0	0.0	0.3	0.4	0.0	0.3	0.0	0.0	0.0	0.0
10	0.3	0.0	0.0	0.0	0.0	0.3	0.0	0.0	0.0	0.3	0.0	0.3	0.4	0.3	0.0
9	0.0	0.0	0.0	0.0	0.0	0.0	0.3	0.3	0.0	0.0	0.0	0.0	0.0	0.0	0.0
8	0.0	0.0	0.3	0.0	0.0	0.0	0.4	0.3	0.0	0.0	0.0	0.3	0.0	0.3	0.3
7	0.6	0.3	0.4	0.5	0.4	0.6	0.4	0.3	0.6	0.0	0.5	0.3	0.0	0.3	0.0
6	0.4	0.3	0.0	0.3	0.0	0.0	0.0	0.5	0.0	0.0	0.3	0.3	0.0	0.3	0.4
5	0.4	0.3	0.0	0.3	0.5	0.0	0.4	0.3	0.5	0.5	0.3	0.3	0.5	0.4	0.3
4	0.0	0.0	0.3	0.5	0.4	0.5	0.5	0.5	0.3	0.3	0.4	0.4	0.5	0.5	0.5

Number of input parameters used (j)

Low standard deviation ——— High standard deviation

Table 18: Average goal tolerance in neural network results over 15 identical runs

		Number of hidden layer neurons (2j+i)														
		-7	-6	-5	-4	-3	-2	-1	0	1	2	3	4	5	6	7
Number of input parameters used (j)	23	0.09	0.09	0.06	0.10	0.07	0.08	0.10	0.11	0.09	0.08	0.09	0.11	0.10	0.11	0.09
	22	0.09	0.07	0.07	0.09	0.08	0.05	0.08	0.08	0.09	0.08	0.07	0.11	0.10	0.10	0.08
	21	0.10	0.09	0.09	0.06	0.10	0.09	0.09	0.09	0.07	0.10	0.08	0.11	0.10	0.10	0.11
	20	0.11	0.09	0.08	0.10	0.10	0.11	0.12	0.09	0.11	0.11	0.11	0.10	0.08	0.12	0.10
	19	0.09	0.11	0.06	0.14	0.07	0.09	0.11	0.10	0.10	0.09	0.09	0.10	0.10	0.09	0.14
	18	0.10	0.07	0.10	0.13	0.10	0.08	0.09	0.10	0.12	0.09	0.10	0.10	0.10	0.08	0.11
	17	0.11	0.10	0.09	0.12	0.10	0.10	0.12	0.11	0.12	0.12	0.10	0.10	0.11	0.11	0.12
	16	0.12	0.12	0.11	0.10	0.10	0.08	0.11	0.09	0.10	0.09	0.12	0.11	0.12	0.10	0.09
	15	0.11	0.10	0.11	0.09	0.10	0.12	0.12	0.10	0.08	0.10	0.09	0.12	0.10	0.12	0.09
	14	0.10	0.11	0.10	0.10	0.11	0.12	0.12	0.12	0.10	0.09	0.10	0.12	0.10	0.14	0.10
	13	0.05	0.06	0.05	0.05	0.05	0.06	0.05	0.09	0.06	0.06	0.06	0.06	0.07	0.10	0.04
	12	0.05	0.05	0.05	0.05	0.04	0.04	0.05	0.04	0.05	0.05	0.05	0.05	0.04	0.06	0.04
	11	0.06	0.04	0.06	0.05	0.04	0.05	0.04	0.05	0.07	0.04	0.05	0.04	0.04	0.04	0.04
	10	0.03	0.04	0.03	0.04	0.04	0.05	0.03	0.04	0.04	0.04	0.03	0.04	0.05	0.04	0.04
	9	0.04	0.04	0.03	0.03	0.04	0.04	0.03	0.05	0.03	0.03	0.03	0.04	0.05	0.04	0.04
	8	0.04	0.04	0.05	0.03	0.04	0.04	0.05	0.04	0.04	0.04	0.04	0.05	0.04	0.05	0.05
	7	0.10	0.10	0.11	0.11	0.10	0.10	0.10	0.12	0.09	0.11	0.10	0.08	0.08	0.10	0.09
	6	0.10	0.10	0.10	0.11	0.09	0.09	0.10	0.11	0.11	0.11	0.11	0.12	0.09	0.11	0.09
	5	0.07	0.07	0.08	0.09	0.10	0.08	0.09	0.09	0.08	0.07	0.08	0.10	0.10	0.07	0.09
	4	0.03	0.05	0.08	0.07	0.07	0.07	0.07	0.08	0.07	0.07	0.07	0.07	0.07	0.07	0.08

Low standard deviation → High standard deviation

Table 19: Standard deviation in goal tolerance in neural network results over 15 identical runs

		Number of hidden layer neurons (2j+i)														
		-7	-6	-5	-4	-3	-2	-1	0	1	2	3	4	5	6	7
Number of input parameters used (j)	23	0.05	0.05	0.04	0.06	0.04	0.06	0.06	0.05	0.05	0.05	0.05	0.05	0.05	0.06	0.05
	22	0.05	0.04	0.05	0.05	0.05	0.02	0.06	0.05	0.04	0.04	0.04	0.05	0.06	0.04	0.04
	21	0.05	0.05	0.06	0.04	0.04	0.04	0.05	0.04	0.05	0.05	0.04	0.07	0.05	0.05	0.06
	20	0.06	0.05	0.05	0.06	0.05	0.06	0.05	0.05	0.06	0.06	0.07	0.06	0.05	0.05	0.06
	19	0.06	0.06	0.04	0.06	0.04	0.05	0.05	0.06	0.05	0.06	0.05	0.05	0.07	0.05	0.06
	18	0.06	0.05	0.04	0.06	0.05	0.04	0.04	0.05	0.05	0.05	0.04	0.06	0.05	0.04	0.06
	17	0.04	0.05	0.05	0.06	0.05	0.05	0.05	0.05	0.05	0.05	0.06	0.05	0.07	0.05	0.04
	16	0.06	0.04	0.05	0.05	0.05	0.06	0.04	0.05	0.06	0.05	0.05	0.05	0.04	0.04	0.04
	15	0.04	0.06	0.06	0.05	0.05	0.06	0.04	0.05	0.04	0.06	0.05	0.07	0.04	0.06	0.05
	14	0.04	0.04	0.05	0.05	0.05	0.05	0.05	0.06	0.05	0.03	0.04	0.04	0.03	0.04	0.04
	13	0.02	0.04	0.02	0.03	0.03	0.03	0.03	0.05	0.03	0.03	0.03	0.02	0.04	0.06	0.02
	12	0.04	0.02	0.03	0.01	0.02	0.01	0.04	0.01	0.03	0.02	0.02	0.02	0.01	0.03	0.01
	11	0.05	0.01	0.05	0.04	0.02	0.02	0.01	0.04	0.05	0.01	0.04	0.01	0.02	0.01	0.01
	10	0.01	0.02	0.01	0.01	0.01	0.04	0.01	0.01	0.01	0.03	0.01	0.03	0.03	0.03	0.01
	9	0.02	0.01	0.01	0.02	0.01	0.02	0.01	0.04	0.01	0.01	0.01	0.01	0.01	0.02	0.02
	8	0.01	0.01	0.04	0.01	0.01	0.01	0.04	0.04	0.01	0.01	0.01	0.04	0.01	0.04	0.04
	7	0.04	0.05	0.05	0.04	0.05	0.05	0.03	0.06	0.04	0.05	0.05	0.04	0.03	0.04	0.05
	6	0.02	0.02	0.03	0.02	0.02	0.02	0.04	0.02	0.03	0.03	0.04	0.04	0.03	0.02	0.03
	5	0.04	0.04	0.05	0.05	0.04	0.03	0.05	0.03	0.02	0.03	0.02	0.04	0.04	0.02	0.04
	4	0.01	0.03	0.03	0.03	0.03	0.03	0.03	0.02	0.03	0.03	0.03	0.02	0.03	0.03	0.02

Low average tolerance → High average tolerance

Table 16 to Table 19 show the results obtained from running the specified neural network 15 identical times. The results above are obtained using the `trainlm.m` network training function. This function displayed the best combination of

performance and repeatability. The results for the other tested training functions are given in Appendix E.

Table 17 to Table 19 clearly indicates that at least eight input parameters are to be considered in order to produce a satisfactory network performance. The network seems to show the highest degree of stability between 8 and 13 input parameters but the highest classification performance between 20 and 23 input parameters. The best performance occurred when using 21 input parameters and either 35 or 33 hidden-layer neurons. Here 12 out of the 15 runs produced 100% correct-classification. However, the goal function at these points showed some variance leading to a reasonable degree of uncertainty. The number of hidden-layer neurons does not seem to play a significant role on either performance or repeatability.

5.5. Discussion

The results showed that at certain combinations of input parameter and hidden-layer-node numbers, the network produced a 100% correct classification of the 166 test strides. At these combinations however, the goal function value varied. At other combinations the network was stable, producing a repeatable accuracy of 99.4% (1 misclassified stroke patient stride in 166 test strides). Upon visual investigation of the misclassified stride (using MOVEN Studio software) it was found that that particular patient displayed very little deviation from those of a typical control group stride. This patient has therefore recovered to a point of quasi-normal gait. This occurrence acts as further motivation for the use of a neural network in this type of application. In a case such as this it might be worth analysing the upper-body gait patterns as these may aid in the classification.

Due to limited numbers of suitable stroke patients and limited time to source and test matching able-bodied subjects, an error could have occurred due to differences in the age and sex demographic between the two subject groups. However, only further testing would reveal if these differences in fact plays a significant role in the accuracy of the network results.

As mentioned earlier, one of the main factors hampering the use of IMC in gait analysis is the lack of confidence in its accuracy only because of the relative adolescence of the technology. Physicians require a tested and trusted system with minimal subjectivity in results. With this in mind, it was decided to place a higher worth on network stability which would imply a greater confidence in results. The combination of network and input variables were therefore selected as in Table 20.

The selected network training function and input variables produced a stable diagnostic accuracy of 99.4%. In a study by Lee *et al.* (2000) an accuracy of between 82.5% and 85% was achieved by their neural network. They used a general

- 66 -

regression neural network and joint angles and spatial parameters from still images as input parameters. The high accuracy achieved is most likely due to the use of angles in all three dimensions compared to the one dimensional images used by Lee *et al.* (2000).

Table 20: Selection of neural network input variable

Variable	Selection
Training function	Trainlm
Nr of input parameters	9 (top nine in Table 15)
Goal function	0.03
Nr of hidden-layer neurons	19
Number of epochs*	500

* See MATLAB2007b Help menu for more information

The neural network is limited in the fact that it only distinguishes between stroke patients and normal subjects. It may be that some of the gait abnormalities displayed by stroke patients are also exhibited by patients with other neuromuscular disorders such as Parkinson's disease or cerebral palsy. There is therefore a definite need to increase the complexity of the network output. This may be achieved by adequately training the network with gait data from several patient groups. There are also subcategories within the specific disorder classes. The presented neural network thus serves mainly as a proof of concept and a basis for further development. What the study aims to prove is that the IMC system allows researchers to gather greater amounts of gait data in a shorter amount of time and independent of the available laboratory facilities. And that these capabilities allow for the implementation of semi-automated-diagnosis tools such as the neural network above.

6. CONCLUSION

6.1. Using full-body IMC in everyday activities

From Section 2.1.3.2 and Appendix C it is apparent that the IMC system is slightly sensitive to local magnetic disturbances. Built-in algorithms are only able to compensate for these disturbances for short periods of time by reducing the work of the magnetometer readings in the correction filter. It is therefore essential to ask what effect this limitation has on the use of IMC in clinical gait analysis.

Firstly, the environments in which clinical gait analysis is employed and the associated equipment were considered. In most cases gait studies are performed within laboratories, hospitals or clinics. Gait laboratories often contain specially adapted walkways in which force-plates are housed. These housings may be constructed using ferrous metal which will lead to EMI. Force plates may also affect readings. These problems can however be eliminated by employing wooden floor mountings and special non interfering force-plates. Most hospitals and clinics contain equipment which may cause EMI. Wires, metal water pipes and steel construction material inside floors are also cause for concern. In both the validity and repeatability studies conducted with the IMC system, steps were taken to avoid the presence of magnetic disturbances. This included removing any metal and electrical objects within a 3 m radius of the test area. Before testing commenced the area was tested for EMI using the IMC system which displays a red dot on the screen if there are significant magnetic disturbances.

The evaluated IMC system also compensates for magnetic interference for periods of up to 30 seconds. In a normal gait analysis this would be sufficient. It must however be stated that the calibration procedure should be done in an EMI-free area. Also between trials, uncompensated orientation drift may diminish the accuracy of the system calibration which would lead to reduced between-trial repeatability. These errors were avoided by frequent recalibration of the IMC system.

Another consideration is that of the gait analysis itself. Clinicians often require the use of stairs, chairs and treadmills to assess the gait of a patient. The latter is of most concern as they make use of electric motors to drive the belt. These motors use electromagnetic fields to drive the motors which lead to definite disturbances in local magnetic fields. Mills *et al*. (2007) conducted gait analysis on ten subjects using a treadmill and EMC which is more sensitive to magnetic disturbances than IMC. They used a specially designed treadmill with non-metallic rollers and with the motor located away from the walking surface.

In all the above-mentioned scenarios, careful planning of the measuring environment and appropriate selection of apparatus could eliminate the limitations associated with

IMC. Force-plates and EMG equipment exist, which could easily be combined with the IMC system.

What sets IMC apart from other technologies however, is its ability to measure patients in any environment, inside and outside. This opens the door for its usefulness in the patient's everyday living environment as well as in telemedicine applications which are discussed in the next section.

6.2. Telemedicine

Telemedicine is a term which describes the idea of taking medical services to areas and communities who are unable to travel to urban areas. This concept is of special importance to a country such as South Africa in which this study was conducted. The use of IMC in clinical gait analysis would mean that persons who were previously unable to afford the use of gait laboratories can now be analysed in their local clinic or even at home. The IMC system used is compact, lightweight and relatively affordable. A physician is therefore able to go to a specific area and conduct gait studies on several patients in a relatively short period of time. Alternatively, rural clinics may acquire an IMC system with which unskilled clinicians may make gait recordings and send these via internet streaming or email to a qualified physician.

6.3. Inertial motion capture for clinical gait analysis

To conclude, the objectives of this study were to investigate the validity and repeatability of IMC in the context of clinical gait analysis. This is motivated by the fact that this technology is still largely untested and therefore underutilized in clinical applications. It was found that currently used kinematic gait measuring systems are mostly bound to laboratory use and therefore relatively costly and time consuming. They lack versatility and mobility which is increasingly required from such a system. In order to gain the trust in IMC from physicians and researchers, research studies such as this one is required which quantitatively compare IMC to proven and mature technologies.

To this end, validity and repeatability studies were conducted using a commercially available full-body IMC system. Validity study results showed good correlation between kinematic joint angles in the sagittal and frontal planes for the knees and hips and acceptable comparison in the transverse planes of these joints. The ankle joint angles proved less comparable with average validly results. Discrepancies were accounted to a combination of factors including a misalignment of rotation axes and non-ideal design of the IMC system foot sensor.

Repeatability study results on the other hand were excellent when compared to similar studies using OMC and EMC. Within-day repeatability of IMC measured

results was higher than that recorded using OMC for both frontal and transverse plane angles of all three joint pairs. The sagital plane repeatability performed slightly better in OMC tests. Within-day values recorded using EMC were in most cases slightly higher than those recoded for the IMC system, however the within-day repeatability using IMC was high across the board. Between-day repeatability seems to be where the strength of the IMC system lies. Results show that the IMC system has, for most of the analysed joint angles, superior between-day repeatability when compared to both the OMC and EMC systems. It may therefore be concluded that the IMC system produces repeatable kinematic joint angles patterns from one test day to the next. This is of greater use in rehabilitation studies where changes in gait patterns due to improvements in locomotion are generally small.

Temporal-spatial repeatability was not as good as that of the joint kinematics because of limitations in gait phase identification algorithms, however repeatability values were acceptable for use in clinical gait analysis. Again, a greater degree of repeatability was found in between-day tests than in within-day tests.

Finally an ealuation was made in Section 5 of the diagnostic potential of IMC in a clinical application. Here a neural network was trained and tested using gait parameters from stroke patients and able-bodied subjects in an attempt to automatically distinguish between these two groups. The selected network was tested for repeatability and based on this the network input variables were selected. The result section was a neural network that was 99.4% accurate in determining whether a measured stride came from an able-bodied subject or a stroke patient.

It is therefore concluded that the commercially available, full-body IMC system is suited for use in clinical gait assessments, not only in conventional laboratory tests but also in adverse and rural environments. The tested system is user-friendly, requires little time for calibration and testing, is relatively inexpensive and can easily be combined with semi-automatic diagnosis methods. These aspects address limitations stated by Simon (2004) which have lead to the under-utilization of gait analysis in general patient care.

6.4. Recommendations

Further analysis into the definition of the ankle joint axis is required for both the OMC and IMC systems to determine the root of this difference. In the same context, refinement of the spatial gait phase identification algorithm should be done to better match the heel-strike and toe-off instances found with real values. This may also lead to improved step length calculation.

Improvements of the IMC system foot sensor may include: reducing the sensor size, creating a rounded sensor base adapted to the shape of the foot, or placing the sensor cable attachment on another side of the sensor.

6.5. Future work

The IMC system allows for relatively quick and simple collection of vast amounts of gait data. This includes data from patients and controls. With this in mind a study may be conducted in which a neural network may be trained and tested for a wider variety of gait pathologies. The network could for example distinguish between patients with CP, PD or stroke. A network such as that would be of great use in telemedicine to determine the treatment required for patients without them having to incur the costs involved in travelling to urban areas and seeing a specialist face-to-face.

Another study may combine motion capture with the measure of other physiological parameters in a self-contained bio-measurement suit. The applications of such a suit are endless, especially in sports, medicine and ergonomic studies.
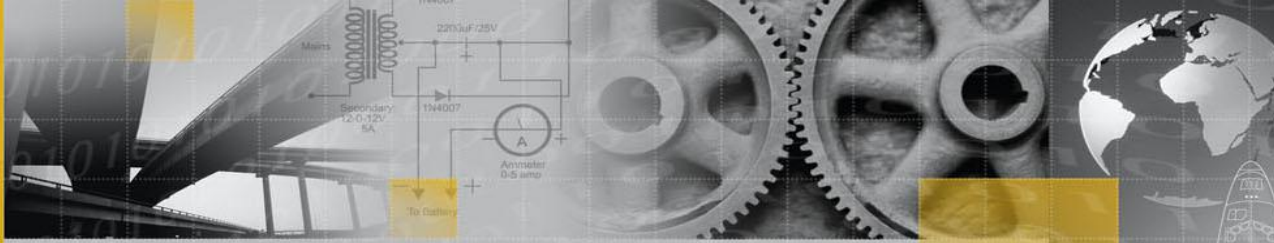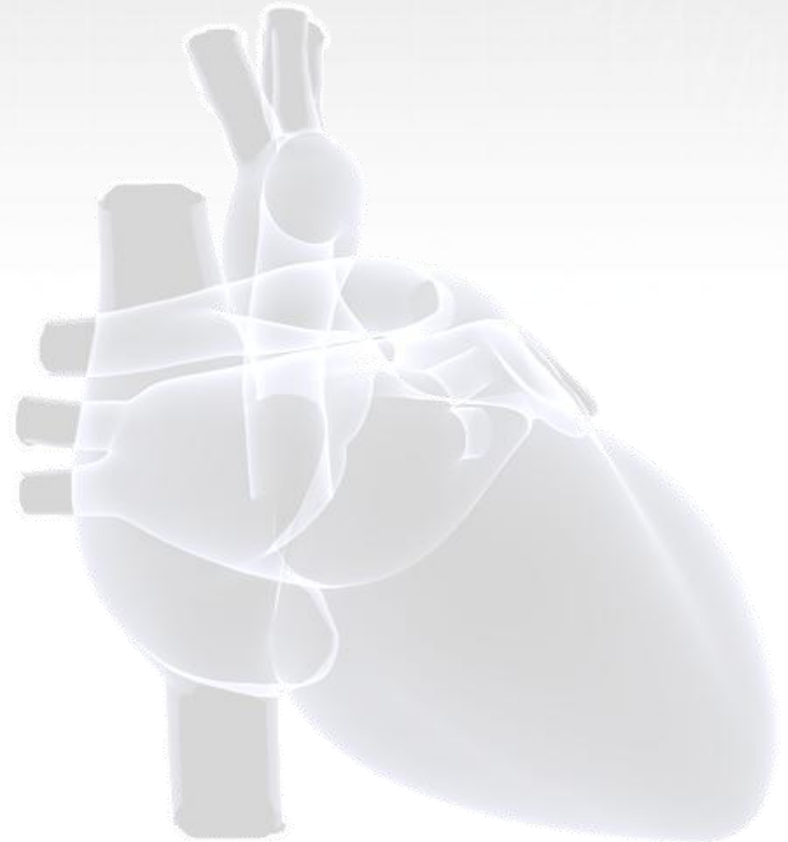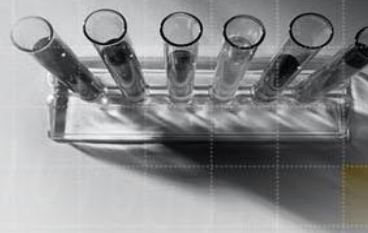
- 71 -

References

7. REFERENCES

Aminian, K., Najafi, B., Büla, C., Leyvraz, P., and Robert, P. (2001). Ambulatory gait analysis using gyroscopes. *In*: *American Society of Biomechanics Annual Meeting, 2001*. San Diego.

Ascension Technology Corporation. (2007). *MotionStar Wireless® 2*. [online]. [Accessed 17 September 2008]. Available form World Wide Web: http://www.ascension-tech.com/products/motionstarwireless.php

Bachmann, E. R. (2000). *Inertial and Magnetic Tracking of Limb Segment Orientation for Inserting Humans Into Synthetic Environments.,*. Monterey, California.

Baker, R. (2007). The history of gait analysis before the advent of modern computers. *Gait and Posture*,Vol. 26(3), pp.331-342.

Besier, T. F., Sturnieks, D. L., Alderson, J. A., and Lloyd, D. G. (2003). Repeatability of gait data using a functional hip joint centre and a mean helical knee axis. *Journal of Biomechanics*,Vol. 36, pp.1159-1168.

Boulgouris, N. V., Hatzinakos, D., and Plataniotis, K. N. (2005). Gait Recognition: A challenging signal processing technology for biometric identification. *IEEE Signal Processing Magazine*, November, pp.78-90.

Bronner, S. (undated). *Instrumented Analysis of Human Motion*. [online]. [Accessed 2 November 2007].

Chen, G., Patten, C., Kothari, D. H., and Zajac, F. E. (2005). Gait differences between individuals with post-stroke hemiparesis and non-disabled controls at matched speeds. *Gait & Posture*,Vol. (22), pp.51-56.

Corazza, S., Mündermann, L., and Andriacchi, T. (2006). Markerless Motion Capture Methods for Estimation of Human Body Kinematics. *In*: *International symposium on the 3D analysis of human motion, 2006*. Valenciennes, France.

Dejnabadi, H., Jolles, B. M., and Aminian, K. (2005). A New Approach to Accurate Measurement of Uniaxial Joint Angles Based on a Combination of Accelerometers and Gyroscopes. *In*: IEEE, (ed). *IEEE Transactions on Biomechanical Engineering, 2005*., pp.1478-1484.

Dejnabadi, H., Jolles, B. M., Casanova, E., Fua, P., and Aminian, K. (2006). Estimation and Visualization of Sagittal Kinematics of Lower Limb Orientation Using Body-Fixed Sensors. *In*: IEEE, (ed). *IEEE Transactions on Biomechanical Engineering, 2006*., pp.1385-1393.

Den Otter, A. R., Geurts, A. C. H., Mulder, T., and Duysens, J. (2007). Abnormalities in the temporal patterning of lower extremity muscle activity in hemiparetic gait. *Gait & Posture*,Vol. (25), pp.342-352.

Diebel, J. (2006). *Representing Attitude: Euler Angles, Unit Quaternions, and Rotation Vectors*. Stanford: Stanford University.

Ebersbach, G., Sojer, M., Valleoriola, F., Wissel, J., Müller, J., Tolosa, E., and Poewe, W. (1999). Comparitive analysis of gait in Parkinson's disease, cerebellar ataxia and subcortical arterioscerotic encephalopathy. *Brain*,Vol. 122, pp.1349-1355.

Ephanov, A. and Hurmuzlu, Y. (2001). *Generating Pathological Gait Patterns via the Use of Robotic Locomotion Models*. [online]. [Accessed 19 January 2007]. Available form World Wide Web: http://engr.smu.edu/me/syslab/papers/Simul_Pathology.pdf

Favre, J., Aissaoui, R., Jolles, B. M., Siegrist, O., de Gruise, J. A., and Aminian, K. (2006). 3D joint rotation measurement using MEMs inertial sensors: Application to the knee joint. *In*: *International symposium on the 3D analysis of human motion , 2006*. Valenciennes, France.

Flavin, P. (1999). *Bipedal Human Gait: A 3d Interactive Model with Animation*. [online]. [Accessed 2 January 2007].

Frey, W., Zyda, M., Mcghee, R., and Cockayne, B. (1996). *Off-the-shelf, real-time, human body motion capture for synthetic environments*. California.

Garg, V. (undated). *Gait disturbances*. [online]. [Accessed 31 May 2007]. Available form World Wide Web: http://pain.health.ivillage.com/armlegpain/gaitdisturbances3.cfm

Gök, H., Ergin, S., and Yavuzer, G. (2002). Kinetic and kinematic characteristics of gait in patients with medial knee arthrosis. *Acta Orthop Scand*,Vol. 73(6), pp.647-652.

Han, J., Jeon, H. S., Jeon, B. S., and Park, K. S. (2006). Gait detection from three dimentional acceleration signals of ankles for tha patient with Parkinson's disease. *In*: *ITAB, 2006*. Ioannina, Epirus.

Huhn, K. (undated). *An overview of instrumentad gait analysis*. [online]. [Accessed 20 June 2007]. Available form World Wide Web: http://www.umdnj.edu/idsweb/tech_reviews/Karen/.

International Society of Biomechanics. (2002). Letter to the editor. *Journal of Biomechanics*,Vol. 35, pp.543-548.

Kadaba, M. P., Ramakrishnan, H. K., Wootten, M. E., Gainey, J., Gorton, G., and Cochran, G. V. B. (1989). Repeatability of Kinematic, Kinetic, and Elevtromyographic Data in Normal Adult Gait. *Journal of Orthopedic Research*,Vol. 7, pp.849-860.

Kim, C. M. and Eng, J. J. (2004). Magnitude and pattern of 3D kinematic and kinetic gait profiles in persons with stroke: relationship to walking speed. *Gait and Posture*,Vol. (20), pp.140-146.

Lackovic, I., Bilas, V., Santic, A., and Nikolic, V. (2000). Measuring of gait parameters from free moving subjects. *Measurement*,Vol. 27, pp.121-131.

Lee, H., Guan, L., and Burne, J. A. (2000). Human gait and posture analysis for diagnosing neurological disorders. *In*: *International Conference on Image Processing, 2000.*, pp.435-438.

Lucchetti, L., Cappozzo, A., Cappello, A., and Della Croce, U. (1998). Skin movement artifact assessment and compensation in the estimation of knee-joint kinematics. *Journal of Biomechanics*,Vol. 31, pp.977-984.

Luinge, H. J. (2002). *Inertial Sensing of Human Movement*. Twente: Univercity of Twente.

Luinge, H. J. and Veltink, P. H. (2005). Measuring orientation of human body segmants using miniature gyroscopes and accelerometers. *Medical and Biological Engineering and Computing*,Vol. 43, pp.273-282.

Mackey, A. H., Walt, S. E., Lobb, G. A., and Stott, N. S. (2005). Reliability of upper and lower limb three-dimentional kinematics in children with hemiplegia. *Gait and Posture*,Vol. 22, pp.1-9.

Mdlanzi, L., Marwala, T., Stander, C. J., Scheffer, C., and Heyns, P. S. (2007). *Principal component analysis and automatic relevance determination in damage identification*. [online]. [Accessed 29 September 2008]. Available form World Wide Web: http://arxiv.org/abs/0705.1672

MIE Medical Research Ltd. (undated). *Gait analysis system*. [online]. [Accessed 3 April 2007]. Available form World Wide Web: http://www.mie-uk.com/gait/index.htm

Miller, N., Jenkins, O. C., Kallmann, M., and Matarić, M. J. (2004). Motion capture from inertial sensing for untethered humanoid teleoperation. *In*: *4th IEEE/RAS International Conference on Humanoid Robots, 10 Nov 2004*. World Scientific Publishing Company, pp.547-565.

Mills, P. M., Morrison, S., Lloyd, D. G., and Barrett, R. S. (2007). Repeatability of 3D gait kinematics obtained from an electromagnetid tracking system during treadmill locomotion. *Journal of Biomechanics*,Vol. (40), pp.1504-1511.

Molson Medical Informatics. (1999). *Normal Gait*. [online]. [Accessed 3 April 2007]. Available form World Wide Web: http://sprojects.mmi.mcgill.ca/gait/normal/intro.asp

Mulroy, S., Gronley, J., Weiss, W., Newsam, C., and Perry, J. (2003). Use of cluster analysis for gait pattern classification of patients in the early and late recovery phases following stroke. *Gait and Posture*,Vol. (18), pp.114-125.

Olney, J. and Richards, C. (1996). Hemiparetic gait following stroke. Part I: Characteristics. *Gait & Posture*,Vol. (4), pp.136-148.

Richards, J. (2008). *Biomechanics in Clinic and Research*. Preston: Elsevier.

Roetenberg, D. (2006). *Inertial and Magnetic Sensing of Human Motion*. Twente.

Roetenberg, D., Baten, C. T. M., and Veltink, P. H. (2007a). Estimating body segment orientation by applying inertial and magnetic sensing near ferromagnetic materials. *IEEE Trans Neural Syst Rehabil Eng*,Vol. 15(3), pp.469-471.

Roetenberg, D., Luinge, H., and Slycke, P. (2007b). Moven: Full 6DOF Human Motion Tracking Using Miniture Inertial Sensors. *Unpublished*.

Roetenberg, D., Slycke, P. J., and Veltink, P. H. (2007c). Ambulatory Position and Orientation Tracking Fusing Magnetic and Inertial Sensing. *IEEE Trans of Biomedical Engineering*,Vol. 54(5), pp.883-890.

Salarian, A., Russmann, H., Vingerhoets, F. J., Dehollain, C., Blanc, Y., Burkhard, P. R., and Aminian, K. (2004). Gait Assessment in Parkinson's Disease: Toward an Ambulatory System for Long-Term Monitoring. *In*: *IEEE Transactions on Biomechanical Engineering, 2004.*, pp.1434-1443.

Simon, S. R. (2004). Quantification of human motion: gait analysis-benefits and limitations to its application to clinical problems. *Journal of Biomechanics*,Vol. 37, pp.1869-1880.

Steinwender, G., Saraph, V., Scheiber, S., Zwick, E. B., Uitz, C., and Hackl, K. (2000). Intrasubject repeatability of gait analysis data in normal and spastic children. *Clinical Biomechanics*,Vol. 15, pp.134-139.

Stolse, H., Kuhtz-Buschbeck, J. P., Drücke, H., Jöhnk, K., Illert, M., and Deuschl, G. (2001). Comparitive analysis of the gait disorder of normal pressure hydrocephalus and Parkinson's disease. *Journal for Neurology, Neurosurgery and Psychiatry*,Vol. 70, pp.289-297.

Su, F.-C. and Wu, W.-L. (2000). Design and testing of a generic algorithm neural network in the assessment of gait patterns. *Medical Engineering & Physics*,Vol. (22), pp.67-74.

Thies, S. B., Tresadern, P., Kenney, L., Howard, D., Goulermas, J. Y., Smith, C., and Rigby, J. (2007). Comparison of linear accelerations from three measurement systems during 'reach & grasp'. *Medical Engineering and Physics*,Vol. 29(9), pp.967-972.

Vardaxis, V. G., Allard, P., Lachance, R., and Duhaime, M. (1998). Classification of able-bodied gait using 3-D muscle powers. *Human Movement Science*,Vol. 17, pp.121-136.

Vlasic, D., Adelsberger, R., Vannucci, G., Barnwell, J., Gross, M., Matusik, W., and Popović, J. (2007). Practical Motion Capture in Everyday Surroundings. *In*: *ACM Transactions on Graphics, 2007*.

von Acht, V., Bongers, E., Lambert, N., and Verberne, R. (2007). Miniature Wireless Inertial Sensors for Measuring Human Motion. *In*: *29th Annual International Conference of the IEEE EMBS, 2007*. Lyon:, pp.6278-6281.

Weisstein, E. W. (undated). *Correlation Coefficient*. [online]. Available form World Wide Web: http://mathwolrd.wolfram.com/CorrelationCoefficient.html

Welch, G. and Foxlin, E. (2002). Motion Tracking: No Silver Bullet, but a Respectable Arsenal. *IEEE Computer Graphics and Applications*,Vol. 22(6), pp.24-38.

White, S. C., Yack, H. J., and Winter, D. (1989). A three-dimensional musculoskeletal model for gait analysis. Anatomical variability estimates. *Journal of Biomechanics*,Vol. 22(8-9), pp.885-893.

Whiting, W. C. and Rugg, S. (2006). *Dynatomy: Dynamic Human Anatomy*. USA: Human Kinematics.

Whittle, M. W. (1996). Clinical gait analysis: A review. *Human Motion Science*,Vol. 15, pp.369-387.

Xsens Technologies. (2007). *Moven - Inertial motion capturing*. [online]. [Accessed 16 March 2007]. Available form World Wide Web: http://www.xsens.com/index.php?mainmenu=products&submenu=human_motion&subsubmenu=Moven

Xsens Technologies. (2008). *Moven*. Enschede.

Yavuzer, G., Öken, Ö., Elhan, A., and Stam, H. J. (2006). Repeatability of lower limb three-dimensional kinematics in patients with stroke. *Gait & Posture*,Vol. 24(2), pp.S188 - S190.

Zhou, H. and Hu, H. (2004). *A Survey - Human Tracking and Stroke Rehabilitation*. Essex.

- R5 -
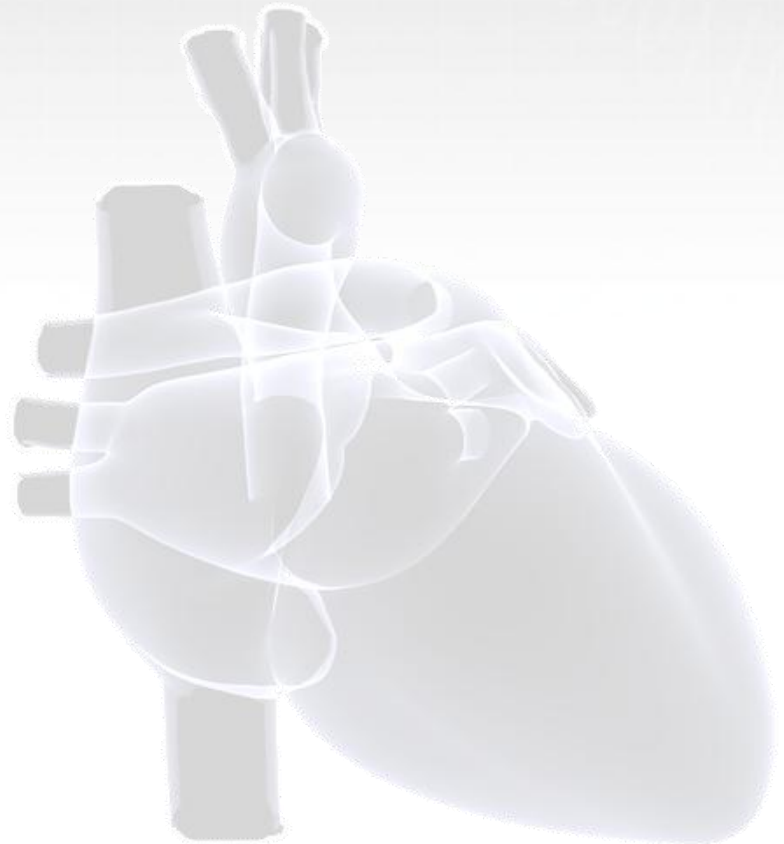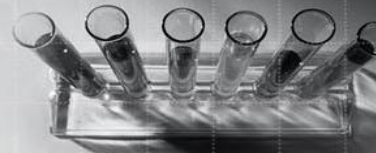
Appendices

FAKULTEIT INGENIEURSWESE
FACULTY OF ENGINEERING
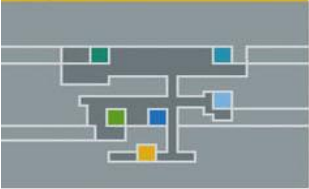
UNIVERSITEIT
STELLENBOSCH
UNIVERSITY

8. APPENDICES

8.1. Appendix A: Gait parameters

8.1.1. Temporal parameters
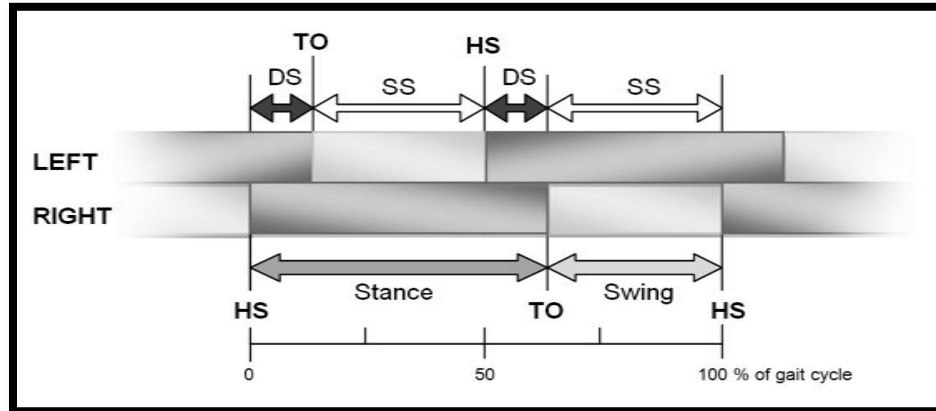
Figure 26: Temporal gait parameters

Parameter	Location/Description
Step Time	The time elapsed from the first contact of one foot to the first contact of the opposite foot
Stride Time (Gait Cycle)	The elapsed time between the first contact of two consecutive footfalls of the same foot
Cadence	The step rate, measured in steps per minute, usually calculated as an average for a full walking measurement
Ambulation Time	The time elapsed between the first contacts of the first and the last footfalls
Velocity	Obtained by dividing the Distance by the Ambulation time. Also step length multiplied by cadence
Mean Normalized Velocity	Obtained by dividing the Velocity by the Average Leg Length and it is expressed in leg length per second (LL/sec). The average Leg Length is computed (left leg length + right leg length)/2
Single Support time [SS]	The time elapsed between the Last Contact of the current footfall to the First Contact of the next footfall of the same foot. This is equal to the Swing Time of the opposite foot
Double Support [DS]	The time elapsed between First Contact of the current footfall and the Last Contact of the previous footfall, added to the time elapsed between the Last Contact of the current footfall and the First Contact of the next footfall
Stance Time	The time elapsed between the First Contact and the Last Contact of two consecutive footfalls on the same foot. It is also presented as a percentage of the Gait Cycle of the same foot
Swing Time	The time elapsed between the Last Contact of the current footfall to the First Contact of the next footfall on the same foot. It is also presented as a percentage of the Gait Cycle of the same foot. The Swing Time is equal to the Single Support time of the opposite foot
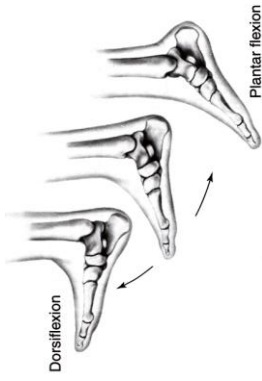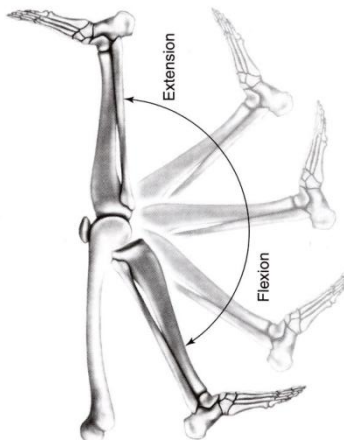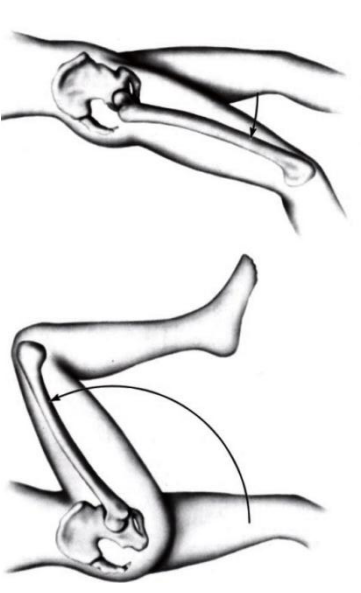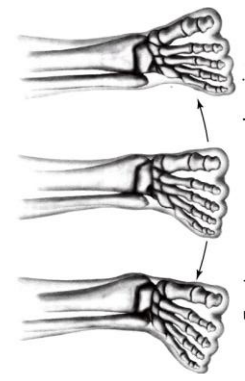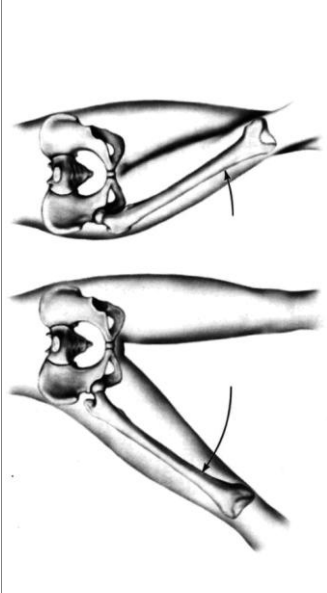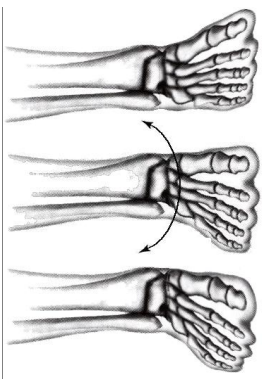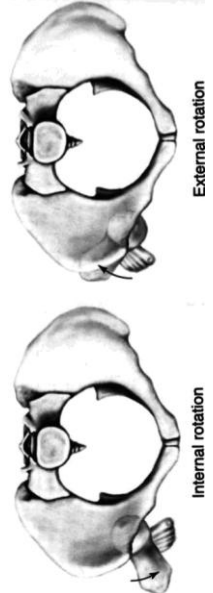
8.1.2. Spatial parameters
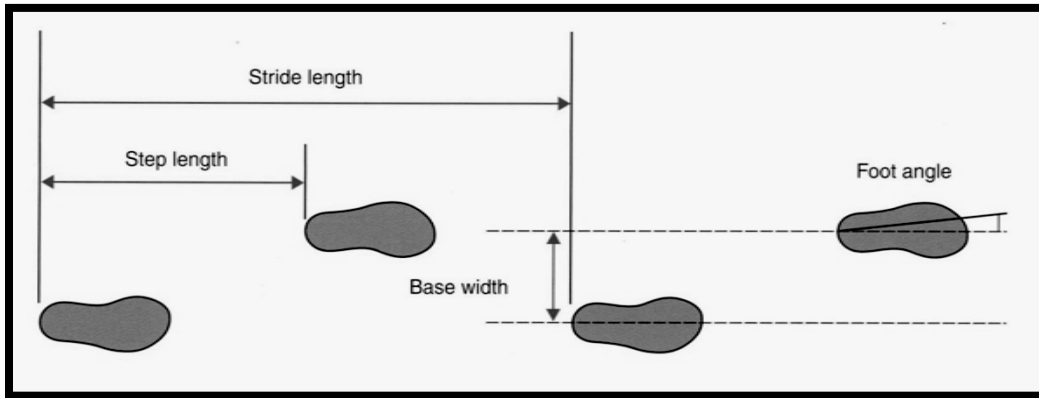
Figure 27: Spatial gait parameters
Source: Richards, 2008

Parameter	Location/Description
Step Length	Measured on the horizontal axis of the walkway from the heel point of the current footfall to the heel point of the previous footfall on the opposite foot. The step length can be a negative value if the patient fails to bring the landing foot heel point forward of the stationary foot heel point
Stride Length	Measured on the line of progression between the heel points of two consecutive footfalls of the same foot (left to left, right to right)
Step/Extremity Ratio	Step Length divided by the Leg Length of the same leg
Step width (Base width)	The measured distance between an equivalent point on the right and left heels for one step (May also be averaged over several steps)
Vertical foot clearance	Vertical distance between the lowest part of the foot and the walking surface
Toe In / Toe Out (Foot angle)	The angle between the line of progression and the line connecting the heel point to the forward point of the footfall. This angle is reported positive for toe out and negative for toe in
H-H Base of Support	The perpendicular distance from heel point of one footfall to the line of progression of the opposite foot
Distance	Measured on the horizontal axis from the heel point of the first footfall to the heel point of the last footfall

- A2 -

8.1.3. Joint angles

8.2. Appendix B: Pathological gait

Gait abnormalities can generally be divided in structural and neurological gait although these overlap significantly. The table below shows the most common gait disturbances: (Garg, 2007)

	Disturbance	Location/Description
Structural gait disturbances	Limp	A jerky, uneven gait that may be caused by pain, weakness or deformity. *Antalgic* gait, a type of limp, is the most common gait disturbance. It is caused by pain and compensates for that pain by keeping weight off of a painful part as much as possible
	Spastic gait	A stiff gait where the toes catch and drag, the legs are held together and the hips and knees are kept in a slightly bent position
	Hemiplegic gait	This gait is characteristic of paralysis or weakness in one leg and is common after a stroke. The patient swings the paralyzed leg around to bring the foot in front. This gait avoids placing weight on the affected leg
	Senile gait	This gait is usually seen in the elderly. It is associated with a stooped posture, with knees and hips bent. Arm swinging is lessened and there is stiffness in turning. Steps are small and broad-based
	Waddling gait	The feet are held wide apart and the patient walks somewhat like a duck. This is a common gait disturbance in late pregnancy
Neurological gait disturbances	Festinating gait	In this gait disturbance, the patient walks on the toes as if being pushed. Steps start slowly and increase in speed. Often, the patient cannot stop until grasping or running into something
	Parkinson's gait	This is a form of festinating gait characteristic of Parkinson's disease. Steps are short and shuffling, with feet scrapping the ground. They start slow and build up speed. The patient's upper body is bent forward, head down, and arms, elbows, hips and knees are bent
	Magnetic gait	Also called glue-footed gait. The patient seems to have difficulty taking the first step, as though the feet had been glued to the ground. Once the first step is made, subsequent steps are small and shuffling
	Double-step gait	In this gait disturbance, alternating steps are made of different length or rate. The stride of one side does not match the other
	Helicopod gait	The patient swings one or both feet in a half circle with each step
	Scissor gait	In this gait, the legs cross in walking. The left leg moves too far to the right and the right leg moves too far to the left
Structural and Neurological gait disturbances	Ataxic gait	A staggering, unsteady and uncoordinated gait typically caused by abnormalities of the nervous system. A variation of this is the *tabetic gait*, a high-stepping ataxic gait where the feet slap the ground
	Toe-walking gait	This is a common gait disturbance in which the patient walks on the toes. A variation on this is the equine gait, which is a high-stepping toe-walking gait
	Steppage gait	Commonly seen with foot drop, where the foot appears to hang limp at the ankle. The foot is lifted high so that the toes do not drag on the ground and the toes touch ground first. The hip and knee are typically bent more than normal in order to clear the toes from the ground

- A4 -

8.3. Appendix C: Gait parameter calculation script

Since the IMC manufacturer software does not include the functionality of calculating gait parameters, these calculations had to be done with the aid of custom software. MATLAB 2007b was used to manipulate position and orientation data into useful temporal-spatial and joint angle values. The diagram below systematically describes the data processing and calculations used and is followed by a short description of each of the functions used (e.g. `gaitpar.m`).
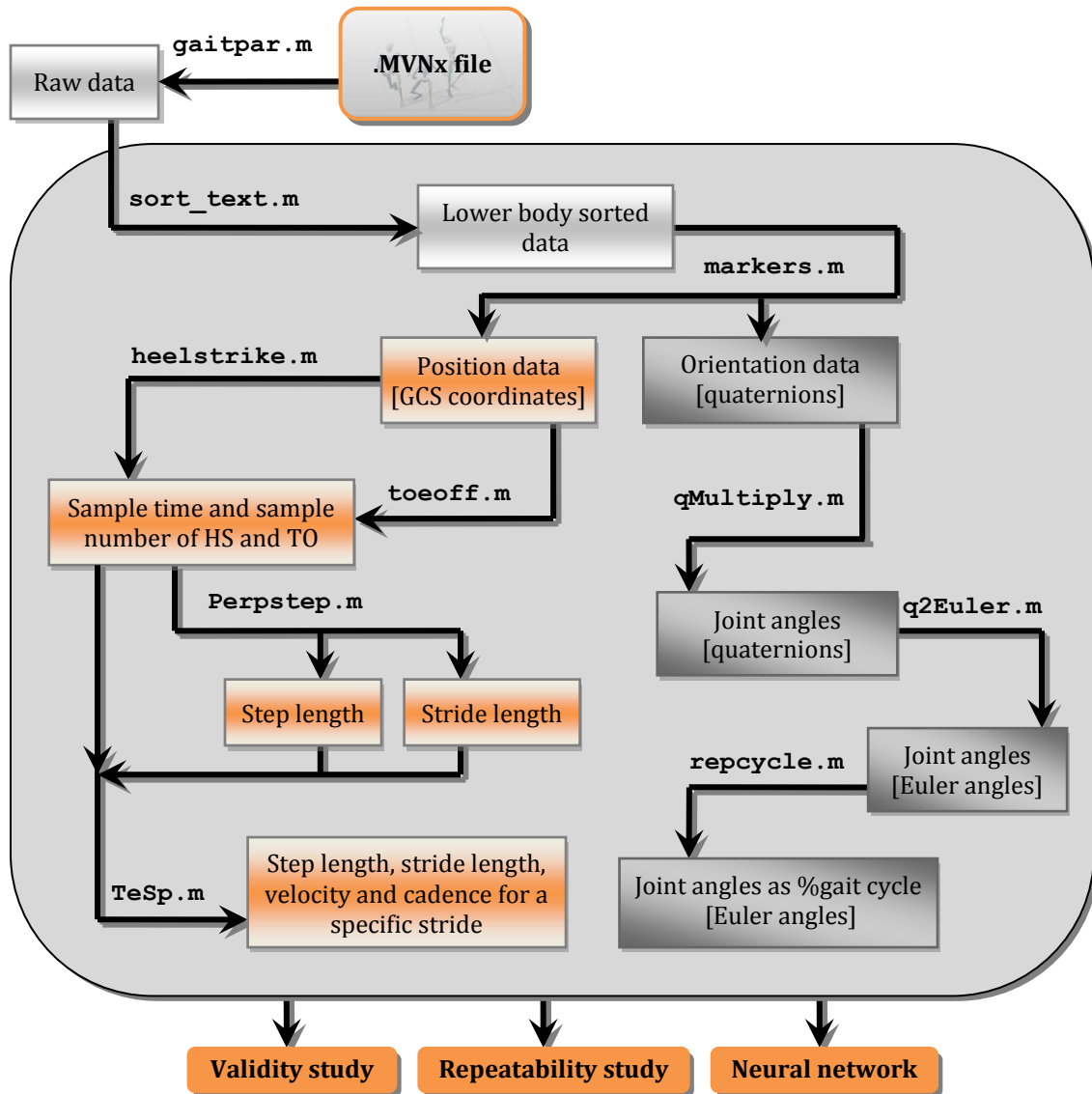
Figure 28: Schematic of gait parameter calculation script

```
gaitpar.m
```

This function was used in each of the three main sections to calculate the required gait parameters from a specific *.MVNx file. The function controls several sub-functions as shown in Figure 28. These are described below. Some calculations such as those for step and stride lengths are completed within this function.

```
sort_text.m
```

The Xsens proprietary MVNx file described in Appendix C contains several lines of initialization parameters as well as miscellaneous data such as the date of recording. Following these lines of information is a large matrix containing position and orientation data of each of the 23 body model segments. This function reads this matrix along with the number of recorded frames and the recording frame-rate.

```
markers.m
```

To simplify orientation and position data handling, these values were sorted into manageable variables named according to the specific segment and a hyphenated p or q for position and orientation respectively (e.g. the left-foot-segment position and orientation variables are LF_p and LF_q. Here position variables are three-column matrices with each row containing the segment position components in the GCS for each time frame. Orientation variables consist of four-column matrices with each row consisting of four unit quaternions also in the GCS). As this study focused only on the lower body gait parameters, only these were sorted for further use.

```
heelstrike.m
```

This function uses the position vectors of the feet to calculate the heel-strike instances. x- and y-plane coordinates are differentiated over time to show when the respective foot is in motion at a specific time frame. These values of $\dot{x}$ and $\dot{y}$ are multiplied to produce a plot of velocity vs. time. Values are then forced into binary form by taking the twelfth power of velocity and then applying a threshold filter. The exponential multiplication was done to force low values to zero and higher values to very high values. A threshold was applied with the aid of the `peakdet.m` built-in MATLAB function. After this step a running loop was created to find the rising edges which were taken as the points of heel-strike. This is similar to the approach followed by Han *et al.* (2006).

```
toeoff.m
```

This function is identical to heelstrike.m except that the falling edges are found and taken as the points of toe-off.

- A6 -

PerpStep.m

The Vicon OMC calibrates its spatial test volume in such a way that the subject walks parallel to the y-axis. This simplifies step length calculations as the x-coordinates can be employed directly. The Moven IMC calibrates to a pose which faces in the direction of magnetic north. For this reason, a direction vector (simulating the y-axis of the Vicon) had to be determined. The step and stride lengths were then found by taking the component of foot displacement parallel to the direction vector.

TeSp.m

As mentioned above, step and stride lengths are calculated within `PerpStep.m`. These lengths are calculated for the entire recording. From these values `TeSp.m` isolates the step and stride length for a specific studied stride. It also calculates the velocity and cadence for that specific stride. Velocity is taken as the absolute displacement of the pelvis from one heel-strike to the next divided by the time between these consecutive instances. From this cadence is calculated by *Cadence = (Velocity x 60) / Step length*.

qMultiply.m

In order to find the segment orientation, the formula, as proposed by Roetenberg, Luinge and Slycke (2007), was used. In this formula the quaternion multiplication of the complex conjugate of the proximal segment and the distal segments are calculated producing the BCS joint angle in quaternion form.

q2Euler.m

Most commercial gait packages represent measured parameters by means of Euler angles as discussed in Section 3.4.1. This function was therefore employed to convert joint angles from quaternions to Euler angles using the formula given in Section 3.4.1 by Diebel (2006). The formula was derived for the xyz Cardan sequence also known as the JCS as proposed by Grood and Suntay (1983).

repcycle.m

Finally a function was required to normalize the joint angles of any given isolated stride to a percentage of the gait cycle. The function `repcycle.m` uses the MATLAB function `resample` to resample the isolated stride to 100 data point, each representing 1% of the gait cycle.

8.4. Appendix D: Validity study results

8.4.1. Temporal-spatial validity results

Table 21: Temporal-spatial validity results - Slow walk (Suit)

	Gait parameters		Difference
	IMC	OMC	
	Mean ± SD	Mean ± SD	E_{RMS} #
Stride length#	0.839 ± 0.21	0.862 ± 0.07	0.067
Step length	0.444 ± 0.05	0.433 ± 0.05	0.194
Velocity	0.474 ± 0.06	0.469 ± 0.04	0.045
Cadence	64.44 ± 8.19	65.87 ± 10.0	12.357

\# Units for gait parameters are as follows: Stride length [m], step length [m], velocity [m/s] and cadence [steps/min]

Table 22: Temporal-spatial validity results - Normal walk (Suit)

	Gait parameters		Difference
	IMC	OMC	
	Mean ± SD	Mean ± SD	E_{RMS} #
Stride length#	1.50 ± 0.14	1.49 ± 0.13	0.046
Step length	0.759 ± 0.08	0.751 ± 0.07	0.067
Velocity	1.329 ± 0.14	1.315 ± 0.12	0.060
Cadence	105.1 ± 5.15	105.0 ± 4.0	5.670

\# Units for gait parameters are as follows: Stride length [m], step length [m], velocity [m/s] and cadence [steps/min]

Table 23: Temporal-spatial validity results - Slow walk (Straps)

	Gait parameters		Difference
	IMC	OMC	
	Mean ± SD	Mean ± SD	E_{RMS} #
Stride length#	1.070 ± 0.27	0.981 ± 0.11	0.028
Step length	0.534 ± 0.06	0.536 ± 0.06	0.300
Velocity	0.657 ± 0.10	0.659 ± 0.11	0.020
Cadence	74.46 ± 13.08	74.45 ± 13.48	4.091

\# Units for gait parameters are as follows: Stride length [m], step length [m], velocity [m/s] and cadence [steps/min]

Table 24: Temporal-spatial validity results - Normal walk (Straps)

	Gait parameters		Difference
	IMC	OMC	
	Mean ± SD	Mean ± SD	E_{RMS} #
Stride length#	1.38 ± 0.12	1.41 ± 0.13	0.045
Step length	0.685 ± 0.06	0.713 ± 0.07	0.051
Velocity	1.281 ± 0.17	1.297 ± 0.18	0.037
Cadence	111.9 ± 7.5	109.1 ± 10.1	5.749

\# Units for gait parameters are as follows: Stride length [m], step length [m], velocity [m/s] and cadence [steps/min]

- A8 -

8.4.2. Joint angle validity results

Table 25: Slow walk joint angle validity results (Suit)

	E_{RMS} [°]		E_{RMS} (adjusted) [°]		R	
	Right Mean ± SD	Left Mean ± SD	Right Mean ± SD	Left Mean ± SD	Right Mean ± SD	Left Mean ± SD
φ_h	5.146 ± 2.106	2.706 ± 1.494	4.530 ± 1.924	1.306 ± 0.782	**0.740** ± 0.103	**0.771** ± 0.355
θ_h	12.770 ± 6.071	34.170 ± 64.003	1.761 ± 0.395	23.045 ± 55.876	**0.994** ± 0.004	**0.990** ± 0.007
ψ_h	9.459 ± 4.475	8.151 ± 5.297	4.247 ± 2.256	3.528 ± 1.119	**0.712** ± 0.193	**0.672** ± 0.212
φ_k	4.045 ± 3.251	6.135 ± 2.380	2.446 ± 1.573	3.968 ± 1.481	**0.658** ± 0.277	**0.541** ± 0.309
θ_k	7.569 ± 4.238	19.002 ± 39.711	2.081 ± 0.512	13.672 ± 29.378	**0.993** ± 0.004	**0.940** ± 0.144
ψ_k	7.757 ± 4.824	13.778 ± 8.689	3.439 ± 1.880	4.287 ± 4.667	0.356 ± 0.259	0.484 ± 0.338
φ_a	6.124 ± 4.071	5.545 ± 0.862	5.322 ± 3.444	4.616 ± 1.490	0.335 ± 0.216	0.316 ± 0.096
θ_a	16.716 ± 4.335	16.073 ± 4.171	15.101 ± 4.048	15.099 ± 4.150	**0.565** ± 0.188	0.403 ± 0.199
ψ_a	8.532 ± 5.577	12.735 ± 6.677	3.003 ± 1.085	4.006 ± 2.873	**0.629** ± 0.127	0.493 ± 0.158

Values in bold and colour are those with correlation coefficient > 0.5

Table 26: Normal walk joint angle validity results (Suit)

	E_{RMS} [°]		E_{RMS} (adjusted) [°]		R	
	Right Mean ± SD	Left Mean ± SD	Right Mean ± SD	Left Mean ± SD	Right Mean ± SD	Left Mean ± SD
φ_h	5.835 ± 2.475	5.278 ± 4.297	4.855 ± 1.963	2.112 ± 0.389	**0.831** ± 0.121	**0.840** ± 0.037
θ_h	13.621 ± 6.709	11.778 ± 4.736	2.800 ± 0.985	3.405 ± 1.071	**0.995** ± 0.003	**0.988** ± 0.013
ψ_h	10.418 ± 4.543	14.433 ± 11.580	5.613 ± 0.715	6.260 ± 2.741	**0.561** ± 0.210	0.422 ± 0.269
φ_k	7.477 ± 5.821	8.938 ± 3.489	5.023 ± 3.229	7.246 ± 2.797	**0.588** ± 0.345	0.490 ± 0.305
θ_k	6.924 ± 3.636	8.989 ± 9.118	3.020 ± 1.070	4.830 ± 2.423	**0.990** ± 0.009	**0.986** ± 0.008
ψ_k	10.451 ± 4.426	11.936 ± 7.825	5.395 ± 2.842	5.023 ± 1.028	0.365 ± 0.225	**0.582** ± 0.229
φ_a	6.813 ± 3.227	7.357 ± 4.529	5.837 ± 2.213	6.782 ± 4.409	**0.525** ± 0.222	0.371 ± 0.256
θ_a	26.551 ± 4.700	27.895 ± 2.320	22.611 ± 2.684	24.885 ± 2.791	0.142 ± 0.111	0.312 ± 0.271
ψ_a	11.210 ± 7.424	14.336 ± 10.894	3.530 ± 0.942	6.790 ± 5.314	0.488 ± 0.330	0.427 ± 0.265

Values in bold and colour are those with correlation coefficient > 0.5

Table 27: Fast walk joint angle validity results (Suit)

	E_{RMS} [°]		E_{RMS} (adjusted) [°]		R	
	Right Mean ± SD	Left Mean ± SD	Right Mean ± SD	Left Mean ± SD	Right Mean ± SD	Left Mean ± SD
φ_h	9.238 ± 2.314	8.431 ± 6.194	8.184 ± 2.565	3.050 ± 1.040	**0.633** ± 0.257	**0.803** ± 0.126
θ_h	13.487 ± 4.138	10.859 ± 3.915	5.181 ± 2.482	4.806 ± 2.134	**0.977** ± 0.030	**0.977** ± 0.023
ψ_h	11.889 ± 1.931	13.455 ± 12.152	10.011 ± 2.027	8.871 ± 3.600	0.422 ± 0.217	0.297 ± 0.196
φ_k	4.465 ± 1.474	12.517 ± 7.450	3.273 ± 0.639	10.969 ± 7.790	**0.599** ± 0.273	0.482 ± 0.100
θ_k	10.420 ± 6.741	7.603 ± 7.699	4.769 ± 2.827	4.120 ± 1.522	**0.972** ± 0.031	**0.975** ± 0.038
ψ_k	7.473 ± 2.576	14.180 ± 10.832	5.947 ± 1.725	8.006 ± 6.367	0.382 ± 0.178	**0.614** ± 0.175
φ_a	5.781 ± 1.950	7.054 ± 5.072	5.235 ± 1.576	6.071 ± 4.239	0.392 ± 0.288	0.354 ± 0.156
θ_a	29.257 ± 4.034	32.941 ± 3.566	27.977 ± 4.486	31.707 ± 4.416	0.140 ± 0.077	0.421 ± 0.240
ψ_a	10.691 ± 4.097	13.530 ± 12.688	5.192 ± 1.867	7.116 ± 5.919	**0.555** ± 0.287	0.270 ± 0.261

Values in bold and colour are those with correlation coefficient > 0.5

- A9 -

	E_{RMS} [°]		E_{RMS} (adjusted) [°]		R	
	Right	Left	Right	Left	Right	Left
	Mean ± SD	Mean ± SD	Mean ± SD	Mean ± SD	Mean ± SD	Mean ± SD
φ_h	2.655 ± 1.558	2.115 ± 1.065	1.490 ± 0.468	1.616 ± 0.622	**0.949** ± 0.041	**0.891** ± 0.087
θ_h	14.918 ± 7.059	14.981 ± 6.717	2.498 ± 0.948	2.777 ± 0.703	**0.984** ± 0.013	**0.983** ± 0.011
ψ_h	8.256 ± 3.892	8.851 ± 2.833	3.581 ± 1.759	4.258 ± 1.642	0.528 ± 0.252	**0.559** ± 0.192
φ_k	7.249 ± 1.035	6.362 ± 1.133	4.326 ± 1.305	4.862 ± 1.132	**0.561** ± 0.299	**0.615** ± 0.177
θ_k	8.912 ± 3.783	7.773 ± 5.225	2.515 ± 1.029	3.413 ± 1.877	**0.990** ± 0.007	**0.978** ± 0.023
ψ_k	12.243 ± 6.100	15.865 ± 6.755	3.231 ± 1.164	3.385 ± 1.421	**0.700** ± 0.250	**0.522** ± 0.275
φ_a	6.083 ± 1.173	7.636 ± 1.741	5.329 ± 0.748	7.157 ± 1.270	0.191 ± 0.206	0.271 ± 0.131
θ_a	21.734 ± 3.100	19.255 ± 1.524	19.158 ± 3.089	17.497 ± 0.855	0.283 ± 0.086	0.330 ± 0.154
ψ_a	5.760 ± 1.404	16.050 ± 8.308	3.864 ± 1.045	4.916 ± 0.671	0.442 ± 0.153	0.367 ± 0.142

Values in bold and colour are those with correlation coefficient > 0.5

	E_{RMS} [°]		E_{RMS} (adjusted) [°]		R	
	Right	Left	Right	Left	Right	Left
	Mean ± SD	Mean ± SD	Mean ± SD	Mean ± SD	Mean ± SD	Mean ± SD
φ_h	3.268 ± 1.711	3.123 ± 0.645	2.055 ± 0.475	2.291 ± 0.271	**0.911** ± 0.078	**0.864** ± 0.056
θ_h	17.819 ± 7.228	17.258 ± 5.694	3.839 ± 1.731	3.462 ± 1.007	**0.971** ± 0.028	**0.982** ± 0.020
ψ_h	9.678 ± 4.702	10.650 ± 3.830	4.515 ± 2.513	5.553 ± 1.890	**0.503** ± 0.245	0.438 ± 0.270
φ_k	8.859 ± 1.011	8.094 ± 0.890	5.558 ± 2.621	6.688 ± 0.749	0.492 ± 0.281	0.394 ± 0.287
θ_k	7.760 ± 4.507	7.897 ± 3.287	3.412 ± 0.858	3.043 ± 0.833	**0.986** ± 0.003	**0.988** ± 0.007
ψ_k	10.479 ± 5.161	15.609 ± 7.929	3.947 ± 0.963	4.404 ± 1.271	**0.779** ± 0.154	**0.572** ± 0.290
φ_a	6.119 ± 2.312	8.664 ± 3.168	5.348 ± 1.042	7.504 ± 1.937	0.282 ± 0.161	0.229 ± 0.179
θ_a	25.570 ± 5.069	22.567 ± 2.230	21.422 ± 2.783	20.653 ± 2.234	0.253 ± 0.109	0.280 ± 0.072
ψ_a	6.644 ± 2.129	15.330 ± 7.092	4.860 ± 2.420	6.802 ± 1.322	0.412 ± 0.295	0.129 ± 0.128

Values in bold and colour are those with correlation coefficient > 0.5

	E_{RMS} [°]		E_{RMS} (adjusted) [°]		R	
	Right	Left	Right	Left	Right	Left
	Mean ± SD	Mean ± SD	Mean ± SD	Mean ± SD	Mean ± SD	Mean ± SD
φ_h	5.224 ± 2.265	3.609 ± 1.023	3.874 ± 1.926	2.805 ± 0.349	**0.855** ± 0.088	**0.895** ± 0.034
θ_h	17.376 ± 6.714	14.248 ± 7.849	4.382 ± 1.074	4.318 ± 1.211	**0.987** ± 0.007	**0.981** ± 0.017
ψ_h	8.905 ± 5.198	11.532 ± 2.398	5.281 ± 2.238	6.499 ± 2.411	**0.596** ± 0.181	0.433 ± 0.322
φ_k	8.047 ± 1.433	9.796 ± 1.929	4.684 ± 2.366	7.978 ± 0.876	0.398 ± 0.361	0.383 ± 0.127
θ_k	11.430 ± 5.494	7.844 ± 4.411	3.479 ± 0.724	3.169 ± 0.520	**0.989** ± 0.006	**0.991** ± 0.004
ψ_k	11.589 ± 5.318	14.030 ± 3.624	5.182 ± 1.307	5.647 ± 1.972	**0.764** ± 0.191	**0.555** ± 0.198
φ_a	5.396 ± 1.761	8.757 ± 5.051	4.910 ± 1.602	8.373 ± 4.496	0.391 ± 0.120	0.240 ± 0.080
θ_a	28.354 ± 4.618	24.277 ± 1.720	26.521 ± 5.691	22.058 ± 1.289	0.300 ± 0.028	0.188 ± 0.073
ψ_a	6.614 ± 0.800	13.184 ± 7.669	5.893 ± 0.861	6.155 ± 1.137	0.485 ± 0.151	0.397 ± 0.250

Values in bold and colour are those with correlation coefficient > 0.5

- A10 -

8.4.3. Joint angle validity results - Suit vs. straps

The difference values given in the tables below simply display the difference between the average results obtained from tests using first the suit and then the straps. Values in bold indicate those in which the results obtained using straps showed higher correlation than those measured using the Lycra suit. The results show that the straps have a significant advantage over the suit only during fast walk trials.

Table 31: Difference between joint angle validity results of suit and straps - Slow walk

	ΔE_{RMS} [°]		ΔE_{RMS} (adjusted) [°]		ΔE_R	
	Right	Left	Right	Left	Right	Left
φ_h	**2.491**#	**0.591**	**3.040**	0.310	**0.210**	**0.120**
θ_h	2.147	**19.189**	0.736	**20.268**	0.010	0.008
ψ_h	**1.203**	0.700	**0.666**	0.730	0.184	0.113
φ_k	3.204	0.227	1.879	0.893	0.097	**0.074**
θ_k	1.344	**11.229**	0.433	**10.260**	0.003	**0.038**
ψ_k	4.486	2.088	**0.208**	**0.902**	**0.344**	**0.039**
φ_a	**0.042**	2.091	0.006	2.541	0.144	0.044
θ_a	5.019	3.182	4.057	2.398	0.282	0.073
ψ_a	**2.771**	3.315	0.862	0.910	0.187	0.126

#Values in bold and colour is where straps showed higher correlation than the suit

Table 32: Difference between joint angle validity results of suit and straps - Normal walk

	ΔE_{RMS} [°]		ΔE_{RMS} (adjusted) [°]		ΔE_R	
	Right	Left	Right	Left	Right	Left
φ_h	**2.567**	**2.155**	**2.800**	0.179	**0.080**	**0.024**
θ_h	4.198	5.479	1.040	0.057	0.024	0.006
ψ_h	**0.740**	**3.783**	**1.098**	**0.706**	0.059	**0.016**
φ_k	1.381	**0.844**	0.535	**0.558**	0.096	0.096
θ_k	0.835	**1.092**	0.392	**1.787**	0.003	**0.003**
ψ_k	0.027	3.673	**1.448**	**0.619**	**0.414**	0.009
φ_a	**0.694**	1.307	**0.489**	0.722	0.243	0.142
θ_a	**0.981**	**5.327**	**1.189**	**4.233**	**0.112**	0.032
ψ_a	**4.566**	0.994	1.330	0.012	0.076	0.298

#Values in bold and colour is where straps showed higher correlation than the suit

Table 33: Difference between joint angle validity results of suit and straps - Fast walk

	ΔE_{RMS} [°]		ΔE_{RMS} (adjusted) [°]		ΔE_R	
	Right	Left	Right	Left	Right	Left
φ_h	**4.014**	**4.821**	**4.310**	**0.244**	**0.221**	**0.092**
θ_h	3.889	3.389	**0.799**	**0.488**	**0.009**	**0.004**
ψ_h	**2.984**	**1.923**	**4.730**	**2.372**	**0.174**	**0.137**
φ_k	3.582	**2.721**	1.412	**2.991**	0.201	0.099
θ_k	1.009	0.241	**1.290**	**0.950**	**0.017**	**0.016**
ψ_k	4.116	**0.150**	**0.765**	**2.359**	**0.382**	0.059
φ_a	**0.385**	1.703	**0.325**	2.302	0.001	0.113
θ_a	**0.903**	**8.663**	**1.456**	**9.649**	**0.161**	0.233
ψ_a	**4.077**	**0.347**	0.701	**0.961**	0.070	**0.128**

#Values in bold and colour is where straps showed higher correlation than the suit

- A11 -

8.5. Appendix E: Neural network results

8.5.1. TRAINLM

Table 34: Average misclassifications in neural network results over 15 identical runs

		-7	-6	-5	-4	-3	-2	-1	0	1	2	3	4	5	6	7
	23	0.6	0.6	0.3	1.1	0.9	1.2	1.1	0.9	0.5	1.1	0.5	1.2	0.6	0.8	0.5
	22	0.6	0.7	0.7	0.7	0.5	0.7	0.7	0.8	0.8	0.5	0.6	0.7	0.6	1.2	1.0
	21	0.2	0.3	0.2	0.9	0.5	0.7	0.3	0.7	0.8	0.9	0.9	0.5	0.5	0.6	0.6
	20	0.5	0.5	0.9	0.8	1.1	0.9	0.7	0.9	0.9	0.9	1.2	1.3	0.6	0.7	1.1
	19	2.0	1.5	1.7	1.1	2.0	1.4	1.9	1.7	1.7	1.8	1.9	2.1	1.7	2.0	1.5
	18	1.3	1.4	1.2	1.2	1.1	1.4	1.1	1.1	1.2	1.1	1.3	1.5	1.5	1.6	1.5
	17	1.6	1.8	1.5	1.5	1.7	1.1	1.1	1.3	1.4	1.0	1.5	1.1	0.7	0.9	1.5
	16	1.3	1.3	1.4	1.7	1.1	1.7	1.3	1.5	1.5	1.4	1.3	1.3	1.1	1.2	1.5
Number of input parameters used (j)	**15**	1.4	1.6	1.0	1.7	1.7	1.3	1.3	1.5	1.5	0.8	1.4	1.1	1.3	1.5	1.3
	14	1.8	1.5	1.9	1.9	1.3	1.7	1.7	1.6	1.6	1.7	1.5	1.5	1.3	1.1	1.7
	13	1.1	1.1	1.0	1.1	1.0	1.1	1.1	0.9	1.0	1.0	1.1	1.1	1.1	0.9	1.1
	12	0.9	1.0	0.9	1.0	1.0	1.0	0.9	1.0	1.0	1.0	1.0	1.0	1.0	1.0	1.0
	11	0.9	1.0	0.9	0.9	1.0	1.0	1.0	0.9	0.8	1.0	0.9	1.0	1.0	1.0	1.0
	10	0.9	1.0	1.0	1.0	1.0	0.9	1.0	1.0	1.0	0.9	1.0	0.9	0.9	0.9	1.0
	9	1.0	1.0	1.0	1.0	1.0	1.0	0.9	0.9	1.0	1.0	1.0	1.0	1.0	1.0	1.0
	8	1.0	1.0	0.9	1.0	1.0	1.0	0.9	0.9	1.0	1.0	1.0	0.9	1.0	0.9	0.9
	7	1.4	1.1	1.2	1.3	0.9	1.2	1.1	0.9	1.3	1.0	1.1	1.1	1.0	1.1	1.0
	6	1.1	1.1	1.0	0.9	1.0	1.0	1.0	1.1	1.0	1.0	0.9	0.9	1.0	0.9	1.0
	5	0.9	0.9	1.0	0.9	0.9	1.0	0.8	0.9	0.9	0.9	1.1	0.9	1.1	0.8	0.9
	4	1.0	1.0	0.9	0.7	0.8	0.7	0.7	0.7	0.9	0.9	0.8	0.8	0.7	0.5	0.7

Number of hidden layer neurons (2j+i)

Low misclassification ◄───────────────────► High misclassification

Table 35: Standard deviation in neural network results over 15 identical runs

		-7	-6	-5	-4	-3	-2	-1	0	1	2	3	4	5	6	7
	23	1.1	0.8	0.5	1.0	1.0	1.5	1.4	0.6	0.7	0.8	0.8	1.4	1.3	0.9	0.6
	22	0.9	1.0	0.8	0.7	0.6	0.8	0.9	0.9	0.8	0.7	0.7	1.2	0.6	1.1	0.9
	21	0.4	0.8	0.4	1.2	0.7	1.0	0.5	0.9	0.9	0.7	1.2	0.7	0.6	0.7	0.7
	20	1.1	0.6	0.8	0.9	1.0	0.7	0.7	0.9	0.7	0.7	1.2	0.8	0.7	0.7	1.1
	19	0.5	0.6	0.8	1.0	0.8	0.6	0.8	0.9	0.7	0.7	1.0	1.0	0.5	1.3	1.4
	18	0.6	0.9	0.8	0.9	0.6	0.6	0.6	0.8	0.9	0.8	0.7	0.5	0.6	0.7	1.0
	17	0.6	0.9	0.7	0.6	1.0	0.8	0.5	0.7	0.6	0.8	0.8	0.7	0.6	0.5	0.8
	16	0.6	0.9	0.5	0.9	0.5	0.6	0.6	0.6	0.8	0.5	0.5	0.9	1.1	0.8	0.5
Number of input parameters used (j)	**15**	0.7	0.7	1.1	1.1	0.8	0.5	0.6	0.6	0.6	0.6	0.5	0.7	0.8	0.5	0.8
	14	0.7	0.8	0.8	0.9	0.7	0.8	0.6	0.6	0.8	0.7	0.6	0.6	0.6	0.7	0.5
	13	0.3	0.3	0.0	0.3	0.0	0.4	0.5	0.4	0.0	0.0	0.4	0.4	0.5	0.5	0.3
	12	0.3	0.0	0.3	0.0	0.0	0.0	0.3	0.0	0.0	0.0	0.0	0.0	0.0	0.0	0.0
	11	0.4	0.0	0.4	0.3	0.0	0.0	0.0	0.3	0.4	0.0	0.3	0.0	0.0	0.0	0.0
	10	0.3	0.0	0.0	0.0	0.0	0.3	0.0	0.0	0.0	0.3	0.0	0.3	0.4	0.3	0.0
	9	0.0	0.0	0.0	0.0	0.0	0.0	0.3	0.3	0.0	0.0	0.0	0.0	0.0	0.0	0.0
	8	0.0	0.0	0.3	0.0	0.0	0.0	0.4	0.3	0.0	0.0	0.0	0.3	0.0	0.3	0.3
	7	0.6	0.3	0.4	0.5	0.4	0.6	0.4	0.3	0.6	0.0	0.5	0.3	0.0	0.3	0.0
	6	0.4	0.3	0.0	0.3	0.0	0.0	0.0	0.5	0.0	0.0	0.3	0.3	0.0	0.3	0.4
	5	0.4	0.3	0.0	0.3	0.5	0.0	0.4	0.3	0.5	0.5	0.3	0.3	0.5	0.4	0.3
	4	0.0	0.0	0.3	0.5	0.4	0.5	0.5	0.5	0.3	0.3	0.4	0.4	0.5	0.5	0.5

Number of hidden layer neurons (2j+i)

Low standard deviation ◄───────────────────► High standard deviation

- A12 -

Table 36: Average goal tolerance in neural network results over 15 identical runs

						Number of hidden layer neurons (2j+i)									
		-7	-6	-5	-4	-3	-2	-1	0	1	2	3	4	5	6	7
	23	0.05	0.05	0.04	0.06	0.04	0.06	0.06	0.05	0.05	0.05	0.05	0.05	0.05	0.06	0.05
	22	0.05	0.04	0.05	0.05	0.05	0.02	0.06	0.05	0.04	0.04	0.04	0.05	0.06	0.04	0.04
	21	0.05	0.05	0.06	0.04	0.04	0.04	0.05	0.04	0.05	0.05	0.04	0.07	0.05	0.05	0.06
	20	0.06	0.05	0.05	0.06	0.05	0.06	0.05	0.05	0.06	0.06	0.07	0.06	0.05	0.05	0.06
	19	0.06	0.06	0.04	0.06	0.04	0.05	0.05	0.06	0.05	0.06	0.05	0.05	0.07	0.05	0.06
	18	0.06	0.05	0.04	0.06	0.05	0.04	0.04	0.05	0.05	0.05	0.04	0.06	0.05	0.04	0.06
Number of input parameters used (j)	17	0.04	0.05	0.05	0.06	0.05	0.05	0.05	0.05	0.05	0.05	0.06	0.05	0.07	0.05	0.04
	16	0.06	0.04	0.05	0.05	0.05	0.06	0.04	0.05	0.06	0.05	0.05	0.05	0.04	0.04	0.04
	15	0.04	0.06	0.06	0.05	0.05	0.06	0.04	0.05	0.04	0.06	0.05	0.07	0.04	0.06	0.05
	14	0.04	0.04	0.05	0.05	0.05	0.05	0.05	0.06	0.05	0.03	0.04	0.04	0.03	0.04	0.04
	13	0.02	0.04	0.02	0.03	0.03	0.03	0.03	0.05	0.03	0.03	0.03	0.02	0.04	0.06	0.02
	12	0.04	0.02	0.03	0.01	0.02	0.01	0.04	0.01	0.03	0.02	0.02	0.02	0.01	0.03	0.01
	11	0.05	0.01	0.05	0.04	0.02	0.02	0.01	0.04	0.05	0.01	0.04	0.01	0.02	0.01	0.01
	10	0.01	0.02	0.01	0.01	0.01	0.04	0.01	0.01	0.01	0.03	0.01	0.03	0.03	0.03	0.01
	9	0.02	0.01	0.01	0.02	0.01	0.02	0.01	0.04	0.01	0.01	0.01	0.01	0.01	0.02	0.02
	8	0.01	0.01	0.04	0.01	0.01	0.01	0.04	0.04	0.01	0.01	0.01	0.04	0.01	0.04	0.04
	7	0.04	0.05	0.05	0.04	0.05	0.05	0.03	0.06	0.04	0.05	0.05	0.04	0.03	0.04	0.05
	6	0.02	0.02	0.03	0.02	0.02	0.02	0.04	0.02	0.03	0.03	0.04	0.04	0.03	0.02	0.03
	5	0.04	0.04	0.05	0.05	0.04	0.03	0.05	0.03	0.02	0.03	0.02	0.04	0.04	0.02	0.04
	4	0.01	0.03	0.03	0.03	0.03	0.03	0.03	0.02	0.03	0.03	0.03	0.02	0.03	0.03	0.02

Low average tolerance — High average tolerance

Table 37: Standard deviation in goal tolerance in neural network results over 15 identical runs

							Number of hidden layer neurons (2j+i)									
		-7	-6	-5	-4	-3	-2	-1	0	1	2	3	4	5	6	7
	23	0.09	0.09	0.06	0.10	0.07	0.08	0.10	0.11	0.09	0.08	0.09	0.11	0.10	0.11	0.09
	22	0.09	0.07	0.07	0.09	0.08	0.05	0.08	0.08	0.09	0.08	0.07	0.11	0.10	0.10	0.08
	21	0.10	0.09	0.09	0.06	0.10	0.09	0.09	0.09	0.07	0.10	0.08	0.11	0.10	0.10	0.11
	20	0.11	0.09	0.08	0.10	0.10	0.11	0.12	0.09	0.11	0.11	0.11	0.10	0.08	0.12	0.10
	19	0.09	0.11	0.06	0.14	0.07	0.09	0.11	0.10	0.10	0.09	0.09	0.10	0.10	0.09	0.14
	18	0.10	0.07	0.10	0.13	0.10	0.08	0.09	0.10	0.12	0.09	0.10	0.10	0.10	0.08	0.11
Number of input parameters used (j)	17	0.11	0.10	0.09	0.12	0.10	0.10	0.12	0.11	0.12	0.12	0.10	0.10	0.11	0.11	0.12
	16	0.12	0.12	0.11	0.10	0.10	0.08	0.11	0.09	0.10	0.09	0.12	0.11	0.12	0.10	0.09
	15	0.11	0.10	0.11	0.09	0.10	0.12	0.12	0.10	0.08	0.10	0.09	0.12	0.10	0.12	0.09
	14	0.10	0.11	0.10	0.10	0.11	0.12	0.12	0.12	0.10	0.09	0.10	0.12	0.10	0.14	0.10
	13	0.05	0.06	0.05	0.05	0.05	0.06	0.05	0.09	0.06	0.06	0.06	0.06	0.07	0.10	0.04
	12	0.05	0.05	0.05	0.05	0.04	0.04	0.05	0.04	0.05	0.05	0.05	0.05	0.04	0.06	0.04
	11	0.06	0.04	0.06	0.05	0.04	0.05	0.04	0.05	0.07	0.04	0.05	0.04	0.04	0.04	0.04
	10	0.03	0.04	0.03	0.04	0.04	0.05	0.03	0.04	0.04	0.04	0.03	0.04	0.05	0.04	0.04
	9	0.04	0.04	0.03	0.03	0.04	0.04	0.03	0.05	0.03	0.03	0.03	0.04	0.05	0.04	0.04
	8	0.04	0.04	0.05	0.03	0.04	0.04	0.05	0.04	0.04	0.04	0.04	0.05	0.04	0.05	0.05
	7	0.10	0.10	0.11	0.11	0.10	0.10	0.10	0.12	0.09	0.11	0.10	0.08	0.08	0.10	0.09
	6	0.10	0.10	0.10	0.11	0.09	0.09	0.10	0.11	0.11	0.11	0.11	0.12	0.09	0.11	0.09
	5	0.07	0.07	0.08	0.09	0.10	0.08	0.09	0.09	0.08	0.07	0.08	0.10	0.10	0.07	0.09
	4	0.03	0.05	0.08	0.07	0.07	0.07	0.07	0.08	0.07	0.07	0.07	0.07	0.07	0.07	0.08

Low standard deviation — High standard deviation

8.5.2. TRAINGDM

Table 38: Average misclassifications in neural network results over 15 identical runs

		Number of hidden layer neurons (2j+i)													
j	**-7**	**-6**	**-5**	**-4**	**-3**	**-2**	**-1**	**0**	**1**	**2**	**3**	**4**	**5**	**6**	**7**
23	4.13	4.47	5.33	4.33	4.73	4.40	4.60	3.93	4.20	3.87	4.53	5.00	4.27	3.60	4.13
22	3.33	3.93	2.73	2.47	3.87	2.73	3.27	2.80	3.20	3.73	3.80	3.80	3.13	3.33	3.20
21	2.80	2.80	2.60	2.33	2.80	3.13	2.53	2.93	2.60	2.60	2.60	3.00	2.20	2.07	2.67
20	2.53	2.53	2.07	2.27	2.07	2.67	2.53	2.20	2.40	2.80	2.20	2.67	2.20	2.53	2.60
19	4.40	4.13	4.33	4.00	3.87	4.20	4.07	4.07	4.67	4.67	3.87	4.67	3.47	4.40	4.20
18	3.00	3.00	3.53	3.33	3.40	3.33	3.33	3.33	3.27	3.40	3.20	2.80	3.40	3.00	2.87
17	3.47	3.20	3.07	2.93	2.93	3.67	3.40	2.87	3.20	3.53	3.87	3.67	3.67	2.67	2.87
16	3.00	2.80	3.73	3.47	3.07	3.60	3.47	3.27	3.20	3.60	3.60	3.20	3.07	3.27	3.20
15	2.73	3.20	2.73	2.40	2.40	3.27	3.07	3.00	3.00	3.33	2.73	3.07	3.53	2.53	3.33
14	2.53	3.73	2.87	3.20	3.33	3.20	3.80	3.33	3.13	2.73	3.60	3.33	3.33	3.20	3.07
13	3.00	2.80	3.27	2.40	2.87	3.00	3.73	3.20	2.93	2.87	3.33	2.73	2.47	2.67	2.80
12	3.07	3.33	3.20	2.93	2.53	3.00	2.93	3.13	3.20	2.80	3.20	3.13	2.67	3.00	2.73
11	2.53	2.93	2.60	3.20	3.00	2.80	3.13	3.20	3.00	2.67	3.13	3.00	3.13	2.60	2.27
10	3.07	2.40	2.73	2.20	3.00	3.53	2.87	2.20	2.67	3.00	2.87	3.07	2.73	3.07	2.53
9	3.13	3.53	3.73	3.00	3.27	3.53	3.13	3.07	3.93	2.73	3.07	3.07	2.87	2.93	3.13
8	3.47	2.93	3.33	3.00	2.87	2.87	2.67	2.87	2.53	1.67	2.73	2.40	2.87	2.67	2.80
7	2.67	3.40	3.13	2.87	3.07	2.73	2.60	2.60	3.67	2.73	2.73	3.13	2.73	1.87	2.47
6	3.53	3.13	3.20	2.60	2.53	2.80	2.40	2.40	3.00	2.73	2.47	2.60	2.67	2.73	3.00
5	4.33	4.47	4.47	4.13	4.00	3.33	3.13	3.47	3.00	3.53	3.47	3.00	2.53	2.53	2.33
4	5.00	4.53	3.40	3.27	3.80	3.40	3.07	3.33	3.13	3.60	2.87	2.93	3.27	2.93	2.93

Number of input parameters used (j)

Low misclassification   High misclassification

Table 39: Standard deviation in neural network results over 15 identical runs

		Number of hidden layer neurons (2j+i)													
j	**-7**	**-6**	**-5**	**-4**	**-3**	**-2**	**-1**	**0**	**1**	**2**	**3**	**4**	**5**	**6**	**7**
23	1.36	1.88	1.68	1.63	1.62	1.64	2.06	1.39	1.37	2.20	1.88	2.17	2.66	1.64	1.19
22	1.80	2.05	1.28	1.41	1.77	0.88	2.05	1.47	1.52	1.62	1.37	0.94	2.20	1.45	1.70
21	1.21	1.32	1.12	1.45	1.78	1.19	0.83	1.62	1.50	1.18	1.30	1.96	1.42	1.28	0.90
20	1.13	1.36	1.16	1.16	1.22	1.72	1.36	1.26	1.18	1.01	1.82	1.11	1.15	1.06	1.12
19	1.30	2.03	1.23	1.36	1.46	2.40	1.44	1.44	1.11	1.88	1.60	1.35	1.51	1.45	1.47
18	1.00	1.36	0.92	1.05	0.91	1.18	0.90	0.82	1.22	0.99	1.47	1.32	1.50	0.93	0.83
17	0.83	0.68	0.80	0.96	0.70	1.35	0.91	0.99	0.86	0.83	0.64	0.90	1.45	0.98	1.13
16	1.00	1.08	0.59	1.06	1.16	1.18	1.46	0.70	1.21	1.45	0.91	0.77	0.88	0.96	1.15
15	1.16	1.01	1.22	1.30	1.45	0.88	0.80	1.07	0.76	1.68	1.10	1.22	0.99	0.83	1.23
14	1.13	1.10	1.06	1.32	1.72	1.08	1.52	1.35	1.30	1.10	0.91	0.98	0.72	1.26	1.16
13	1.20	0.94	0.88	0.63	1.51	1.25	1.16	1.32	1.22	0.64	1.18	0.96	1.06	0.82	1.15
12	1.58	1.45	1.61	1.39	0.99	1.13	1.62	1.36	1.32	0.56	0.94	0.99	0.90	1.20	1.28
11	1.46	1.33	1.45	1.37	1.36	1.26	0.74	1.21	0.85	1.18	1.30	0.93	1.30	1.24	1.10
10	1.28	0.99	1.44	1.21	1.51	1.96	1.13	1.42	1.50	0.93	1.06	1.16	0.96	1.10	1.55
9	1.13	1.51	1.44	1.56	1.28	1.46	1.41	0.96	2.05	0.96	1.33	0.96	0.99	1.39	0.92
8	1.85	1.71	1.80	1.46	1.30	1.55	1.18	1.41	1.06	0.98	0.96	1.12	1.46	0.90	1.15
7	1.45	1.35	1.19	1.85	1.53	1.39	1.45	1.35	1.63	1.58	1.10	1.13	1.39	1.30	1.13
6	2.13	2.10	1.21	1.35	1.13	0.94	1.18	1.12	1.36	1.10	1.13	1.45	1.35	0.88	1.51
5	1.63	1.30	1.64	0.83	1.41	1.11	0.83	0.92	1.20	1.13	0.74	1.00	0.83	0.92	0.90
4	1.07	2.13	0.99	1.16	1.21	0.83	0.80	0.98	0.83	0.91	0.99	0.96	0.88	0.88	0.80

Number of input parameters used (j)

Low average tolerance   High average tolerance

Table 40: Average goal tolerance in neural network results over 15 identical runs

					Number of hidden layer neurons (2j+i)											
		-7	-6	-5	-4	-3	-2	-1	0	1	2	3	4	5	6	7
	23	0.09	0.11	0.13	0.14	0.10	0.11	0.11	0.11	0.10	0.10	0.10	0.11	0.09	0.11	0.08
	22	0.12	0.11	0.07	0.10	0.13	0.09	0.10	0.13	0.10	0.08	0.08	0.10	0.13	0.12	0.10
	21	0.08	0.10	0.10	0.12	0.10	0.11	0.08	0.08	0.11	0.11	0.10	0.12	0.10	0.12	0.12
	20	0.08	0.08	0.12	0.08	0.11	0.07	0.09	0.10	0.11	0.12	0.09	0.09	0.09	0.09	0.12
	19	0.09	0.11	0.11	0.15	0.11	0.12	0.10	0.09	0.11	0.10	0.09	0.12	0.13	0.07	0.13
	18	0.08	0.10	0.10	0.09	0.10	0.11	0.10	0.12	0.11	0.09	0.10	0.10	0.09	0.10	0.10
Number of input parameters used (j)	17	0.09	0.09	0.12	0.08	0.10	0.11	0.12	0.11	0.12	0.09	0.08	0.08	0.09	0.09	0.11
	16	0.11	0.12	0.10	0.12	0.10	0.12	0.10	0.10	0.11	0.10	0.10	0.10	0.11	0.10	0.11
	15	0.10	0.11	0.12	0.10	0.10	0.09	0.10	0.12	0.10	0.08	0.10	0.10	0.08	0.11	0.10
	14	0.14	0.11	0.09	0.08	0.07	0.06	0.09	0.10	0.09	0.08	0.09	0.09	0.10	0.10	0.08
	13	0.07	0.10	0.11	0.11	0.10	0.09	0.09	0.08	0.10	0.11	0.10	0.09	0.09	0.10	0.12
	12	0.10	0.11	0.12	0.11	0.10	0.10	0.10	0.11	0.09	0.12	0.11	0.09	0.07	0.10	0.12
	11	0.12	0.12	0.10	0.09	0.10	0.11	0.11	0.09	0.08	0.14	0.07	0.08	0.09	0.12	0.13
	10	0.12	0.11	0.10	0.10	0.09	0.11	0.11	0.11	0.12	0.12	0.10	0.08	0.09	0.11	0.11
	9	0.10	0.11	0.11	0.09	0.11	0.07	0.11	0.11	0.10	0.09	0.11	0.12	0.10	0.12	0.12
	8	0.09	0.09	0.09	0.09	0.11	0.11	0.08	0.10	0.12	0.10	0.10	0.11	0.09	0.12	0.09
	7	0.13	0.11	0.11	0.10	0.12	0.11	0.11	0.07	0.09	0.12	0.10	0.09	0.12	0.10	0.12
	6	0.09	0.09	0.09	0.11	0.12	0.11	0.08	0.12	0.09	0.10	0.11	0.10	0.09	0.12	0.10
	5	0.09	0.10	0.08	0.10	0.06	0.11	0.09	0.11	0.08	0.08	0.13	0.09	0.10	0.10	0.07
	4	0.11	0.09	0.11	0.12	0.10	0.11	0.12	0.11	0.09	0.11	0.10	0.10	0.11	0.08	0.10

Low average tolerance   High average tolerance

Table 41: Standard deviation in goal tolerance in neural network results over 15 identical runs

						Number of hidden layer neurons (2j+i)											
		-7	-6	-5	-4	-3	-2	-1	0	1	2	3	4	5	6	7
	23	0.04	0.06	0.05	0.05	0.06	0.04	0.05	0.05	0.06	0.06	0.05	0.06	0.06	0.06	0.06
	22	0.06	0.08	0.05	0.06	0.06	0.07	0.06	0.06	0.06	0.05	0.06	0.05	0.06	0.06	0.06
	21	0.04	0.06	0.05	0.07	0.06	0.06	0.06	0.06	0.06	0.06	0.06	0.06	0.05	0.05	0.06
	20	0.04	0.04	0.06	0.06	0.06	0.04	0.06	0.07	0.06	0.06	0.06	0.05	0.05	0.06	0.05
	19	0.06	0.06	0.06	0.06	0.07	0.06	0.07	0.04	0.05	0.06	0.04	0.06	0.04	0.06	0.06
	18	0.05	0.05	0.05	0.05	0.05	0.06	0.05	0.07	0.06	0.06	0.06	0.04	0.04	0.06	0.05
Number of input parameters used (j)	17	0.05	0.06	0.05	0.05	0.06	0.06	0.07	0.06	0.06	0.06	0.05	0.07	0.06	0.06	0.06
	16	0.06	0.05	0.06	0.06	0.05	0.07	0.07	0.07	0.06	0.06	0.07	0.05	0.05	0.05	0.07
	15	0.05	0.07	0.06	0.07	0.05	0.06	0.06	0.07	0.06	0.04	0.05	0.06	0.04	0.07	0.05
	14	0.06	0.06	0.06	0.05	0.06	0.04	0.05	0.05	0.06	0.05	0.05	0.06	0.06	0.06	0.06
	13	0.06	0.05	0.05	0.07	0.06	0.06	0.06	0.04	0.06	0.04	0.07	0.05	0.04	0.06	0.06
	12	0.06	0.05	0.06	0.06	0.06	0.06	0.06	0.06	0.06	0.05	0.07	0.05	0.05	0.05	0.06
	11	0.07	0.05	0.06	0.05	0.05	0.06	0.05	0.05	0.05	0.05	0.03	0.05	0.06	0.06	0.06
	10	0.07	0.05	0.06	0.06	0.05	0.06	0.06	0.07	0.06	0.06	0.04	0.05	0.04	0.06	0.06
	9	0.06	0.06	0.05	0.05	0.06	0.04	0.05	0.06	0.06	0.04	0.05	0.06	0.06	0.06	0.07
	8	0.05	0.07	0.05	0.07	0.06	0.06	0.05	0.06	0.06	0.06	0.07	0.07	0.05	0.06	0.05
	7	0.06	0.06	0.05	0.05	0.06	0.06	0.06	0.04	0.06	0.06	0.06	0.06	0.06	0.04	0.04
	6	0.05	0.06	0.06	0.05	0.06	0.07	0.06	0.07	0.06	0.06	0.05	0.06	0.06	0.06	0.06
	5	0.06	0.06	0.04	0.05	0.05	0.06	0.05	0.04	0.05	0.05	0.06	0.06	0.06	0.05	0.04
	4	0.06	0.05	0.07	0.04	0.05	0.06	0.06	0.05	0.04	0.06	0.05	0.06	0.06	0.06	0.04

Low standard deviation   High standard deviation

- A15 -

8.5.3. TRAINGDX

Table 42: Average misclassifications in neural network results over 15 identical runs

							Number of hidden layer neurons (2j+i)								
		-7	-6	-5	-4	-3	-2	-1	0	1	2	3	4	5	6	7
Number of input parameters used (j)	23	1.20	1.93	1.47	1.07	1.47	1.80	1.73	1.40	1.87	1.53	2.07	1.27	1.73	1.33	1.87
	22	1.13	1.20	1.07	1.20	1.67	0.93	1.07	1.53	1.20	1.73	1.27	1.33	1.73	2.00	1.67
	21	0.60	0.67	0.93	1.13	0.60	0.93	0.93	0.87	1.00	0.93	1.47	0.73	1.00	1.53	1.40
	20	0.73	0.87	1.00	1.20	1.13	0.67	1.00	1.40	0.87	1.27	0.73	0.93	0.60	1.00	0.93
	19	2.80	2.73	2.47	2.93	3.07	2.60	3.00	3.00	2.67	2.53	2.80	3.13	2.93	3.27	3.47
	18	1.73	1.60	1.13	1.53	1.73	1.60	1.73	1.93	1.67	1.40	1.53	1.73	1.73	0.87	1.67
	17	2.07	1.93	1.73	2.53	2.07	2.27	2.07	2.07	2.33	1.80	1.80	1.87	2.07	1.40	1.60
	16	2.00	1.80	2.07	2.00	2.13	2.07	1.87	1.53	2.33	1.80	1.60	1.40	2.13	2.27	2.13
	15	2.53	2.47	2.13	1.73	1.93	1.60	1.93	2.07	2.07	1.87	1.40	1.87	2.07	1.60	1.80
	14	2.33	2.33	2.67	2.07	1.73	2.13	1.93	1.80	1.87	1.93	1.93	2.00	1.93	2.13	2.07
	13	1.87	1.73	1.87	1.60	1.60	1.60	1.53	1.33	1.47	1.20	1.33	1.40	1.73	1.20	1.33
	12	1.33	1.87	1.80	1.33	1.40	1.47	1.40	1.60	1.00	1.47	1.40	1.13	0.87	1.13	1.00
	11	2.13	1.47	1.33	1.47	1.47	1.07	1.33	1.20	1.20	1.13	1.07	1.20	0.93	1.00	1.13
	10	2.27	2.13	1.67	1.73	1.93	1.67	1.33	1.27	1.07	1.20	1.20	1.20	1.27	1.00	0.87
	9	2.33	1.87	1.60	2.07	1.53	1.40	1.47	1.27	1.13	1.20	1.07	1.53	1.13	1.47	0.87
	8	1.87	1.93	1.00	1.40	1.40	1.27	1.20	1.00	1.00	1.00	1.20	0.93	0.93	0.87	1.00
	7	2.40	1.80	1.60	1.87	1.67	1.27	1.53	1.53	1.20	1.07	1.33	1.00	1.00	1.00	1.07
	6	1.87	1.47	1.47	1.53	1.53	1.33	1.07	1.13	0.93	1.13	1.27	1.07	1.07	1.07	1.00
	5	2.40	2.33	1.60	1.80	1.73	1.93	1.40	1.27	1.27	1.40	1.27	1.27	1.40	1.60	1.20
	4	2.00	1.80	1.60	1.67	1.73	1.80	1.47	1.53	1.40	1.47	1.47	1.60	1.67	1.47	1.40

Low misclassification — High misclassification

Table 43: Standard deviation in neural network results over 15 identical runs

							Number of hidden layer neurons (2j+i)								
		-7	-6	-5	-4	-3	-2	-1	0	1	2	3	4	5	6	7
Number of input parameters used (j)	23	1.01	0.88	0.99	0.96	0.99	1.08	1.16	0.63	1.36	1.25	1.10	0.88	0.96	1.18	1.46
	22	0.83	0.86	0.88	1.21	1.18	0.96	1.39	1.25	1.08	1.58	1.16	1.18	1.16	1.56	1.29
	21	0.74	0.49	0.70	0.92	0.51	0.96	0.70	0.92	1.00	0.96	0.92	0.70	1.00	0.52	1.50
	20	0.70	0.64	0.93	0.77	0.74	0.72	1.20	0.83	0.92	0.80	0.80	0.70	0.83	1.00	0.88
	19	1.15	0.88	1.13	1.16	0.96	0.99	1.25	1.20	0.82	1.41	1.32	0.83	0.96	1.39	0.92
	18	0.70	0.63	1.06	0.83	0.80	0.83	0.80	0.80	0.98	0.74	0.92	1.03	0.59	0.74	0.49
	17	0.80	1.10	0.70	0.92	0.80	0.80	0.80	0.80	0.82	0.94	0.77	0.83	0.70	0.83	0.83
	16	0.76	0.77	0.70	0.65	0.83	0.70	0.64	0.83	1.11	0.68	0.74	0.74	0.64	0.80	0.83
	15	0.74	0.52	0.92	0.80	0.80	0.83	0.88	0.70	0.59	0.99	0.91	0.74	0.59	0.91	0.56
	14	0.82	0.82	0.72	0.46	0.96	0.64	0.80	0.56	0.64	0.88	0.70	0.76	0.80	0.92	0.59
	13	0.74	0.46	0.64	0.83	0.51	0.83	0.64	0.72	0.74	0.56	0.62	0.51	0.70	0.56	0.72
	12	0.82	0.83	0.56	0.62	0.63	0.52	0.83	0.74	0.53	0.52	0.51	0.35	0.64	0.64	0.38
	11	0.83	0.52	0.90	0.74	0.52	0.59	0.72	0.56	0.56	0.52	0.26	0.77	0.70	0.53	0.52
	10	0.70	0.83	0.90	0.88	0.46	0.72	0.49	0.59	0.26	0.68	0.41	0.77	0.59	0.38	0.64
	9	0.62	0.83	0.51	0.80	0.74	0.51	0.64	0.70	0.52	0.68	0.59	1.06	0.52	0.74	0.35
	8	0.83	0.70	0.38	0.74	0.63	0.46	0.41	0.00	0.38	0.00	0.56	0.26	0.26	0.35	0.00
	7	0.91	0.77	0.63	0.74	0.82	0.80	0.64	0.83	0.56	0.26	0.72	0.00	0.38	0.53	0.26
	6	0.74	0.64	0.74	0.74	0.74	0.62	0.26	0.35	0.26	0.35	0.46	0.26	0.26	0.26	0.00
	5	0.63	0.49	0.63	0.77	0.59	0.59	0.51	0.46	0.46	0.51	0.46	0.46	0.51	0.74	0.41
	4	0.38	0.68	0.63	0.62	0.70	0.68	0.64	0.64	0.51	0.64	0.52	0.74	0.72	0.74	0.51

Low standard deviation — High standard deviation

Table 44: Average goal tolerance in neural network results over 15 identical runs

Number of hidden layer neurons (2j+i)

j	-7	-6	-5	-4	-3	-2	-1	0	1	2	3	4	5	6	7
23	0.09	0.08	0.09	0.10	0.08	0.09	0.08	0.09	0.07	0.07	0.07	0.09	0.07	0.09	0.08
22	0.08	0.08	0.09	0.09	0.10	0.08	0.10	0.08	0.08	0.08	0.09	0.11	0.12	0.11	0.11
21	0.07	0.08	0.08	0.06	0.07	0.07	0.09	0.09	0.09	0.09	0.06	0.11	0.07	0.05	0.07
20	0.06	0.06	0.08	0.08	0.10	0.10	0.08	0.09	0.07	0.06	0.09	0.09	0.09	0.08	0.07
19	0.07	0.08	0.08	0.09	0.10	0.12	0.09	0.09	0.08	0.06	0.08	0.10	0.09	0.11	0.12
18	0.07	0.11	0.10	0.11	0.07	0.09	0.08	0.06	0.07	0.10	0.08	0.07	0.09	0.08	0.07
17	0.07	0.07	0.10	0.08	0.09	0.07	0.07	0.07	0.08	0.07	0.08	0.08	0.08	0.10	0.09
16	0.07	0.11	0.12	0.10	0.06	0.09	0.10	0.07	0.07	0.09	0.09	0.11	0.07	0.10	0.08
15	0.05	0.07	0.08	0.11	0.08	0.08	0.07	0.11	0.07	0.07	0.08	0.08	0.07	0.06	0.07
14	0.08	0.09	0.06	0.09	0.09	0.09	0.07	0.09	0.06	0.08	0.08	0.05	0.07	0.08	0.09
13	0.10	0.07	0.08	0.12	0.08	0.08	0.08	0.06	0.09	0.07	0.09	0.06	0.07	0.08	0.07
12	0.10	0.06	0.08	0.09	0.09	0.05	0.07	0.09	0.08	0.07	0.10	0.07	0.07	0.09	0.10
11	0.06	0.09	0.09	0.08	0.07	0.12	0.09	0.09	0.10	0.08	0.06	0.07	0.08	0.08	0.09
10	0.06	0.08	0.08	0.06	0.10	0.08	0.09	0.07	0.08	0.11	0.09	0.08	0.07	0.10	0.08
9	0.09	0.08	0.10	0.08	0.09	0.08	0.07	0.08	0.06	0.09	0.11	0.08	0.08	0.06	0.07
8	0.07	0.09	0.13	0.10	0.08	0.08	0.08	0.06	0.06	0.07	0.06	0.08	0.08	0.06	0.07
7	0.07	0.10	0.14	0.08	0.08	0.11	0.09	0.07	0.05	0.08	0.08	0.07	0.07	0.06	0.07
6	0.09	0.10	0.09	0.09	0.08	0.10	0.07	0.08	0.09	0.06	0.05	0.07	0.08	0.06	0.08
5	0.05	0.05	0.08	0.08	0.07	0.08	0.08	0.06	0.08	0.07	0.08	0.05	0.09	0.08	0.08
4	0.05	0.06	0.08	0.07	0.06	0.07	0.06	0.07	0.08	0.06	0.09	0.08	0.05	0.11	0.06

Number of input parameters used (j)

Low average tolerance ——————————————— High average tolerance

Table 45: Standard deviation in goal tolerance in neural network results over 15 identical runs

Number of hidden layer neurons (2j+i)

j	-7	-6	-5	-4	-3	-2	-1	0	1	2	3	4	5	6	7
23	0.04	0.04	0.04	0.05	0.06	0.04	0.04	0.06	0.04	0.05	0.05	0.04	0.06	0.05	0.06
22	0.06	0.06	0.05	0.05	0.05	0.05	0.06	0.06	0.04	0.04	0.05	0.06	0.07	0.06	0.04
21	0.05	0.04	0.05	0.05	0.05	0.04	0.05	0.04	0.05	0.06	0.03	0.05	0.04	0.05	0.04
20	0.04	0.03	0.05	0.05	0.05	0.03	0.05	0.06	0.05	0.05	0.06	0.04	0.05	0.05	0.04
19	0.05	0.06	0.05	0.06	0.05	0.06	0.04	0.05	0.05	0.04	0.04	0.07	0.05	0.07	0.06
18	0.04	0.06	0.06	0.06	0.04	0.05	0.05	0.04	0.05	0.06	0.04	0.04	0.06	0.06	0.05
17	0.04	0.06	0.07	0.07	0.05	0.06	0.04	0.04	0.05	0.05	0.06	0.04	0.05	0.05	0.06
16	0.05	0.05	0.06	0.06	0.05	0.06	0.05	0.05	0.03	0.06	0.05	0.05	0.04	0.06	0.05
15	0.04	0.06	0.04	0.06	0.06	0.05	0.04	0.06	0.04	0.06	0.06	0.04	0.05	0.04	0.04
14	0.05	0.06	0.02	0.04	0.05	0.05	0.05	0.05	0.03	0.05	0.05	0.03	0.06	0.05	0.04
13	0.06	0.07	0.04	0.05	0.05	0.05	0.04	0.05	0.06	0.04	0.04	0.03	0.05	0.05	0.04
12	0.06	0.06	0.05	0.06	0.05	0.03	0.03	0.05	0.05	0.04	0.04	0.05	0.05	0.05	0.05
11	0.03	0.05	0.06	0.05	0.05	0.06	0.06	0.05	0.06	0.07	0.03	0.05	0.05	0.06	0.04
10	0.05	0.06	0.05	0.04	0.06	0.06	0.04	0.04	0.05	0.06	0.06	0.04	0.05	0.07	0.06
9	0.07	0.06	0.05	0.05	0.06	0.06	0.04	0.05	0.05	0.06	0.05	0.04	0.04	0.04	0.05
8	0.05	0.07	0.05	0.06	0.04	0.04	0.05	0.03	0.04	0.05	0.03	0.04	0.05	0.06	0.05
7	0.05	0.06	0.05	0.06	0.06	0.06	0.05	0.06	0.04	0.04	0.06	0.04	0.05	0.05	0.06
6	0.06	0.05	0.05	0.06	0.04	0.05	0.04	0.05	0.05	0.03	0.03	0.05	0.04	0.06	0.06
5	0.05	0.02	0.03	0.04	0.04	0.06	0.06	0.04	0.04	0.05	0.05	0.05	0.05	0.05	0.04
4	0.03	0.04	0.05	0.04	0.04	0.05	0.04	0.03	0.05	0.04	0.04	0.05	0.04	0.06	0.04

Number of input parameters used (j)

Low standard deviation ——————————————— High standard deviation

- A17 -